Materials and Transducers Toward Selective Wireless Gas Sensing

Radislav A. Potyrailo, **Cheryl Surman**, **Nandini Nagraj**, and **Andrew Burns**
General Electric Global Research Center, Niskayuna, NY, USA

1. Introduction

Wireless sensors are devices in which sensing electronic transducers are spatially and galvanically separated from their associated readout/display components. The main benefits of wireless sensors, as compared to traditional tethered sensors, include the non-obtrusive nature of their installations, higher nodal densities, and lower installation costs without the need for extensive wiring.[1–3] These attractive features of wireless sensors facilitate their development toward measurements of a wide range of physical, chemical, and biological parameters of interest. Examples of available wireless sensors include devices for sensing of pH, pressure, and temperature in medical, pharmaceutical, animal health, livestock condition, automotive, and other applications.[4–7]

Some implementations of wireless gas sensors can be already found in monitoring of analyte gases (e.g. carbon dioxide, water vapor, oxygen, combustibles) in relatively interference-free industrial and indoor environments.[8,9] However, unobtrusive wireless gas sensors are urgently needed for many more diverse applications ranging from wearable sensors at the workplace, urban environment, and battlefield, to monitoring of containers with toxic industrial chemicals while in transit, to medical monitoring of hospitalized and in-house patients, to detection of food freshness in individual packages, and to distributed networked sensors over large areas (also known as wireless sensor networks, WSNs). Unfortunately, in these and numerous other practical applications, the available wireless gas sensors fall short of meeting emerging measurement needs in complex environments. In particular, existing wireless gas sensors cannot perform highly selective gas detection in the presence of high levels of interferences and cannot quantitate several components in gas mixtures.

1.1. Diversity Of Monitoring Needs Of Volatiles

The monitoring of numerous gases of environmental, industrial, and homeland security concern is needed over the broad range of their regulated exposure concentrations. Figure 1 illustrates the relationships between several regulated exposure levels spanning several orders of magnitude of gas concentrations. Typical examples of concentrations of regulated exposure are presented in Table 1[10–14] for three groups of toxic volatiles such as volatile organic compounds (VOCs), toxic industrial chemicals (TICs), and chemical warfare agents (CWAs). These examples demonstrate the need for gas sensing capabilities with broad measurement dynamic ranges to cover 2 – 4 orders of magnitude in gas concentrations.

Additional needs for detection of volatiles originate from medical diagnostics, food safety, process monitoring, and other areas.[15–17] In those applications, the types and levels of detected volatiles can provide the needed information for further control actions.

1.2. Chemical Interferences As The Key Noise Parameter For Wireless Sensors

Real-world scenarios significantly complicate the detection capabilities of laboratory sensor prototypes. Chemical interferences represent one of the key environmental noise parameters of the sensed environment. Water vapor is the most abundant and high-concentration interferent in ambient air, with the concentration of saturated water vapor pressure (P_0) at ~30,000 ppm at room temperature[18] (100% relative humidity, RH). Thus, if a new sensor under development is thought to detect 1 ppm of a toxic vapor at 50%RH air (water vapor at 0.5 P/P_0), this new sensor must operate at a 15,000-fold overload from water vapor interference. The sensitivity of almost all sensors to water vapor represents the largest challenge for their practical applications even when combined in arrays to form "electronic noses". Importantly, cross-sensitivity to water vapor is not an issue in natural noses because humans and other mammals do not have receptors for water vapor.[19]

In addition to water vapor, there are numerous other potential chemical interferences that add to the complexity of the background. Some examples of chemical interferences include common industrial solvents, firefighting foam, antifreeze, diesel fuel, kerosene, gasoline, lighter fluid, bleach, window cleaner, floor stripper, floor wax, paint thinner, vinegar, insect repellent, and some others coomonly used for detailed evaluation of sensors performance.[20–23] Typical concentration levels of these and other interferences are 0.01 – 0.1 P_0.

1.3. The Goals And Scope Of This Review

The area of wireless sensing attracts tremendous research attention as indicated by the ~30,000 publications in the field (Figure 2). While there are several excellent reviews on different types of wireless and wearable sensors[8,9,24,25] and several books on physical wireless sensor networks,[26,27] no comprehensive review is available to the chemistry research community to address the key aspects in wireless gas sensor development that include (1) analysis of challenges in wireless sensing from the standpoint of sensor selectivity and power-limited operation, (2) analysis of sensing mechanisms and related applicable known or emerging new sensing materials, (3) analysis of transducers and their applicability for wireless gas sensing, (4) analysis of methodologies to provide selective gas response without the use of "classical" sensor arrays, and (5) wireless sensor networks.

Thus, this review has three broad goals in order to stimulate research in this rapidly expanding multi-disciplinary area. The first goal is to link requirements of known and emerging sensing materials with the principles, methodologies, and component/system requirements of wireless gas sensors. The second goal is to critically analyze the current non-satisfactory gas-selectivity performance of battery-free and low-power gas sensors and to facilitate potential solutions to this important problem. The third goal is to demonstrate the breadth of possible applications, highlight success stories, and to initiate new sensing materials and transducer developments for wireless gas sensors.

In this review, we concentrate on sensing materials, transduction technologies, and data analysis techniques for enhancing selectivity and sensitivity in complex environments. Our discussions of sensing materials for wireless gas sensors is focused on the diversity of response mechanisms to different species to enhance selectivity of analyte detection, approaches for nano-engineering of sensing materials, and new sensing schemes that facilitate the detection and independent recognition of material responses. The choice of focus and detail on materials discussed in this review was provided by their current and future potential applicability to wireless gas sensors.

We focus on sensors that employ electromagnetic fields in the radiofrequency and microwave regions of spectrum for their interactions with sensing materials and/or for

communication with the readout components. Importantly, while a tremendous amount of knowledge has been produced with existing sensing materials coupled to low power tethered and passive wireless transducers, these materials were not systematically explored for selective gas sensing outside the philosophy of sensor arrays. Thus, we critically analyze sensing materials from the standpoint of their potential for selective gas response in individual wireless sensors.

Throughout the review, the emphasis is placed on the passive, battery-free sensors with the critical analysis of requirements for their transducer designs and performance of sensing materials. To solve the fundamental selectivity problem, the design approach should involve the strategy of the proper combination of the three key sensor system components such as sensing material, transducer, and signal generation and processing techniques. Using this strategy, an appropriate selection of sensing materials for monitoring of specific gases including organic and inorganic gases, volatile organic compounds, toxic industrial chemicals, and others can be performed. The selected sensing material is coupled to a wireless transducer to meet a permutation of several criteria that include the range of measured gas concentrations, temperature range of operation, classes of interferences, required response time, precision, and accuracy.

1.4. Topics That Are Out Of Scope Of This Review

It is not effective to cover all topics of wireless sensors for the readers of *Chemical Reviews*. Thus, several topics that are out of scope of this review include (1) engineering aspects of wireless and remote sensors;[28] (2) physics of energy harvesting for passive wireless sensors; 29 and (3) remote sensors that utilize optical and terahertz frequencies of spectrum (fiber-optic and stand-off sensors).[30–32]

2. Anatomy of Wireless Gas Sensors

A typical wireless gas sensor has three highly inter-dependent subsystems (see Figure 3). These subsystems include a sensing transducer with its associated means of powering, a sensing material deposited onto the transducer, and a data transmitter. The data transmitter may be a separate component to which a sensor is connected, or the sensor itself can be the data transmitter.[33] The sensing material can be a separate component or it can also act as the transducer.[34] Wireless sensors (sensing nodes) communicate with a readout/display component (sensor reader) or between each other via a WSN. The communication distance depends on several parameters including the power stored on-board the sensor or delivered to the sensor, the power needed for the sensor to operate at a predetermined signal-to-noise ratio, the amount of environmental clutter that reduces sensor performance, and the communication protocol.

2.1. Active And Passive Wireless Sensors

Wireless gas sensors are based on different detection principles depending on the type of sensing materials and associated transducers used to provide the required sensitivity, selectivity, and stability of measurements. Table 2 shows the power requirements for different gas sensing transducers and sensing systems that have been adapted or could be adapted for wireless sensing.[35–55] Depending on the available power for operation, there are two broad types of wireless sensors: active sensors and passive sensors.

Active wireless sensors have an on-board power supply such as a battery, a supercapacitor, or an energy harvester and can transmit signals up to several hundreds of meters. For minimally-obtrusive sensors, some of the most attractive types of batteries are lithium ion batteries with their thin-film versions having energy densities of >200 Wh/kg.[56] Other energy storage sources include electrochemical capacitors (also known as supercapacitors)

that have energy densities of ~ 5 Wh/kg.[57,58] Energy harvesting for wireless sensors can be accomplished using several energy harvesting methods. Table 3 shows the characteristics of various ambient energy sources and harvested power levels from these sources.[58] Active wireless sensors typically contain a standard communication module with an input for capacitive, resistive, or other types of electronic sensors. Optical sensors with light-emitting diode / photodiode pairs and colorimetric chemically sensing films have also been coupled to such standard communication modules.[59,60] Representative examples of battery-powered wireless sensor systems have been described elsewhere.[43,52,59]

Passive wireless sensors lack an on-board power supply and receive their power from the electromagnetic field generated by the sensor reader. While active wireless sensors communicate over greater distances than passive sensors, their larger size and need for power source maintenance are possible limitations in some applications. Without the need for a battery, the life of a passive sensor is limited mainly by the stability of the sensing film and transducer. Thus, while the communication read range of passive sensors is shorter than that of active sensors, passive sensors are attractive as long-lasting, cost-efficient, and inconspicuous devices. Power to passive sensors can be provided by inductive or capacitive coupling[61] with the delivered power dependent on operation frequency, sensor antenna size, pick-up coil size, impedance-matching conditions, and the power of the sensor reader. Short-range wireless communication with small sensors and low power readers (proximity communication) can be implemented where minimizing the effects of ambient clutter are important.

2.2. Transducers For Wireless Passive Sensors

A variety of electronic transducers that have been developed over the years have been also implemented in wireless passive designs. Examples of magnetoelastic,[53] thickness shear mode (TSM), surface acoustic wave (SAW), and resonant LCR (inductor–capacitor-resistor) transducers are illustrated in Figure 4.

Magnetoelastic transducers[45,62] are made of amorphous ferromagnetic materials (e.g. $Fe_{40}Ni_{38}Mo_4B_{18}$, $Fe_{81}B_{13.5}Si_{3.5}C_2$ alloys) or Fe-rich metallic glasses in the form of ribbons that are further coated with a sensing film (Figure 4a). When excited by a time-varying magnetic field, the large magnetostriction of the ferromagnetic materials facilitates a pronounced magnetoelastic resonance in the sensor structure that is measured wirelessly with a pick-up coil. The mechanism of operation of these sensors involves analyte-induced changes to the mass or elasticity of the sensing films and correlation of these changes with shifts in the resonant frequency of sensors. Typical sizes of these sensors range from a few centimeters down to a few millimeters, and the corresponding resonant frequencies range from hundreds of kHz to hundreds of MHz.

TSM transducers,[46,63] also known as quartz crystal microbalances (QCMs), are often made of AT-cut quartz crystals with associated electrodes that are in contact with a sensing material (Figure 4b). These TSM sensors can be wirelessly interrogated by connecting the sensor to an antenna and reading the resonant impedance spectrum with a pick up coil. The mechanism of operation of these sensors involves analyte-induced changes in the mass, elasticity, and/or conductivity of the sensing film and correlation of these changes with changes in the frequency and attenuation response of the sensor. Typical sizes of these sensors are from a few centimeters down to a few millimeters, and the corresponding resonant frequencies range from several MHz to hundreds of MHz.

SAW transducers[47,54,64] are often made of quartz, $LiNbO_3$, $LiTaO_3$, or $La_3Ga_5SiO_{14}$ materials, configured as delay lines or resonators, which are further coated with a sensing film (Figure 4c). These SAW sensors can be wirelessly interrogated by connecting the

sensor to an antenna and reading the frequency response with a pick-up coil. Similar to TSM sensors, the mechanism of operation of SAW sensors involves analyte-induced changes in the mass, elasticity, and/or conductivity of the sensing film and correlation of these changes with changes in the frequency and attenuation response of the sensors. Typical sizes of these sensors are from millimeters down to micrometers, and the corresponding resonant frequencies range from tens of MHz to several GHz.

LCR transducers[48,65–69] are fabricated as planar, highly conducting circuits in contact with a sensing material (Figure 4d). Resonant impedance spectra of the resulting LCR sensors depend on the inductance (L), capacitance (C), and resistance (R) parameters of the circuit and are measured wirelessly with a pick-up coil. The mechanism of operation of these sensors involves the analyte-induced changes to the complex permittivity ($\varepsilon'_r - j\,\varepsilon''_r$) of the sensing film material and correlation of these changes with changes in the resonant impedance spectrum of the sensor. The real part ε'_r of the complex permittivity of the sensing material is also known as dielectric constant. The imaginary part ε''_r of the complex permittivity of the sensing material is directly proportional to its conductivity σ. Typical sizes of these sensors are from a few centimeters down to micrometers, and the corresponding resonant frequencies range from hundreds of kHz to tens of GHz and depend on the L and C values. These sensors can operate up to the terahertz range[70] in stand-off applications.[30] However, terahertz stand-off sensors are beyond the scope of our review.

In addition to transducers illustrated in Figure 4, resistor and capacitor transducers can also be easily applied for wireless passive sensing. To achieve this goal, such a transducer needs to be galvanically coupled to an inductor and a capacitor or a resistor to complete an LCR circuit.[71] The wireless implementation can be provided by the appropriate flat-coil design of the inductor component of the formed LCR structure. Resistor and capacitor transducers can be also implemented in sensors that are described in Section 2.3.

2.3. RFID Sensors

Both active and passive wireless sensors can contain read/write or read-only memory in the form of integrated circuit (IC) memory chips or interdigital reflected power lines. This feature adds a radio-frequency identification (RFID) capability if the operation frequency and the communication protocols meet the regulatory requirements.[61,72] RFID devices (wireless labels or tags with read/write or read-only memory) have been recognized as a disruptive technology and are widely used in diverse applications ranging from asset tracking, to detection of unauthorized opening of containers, and automatic identification of animals.[61,72] Typical operating frequencies of RFID devices are 125 – 135 kHz (LF, low frequency tags), 13.56 MHz (HF, high frequency tags), 868 – 956 MHz (UHF, ultrahigh frequency tags), and 2.45 GHz (microwave tags).[61]

Several representative examples of active and passive RFID sensors are presented in Figure 5. The limiting form factor for active RFID sensors (Figure 5a–b) is the size of their power source. The limiting form factor for passive RFID sensors is the antenna size (Figure 5c–f). Passive LF, HF, and UHF RFID devices are available with analog capacitive or resistive inputs to an IC RFID chip allowing connection of an external capacitor or resistor transducer (Figure 5c–e) with measurement resolution ranging from a single bit (threshold sensing) to 8 – 12 bit, provided by the IC chip. A new passive RFID sensing approach has been recently demonstrated that does not rely on IC memory chips with an analog input but rather implements ubiquitous, passive 13.56 MHz RFID tags as inductively coupled sensors with 16-bit resolution (Figure 5f) provided by the sensor reader. These RFID sensors combine several measured parameters of the resonant sensor antenna with multivariate data analysis to deliver the unique capability of multiparameter sensing with rejection of environmental interferences.[33,73–75] Additional demonstrated approaches for battery-free RFID sensing are

based on chipless RFID sensors,[76,77] and wireless identification and sensing platforms (WISP).[78]

2.4. Key Performance Factors Of Wireless Sensors

The relative performance of different types of wireless sensors and their overall attractiveness depend on several key factors including (1) intrinsic performance properties of a transducer (e.g. dynamic range and sensitivity of response, signal stability under uncontrolled variations of ambient conditions), (2) sensing material type and deposition methods, (3) ability to correct for uncontrolled environmental noise effects, (4) transducer manufacturability, and (5) design of sensor reader.

Given the existing and emerging approaches for providing power to active sensors, improvements in sensitivity and selectivity in *active sensors* are achieved mostly through the design of new or improved sensing materials, the integration of individual transducers into arrays, and the development of system designs that include air-sampling modules. Improvements in sensitivity and selectivity of *passive sensors* are predominantly achieved through the design of new or improved sensing materials, transducers, and data processing algorithms.

2.5. Summary Of Specific Requirements For Wireless Gas Sensors

In summary, there are several deployment attributes for wireless gas sensors. These attributes include (1) unobtrusive nature of installations, (2) limited or no on-board electrical power for sensor operation, (3) long-term unattended operation without comprehensive re-calibration or single-use operation as a reversible device or a dosimeter, (4) limited or no power for gas delivery across the sensor, (5) simplicitity in installation without sensor wiring. These attributes facilitate specific requirements for wireless sensors.

The specific requirements for active and passive wireless sensors vs. tethered sensors include (1) sensor system design with minimal number of individual sensors, (2) operation without active water vapor removal before analyte measurement, (3) operation without active analyte gas preconcentration and release, (4) operation without periodic baseline correction with a blank gas.

Additional requirements for passive wireless sensors include (1) operation without active gas transport to and from the sensor, (2) operation without active control of sensor temperature for correction for fluctuations in ambient temperature.

In tethered sensors, modulation of data acquisition parameters as a function of time during measurements (e.g. temperature, sample/blank gas flow ratio) was shown to provide additional variables into the response of tethered sensors[79] by not only improving sensor steady-state and dynamic selectivity[80] but also by providing the ability to correct for baseline drift.[81] In wireless sensors, these and other signal modulation approaches are becoming progressively difficult due to the limitations of available on-board power.

3. The Need For Transducers With Multiple Response Mechanisms

Unlike the sophisticated analytical approaches used for the detection of unknown gases, existing and intended applications of gas sensors involve situations where analyte gases and interferences are known.[19,82] For these situations, a given sensor system can be calibrated to quantitate 1 – 3 individual gases in their mixtures in the presence of interferences.[83–87] Starting from this calibrated performance, the quality of quantitation degrades in the presence of chemical interferences above the expected levels, uncontrolled temperature fluctuations, film/transducer aging, surface contamination of the sensor, chemical sensor

poisoning, moisture condensation, mechanical damage, and many other end-use factors. From this list of practical problems, the most significant practical problem in chemical sensing is poor selectivity of individual gas sensors.

The requirement for sensor selectivity often conflicts with the requirement for sensor reversibility. Indeed, full reversibility of sensor response is achieved via weak interactions between the analyte and the sensing film, while high selectivity of sensor response is achieved via strong interactions between the analyte gas and the sensing film. As an example, Figure 6 illustrates typical response cross-sensitivity for different types of sensing materials towards a variety of vapors.[88,89] This problem is currently addressed by two broad research directions: the development of new sensing materials and the development of sensor arrays.

One direction involves the development of new sensing materials with improved response selectivity to an analyte of interest and significantly suppressed response to interferences. Over the years, different approaches to develop materials with molecular selectivity have been explored including the use of molecularly imprinted polymers, zeolites, porphyrins, cavitands, metal-organic frameworks (MOFs) and other surpamolecular compounds.[90–98] Unfortunately, highly selective recognition could be associated with high binding energies and, thus, lack of full sensor reversibility. In addition, developing sensing materials that are selective to small, non-reactive molecules such as volatile organic compounds is very challenging.[99–101]

The other direction involves the development of arrays of sensors with partially selective sensing materials and processing the outputs of individual sensors together. This concept was pioneered by Persaud and Dodd in 1982.[102] Typically, one response per individual sensor (e.g. resistance, current, capacitance, work function, mass, temperature, thickness) is measured with data from the array of individual sensors that is processed using multivariate analysis tools.

3.1. Limitations Of Sensor Arrays For Tethered And Wireless Gas Sensin

In principle, a sensor array can quantify several individual gases in their mixtures (see Figure 7a).[85] However, it was shown that the number of individual gases that can be quantified using any sensor array with the same or different response mechanisms of transducers is at most $2 - 3$.[83–85,87] In practice, this situation is more challenging because of the potential for experiencing high levels of interferences. As a result, even sensor arrays often cannot detect minute analyte concentrations in the presence of elevated levels of interferences, e.g., water vapor in air. Figure 7b illustrates typical reduction in the ability of sensor arrays to detect low concentrations of analyte vapors in the presence of relatively high levels of water vapor interference.[103] Thus, it is critical that new wireless sensors will be not adversely affected by interferences that could be at $10^2 - 10^7$ higher concentrations.

Using identical transducers in the array simplifies its fabrication, while combining transducers based on different principles or employing transducers that measure more than one property of a sensing film[79] can improve the array performance through hyphenation.[104] In conventional, tethered sensor systems, minimizing the number of sensors in an array is attractive because it simplifies data analysis, reduces data processing noise, simplifies sensor material deposition as well as device fabrication.[19,105,106] The significant additional force toward simplifying wireless sensor designs is the limited power budget of wireless devices.

3.2. Data Processing

The two main goals of multivariate analysis are (1) to provide qualitative analysis by extracting response patterns and identifying types of analytes detected by the sensor array or

(2) to provide quantitative analysis of concentrations of one or several analytes. Several excellent reviews detail different multivariate techniques employed for analysis of data from sensor arrays.[19,106–108] There are several available multivariate analysis tools to assess the selectivity of sensor arrays, to provide quantitation of individual components in mixtures, to provide baseline correction and de-noising, to perform unsupervised and supervised pattern recognition, to automatically determine faults in sensor performance, and to determine the number of components in mixtures.[101,109–113] Some representative examples include the use of unsupervised pattern recognition[109,113] analyses on dynamic data using evolving factor analysis (EVA) and multivariate curve resolution (MCR),[111] signal-to-noise improvement using wavelet analysis,[112] sensor response quantitation using locally weighted regression (LWR),[109] and cluster analysis using Euclidean[110] and Mahalanobis[101] distances.

The most widely implemented pattern recognition tool for multivariate signals is known as principal components analysis (PCA). This robust, unsupervised pattern recognition technique is described in detail elsewhere[106] and is used not only in laboratory sensor arrays but also in commercially available systems, e.g. it was used by the vast majority of surveyed manufacturers of sensor arrays (also known as electronic noses).[82,107] PCA operates by projecting the data set onto a subspace of lower dimensionality with removed collinearity. PCA achieves this objective by explaining the variance of the data matrix from the sensor array in terms of the weighted sums of the original inputs from each sensor without significant loss of information. These weighted sums of the original variables are called principal components (PCs). Thus, as discussed below using examples from different sensing materials, visualization of selectivity of sensing materials is often performed using PCA by plotting the scores of the first 2 – 3 PCs.

3.3. Multivariate Sensing

Development of multi-transducer sensor arrays based on different detection principles is gaining popularity[79] because this approach provides a way to enhance response selectivity. Examples of such devices include chemiresistor-capacitor[114] and cantilever-capacitor-calorimeter[115] arrays. Operation of acoustic-wave transducers has been combined with optical,[116] electrical conductivity,[117] and field-effect transistor (FET),[118] detection. Simultaneous measurements of capacitance and resistance of sensing materials were also performed.[119,120] Multiparameter gas sensing was also demonstrated using FETs[121,122] and temperature-programmed sensors.[123]

Impedance spectroscopy measurements were performed on TSM[124] and interdigital[125] sensors to extract several independent parameters. Independent output parameters of individual acoustic-wave transducers were measured, for example, wave propagation velocity and attenuation,[126] series-resonant frequency and resonant admittance,[127] material resistance and resonance frequency.[128,129] A capacitive sensor was described that consisted of a parallel plate capacitor and a quartz crystal oscillator.[130] Passive inductive-capacitive or passive inductive-capacitive-resistive sensors were described that measured multiple unrelated physical quantities.[131] Sensors based on dissipation spectroscopy were described that measured the magnitudes of the high frequency conductivity changes of semiconducting sensing films related to different vapors.[132,133]

An attractive solution for further improving the sensor selectivity was recently demonstrated using a single sensor rather than a sensor array.[33,73–75] This new concept involved the combination of a sensing material that exhibited different response mechanisms to different species of interest with a transducer that had multi-variable signal transduction capability to detect these independent changes. Two exemplary developed scenarios for passive wireless sensing using this sensor platform are depicted in Figure 8. In the first approach, a sensing material was applied onto the resonant RFID antenna (Figure 8a) that altered its impedance

response. In another approach, a complementary sensor resistor and/or capacitor was attached across an antenna and an IC memory chip (Figure 8b) that also altered the sensor impedance response.[71] The impedance response of the sensor was correlated to the concentration of the analyte of interest independent of the presence of high levels of background interferences. Measurement of RFID sensor antenna impedance and readout of the calibration parameters of the sensor (stored in the memory chip) were performed via mutual inductance coupling between the RFID sensor antenna and the pick-up coil of the reader. For selective analyte quantitation using individual RFID sensors, impedance spectra of the resonant antenna were measured (Figure 8c) and several parameters from the measured real and imaginary portions of the impedance spectrum were further calculated. By applying multivariate analysis to the impedance spectra or to the calculated parameters, quantitation of analytes and their mixtures with interferences was performed with individual RFID sensors. Depending on the sensing material, transducer geometry, and type of analyzed gas, these developed RFID sensors demonstrated part-per-million, part-per-billion, and part-per-trillion detection limits. Compared to other sensor technologies (summarized in exemplary references[19,79,105]), these RFID sensors exhibited significantly improved response selectivity to analytes, detected several analytes with a single sensor, and rejected effects from interferences.

4. Integration of Sensing Materials with Transducers

Constructing a wireless gas sensor involves the proper combination of transducer and sensing material to meet the needs of a particular application. The mechanisms of transduction in wireless sensors involve the transduction of the analyte-induced changes of mass, elasticity, and complex permittivity of the sensing film material into the corresponding variation in transducer resonant frequency, capacitance, resistance, and other electrical properties. Different classes of sensing materials with diverse requirements for temperature of operation (accommodating ambient temperature or requiring elevated temperature) and with diverse requirements for power (passive vs. active sensors) are outlined in Figure 9 and can be selected based on the mechanisms of their gas response.

The gas responses of different types of sensing materials that are detailed in this review involve numerous mechanisms such as dispersion, polarizability, dipolarity, basicity, acidity, and hydrogen bonding interactions in dielectric polymers; changes in density and charge carrier mobility, swelling, and conformation transitions of chains in conjugated polymers; swelling and an associated increase in material resistance in carbon nanoparticle-filled polymers; dispersion, dipolarity/polarizability, and hydrogen-bond acidity interactions in fullerenes; charge transfer between analytes and p-type semiconducting carbon nanotubes, gas-induced Schottky barrier modulation at carbon nanotube/metal contacts, and/or polarization of molecular adsorbates on carbon nanotubes and graphene; electron tunneling between metal cores and charge hopping along the atoms of the dielectric ligand shell in monolayer-protected metal nanoparticles; adsorption/desorption, reduction/reoxidation, and bulk effects in semiconducting metal oxides; molecular discrimination of gases by size and shape in zeolites; molecular recognition based on complexation interactions of gases in supramolecular materials due to the presence of organic hosts with enforced cavities; hydrogen bonding, polarization, polarity interactions, metal center coordination interactions and molecular arrangements in metalloporphyrins, metallophthalocyanines, and related macrocycles; and van der Waals interactions of the framework surface, coordination to the central metal ion, and hydrogen bonding of the framework surface in MOFs. The analysis of these diverse mechanisms of materials responses should inspire the discoveries of new basic principles of the transduction of surface/bulk chemistry into measurable electrical signals.

4.1. Synthetic Polymers As Sensing Materials

Synthetic polymers, including dielectric polymers, conjugated polymers, their copolymers, and polymeric formulations are among the most diverse, as well as most mature, classes of sensing materials.[134] In modern wireless sensors, one of the main reasons for their attractiveness originates from their ability to operate at room temperature. Recent reviews are available on polymeric materials for gas sensor applications that highlight sorbing polymers and copolymers, conjugated polymers, and formulated polymeric materials.[34,99–101,135–137] Additional selectivity requirements for wireless sensing have driven researchers to develop specific polymers for these applications. Micro- and nano-patterning of these sensing materials and formation of ultrathin sensing films facilitates enhanced vapor diffusion and response speed when compared to conventional polymeric films.

4.1.1. Dielectric Polymers—Both, high- and low-T_g (glassy and rubbery, respectively) polymeric materials have been employed as sensing materials since the 1960s.[134]. The interactions of polymers with vapors can be described using linear solvation energy relationships (LSERs)[138] and include dispersion, polarizability, dipolarity, basicity, acidity, and hydrogen bonding interactions.[137] Sensing mechanisms of dielectric polymers involve analyte-induced changes in dielectric constant,[139] mass,[46] and elasticity[140] of sensing films as well chemical (e.g. acid/base) reactions between analytes and sensing polymers.[141] Transducers implemented for wireless gas sensing with dielectric polymers include capacitors,[139] and TSM,[46] SAW,[64] magnetoelastic,[45] and RF[71] resonators.

Low-T_g polymers are typically employed for the detection of a large variety of organic vapors. Gas diffusion is more rapid in low-T_g polymers as compared to in high-T_g polymers because of the greater free volume and thermal motion of polymer chain segments.[142] High-T_g polymers expand the range of gases that can be detected with polymeric sensing materials including numerous inorganic gases. Wireless and low power sensors have been demonstrated for humidity detection based on polyimide, cellulose acetate (CA), poly cellulose acetate-butyrate (CAB), poly methyl-methacrylate (PMMA), and polyvinylpyrrolidone (PVP).[35,38,143,144] Examples of polymers used for carbon dioxide sensing include acrylamide/isooctylacrylate[45] and amorphous glassy perfluorodioxole copolymers[46,64,145] Ammonia gas sensitivity has been shown for sensors using a poly(acrylic acid-co-isooctylacrylate) sensing film.[146]

High-T_g polymers with aromatic backbones (e.g., polycarbonates, polysulfones, and polyimides) that contain –$C(CF_3)_2$-(6F) groups in the main chain, exhibit enhanced free volume and gas permeability relative to analogous materials without 6F groups[147] and have been used for low power gas sensing.[148] Similar effects may also be achieved by introducing fluoroalkyl groups as side chains in polymers. Amorphous high-T_g perfluorodioxole copolymers are known to have weak interchain interactions that result in uniquely high vapor solubility coefficients.[149] Random copolymers prepared from tetrafluoroethylene (TFE) and 2,2-bis(trifluoromethyl)-4,5-difluoro-1,3-dioxole (BDD) are widely used for sensors. For example, the TFE/BDD composition of 13/87 mol% (known as Teflon AF2400, see Figure 10a) has been applied for measurements of CO_2 in numerous wireless and other sensors.[46,64,145] Detection limits were demonstrated down to several ppm of CO_2, although humidity remained a significant interferent. Interestingly, the humidity effect was of a different magnitude depending on the transduction principle. In capacitance-based sensors, water exerted a 30 times stronger response than CO_2[145] while smaller water effects were found for SAW transducers.[64] It was suggested to use either a complete water removal before CO_2 measurements[145] or to incorporate a separate humidity sensor to

mitigate this issue.[64] An example of a wireless SAW sensor response to CO_2 at different humidity levels is presented in Figure 10b.

Polymers with low glass transition temperatures have been extensively explored for detection of many classes of volatiles. Representative examples of such polymers that became "classic" benchmark sensing materials against which numerous other new materials have been compared are presented in Figure 11. One of these polymers, polyetherurethane (PEUT, Figure 11a),[86] served as a coating on a capacitance transducer in a passive RFID sensor (Figure 5c) and was used to demonstrate detection of volatile organic compounds and water vapor as shown in Figure 12a. Two variable parameters that modulated the capacitance of the sensor were changes in the dielectric constant and swelling of sensing film. Capacitance of the sensor depended on the dielectric constants of the measured vapors as well as the dielectric constant of the sensing film, with the net capacitance either increasing or decreasing upon vapor exposure. For polyetherurethane sensing films (ε'_r = 4.8), the sensor capacitance increased upon exposures to vapors with the dielectric constants higher than the sensing film (e.g. water (ε'_r = 78.5) and tetrahydrofuran (THF, ε_i = 7.5)) and decreased upon exposure to vapors of lower dielectric constant (e.g. toluene (ε'_r = 2.4)). Thus, Figure 12a illustrates the non-selective measurements of vapors with a single capacitance sensor because the responses of the sensor to water and THF vapors were in the same direction and differed only in magnitude. Therefore, it was impossible to differentiate effects from THF or water vapor produced on this sensor, or to obtain selective responses to toluene or THF in the presence of water vapor. However, a single passive RFID sensor with multivariable response was able to easily discriminate between these three vapors (see Figure 12b–d). The individual F_p, F_1, F_2, F_z, Z_p, Z_1 and Z_2 responses (Figure 12b–c) were analyzed using PCA tools with results shown in Figure 12d. Thus, a single multivariable response wireless sensor reliably discriminated between these three example vapors using a "classic" polyetherurethane polymer.

The capabilities of passive multivariable response RFID sensors with polyetherurethane sensing films were also demonstrated under operation in the presence of high levels of interferences (e.g. water vapor) and found to reject these interference effects. While the individually measured parameters were affected by humidity, the resulting multivariable response of this sensor provided the possibility for signal correction and rejection of the water effect. Figure 13a illustrates the PCA scores plot vs. experimental time of sensor response to variable concentrations of toluene vapor in the presence of changing relative humidity. Critical to the success of correcting for humidity effects with a single sensor, polyetherurethane responded to toluene with the same magnitude in the presence of different concentrations of water vapor. A full correction of toluene response at different RH levels was done using multivariate analysis. The resulting multivariate calibration curves at variable RH were identical (Figure 13b) and provided a new capability to quantify vapors at different RH.

Furthermore, passive multivariable response RFID sensors with polyetherurethane sensing films were tested for their selective quantitation of analyte vapors in mixtures with two interferences. Acetone was selected as a model analyte vapor to be quantitated in mixtures with water and ethanol vapors. Figure 14a illustrates the PCA scores plot of sensor response to variable concentrations of acetone vapor in the presence of changing concentrations of water and ethanol vapors. A full correction of acetone response at different levels of water and ethanol vapors was done using a developed PCA model. The resulting multivariate calibration curves for acetone were not affected by the variable levels of water and ethanol vapors (Figure 14b) and provided a new capability to quantify an analyte vapor in the presence of multiple interferences using only one sensor.

Selection of sensing materials with other dielectric constants (e.g. polyisobutylene (PIB, ε'_r = 2.1), ethyl cellulose (EC, ε'_r = 3.4), polyepichlorihydrin (PECH, ε'_r = 7.4), cyanopropyl methyl phenylmethyl silicone (OV-225, ε'_r = 11), dicyanoallyl silicone (OV-275, ε'_r = 33) as shown in Figure 11b–f) provides the ability to tailor the relative direction of sensing response upon exposure to vapors of different dielectric constant.[139,150] The different partition coefficients of vapors into these or other sensing materials further modulate the diversity and relative direction of the response.

More selective recognition of vapors can be achieved by incorporating tailored functionalities into polymeric sensing materials. One class of materials with enhanced selectivity toward highly basic analytes such as nitroaromatic explosives and chemical warfare agents is based on hydrogen bond acid functionality and has been explored with several types of transducers including capacitors,[151] resistors,[152] microcantilevers,[140] and SAW.[153] These materials generally use fluorination to increase the hydrogen bond acidity of aliphatic or phenolic alcohols, which are incorporated as main chain or pendant groups on low-T_g sensing polymers. An example of selective molecular association between dimethyl methylphosphonate (DMMP, chemical warfare agent simulant) and the hexafluoroisopropanol group in a siloxane fluoroalcohol (SXFA) polymer is illustrated in Figure 15.

Because temperature effects are important at all stages of sensor fabrication, testing, and end-use, an understanding of temperature effects is essential to building robust, temperature-corrected transfer functions for sensor performance in order to preserve response sensitivity, selectivity, and baseline stability. Wireless TSM sensors have been implemented for the evaluation of effects of conditioning of Nafion sensing films at different temperatures on the vapor response selectivity patterns.[154] Nafion-coated TSM resonators were conditioned at 22 – 125°C for 12 h followed by exposure to water, ethanol, and acetonitrile vapors. It was found that conditioning the sensing films at 125°C provided an improvement in the linearity in response to ethanol and acetonitrile vapors, an increase in relative response to acetonitrile, and an improvement in the discrimination ability between different vapors compared to room temperature conditioning.

The combined effects of annealing temperature and plasticizers on performance of Nafion sensing films were studied utilizing passive RFID sensors with multivariable response.[155] Nafion was formulated with five phthalate plasticizers as shown in Figure 16a. Sensing film formulations and control sensing films without plasticizers were deposited onto RFID sensors to form a 6 × 8 sensor array (Figure 16b), which was exposed to eight temperatures ranging from 40 to 140 °C using a gradient temperature heater, and their response stability and gas-selectivity response patterns were evaluated upon exposure to water and acetonitrile vapors. The multivariable responses of these sensors were further examined using PCA (see Figure 16c). Nafion sensing films formulated with dimethyl phthalate showed the largest improvement in response diversity to these two vapors as indicated by the largest Euclidean distance. This RFID-based sensing approach demonstrated rapid, cost-effective, combinatorial screening of sensing materials and preparation conditions.

4.1.2. Conjugated Polymers—Conjugated polymers (also known as intrinsically conducting polymers) have been in laboratory use for gas sensing since 1980s.[156,157] Conjugated polymers are unique synthetic sensing materials because recognition and transduction in these materials can be performed within the same chemical moiety. This facilitates an expansion of the range of detectable analytes and an improvement of their detection limits. Conjugated polymers exhibit several mechanisms of molecular gas recognition including changes in density and charge carrier mobility, polymer swelling, and conformational transitions of polymer chains.[135,158] In addition, the inherent electrical

transport and energy migration properties of intrinsically conducting polymers can also facilitate the enhancement of material[159] and readout[135] sensitivity. Transducers implemented for wireless and low-power gas sensing with conjugated polymers include chemiresistors,[160] capacitors,[161] FETs,[162] and TSM,[163] SAW,[164] and RF[74] resonators. Current developments in conjugated polymers involve the implementation of known polymers in new applications, development of new polymers, and exploration of effects of polymer nano-morphology on the vapor-response selectivity and sensitivity.

Examples of conjugated polymers and their derivatives demonstrated for gas sensing with wireless and low power transducers include polyaniline,[165–167] polythiophenes,[160,162,168] polypyrrole,[164,169] bilypyrroles,[170] and poly(vinyl ferrocene).[163] Conjugated polymers (e.g. poly(fluorene)-diphenylpropane) originally developed for organic light emitting diodes have also been demonstrated with wireless resonant sensors as sensing materials with significantly suppressed humidity effects.[71] Formulation of conjugated polymers with different dielectric and highly conducting additives provides an way to expand the diversity of response selectivity to different gases.[100] Recently, two "classic" conjugated polymers with diverse response mechanisms to different vapors were applied to multivariable RFID transducers to detect these independent changes and to demonstrate the power of passive wireless sensors.[74] Poly(3,4-ethylenedioxythiophene) (PEDOT) was formulated with poly(4-styrenesulfonate) (PSS) and employed for sensing of acetonitrile (ACN), ethanol (EtOH), and water (H_2O) vapors (see Figure 17a–b). The response mechanism of PEDOT-PSS to polar organic vapors involves conformational changes within the polymer chains due to the interaction between the dipoles of the vapors and dipoles or charges on the polymer chains.[171,172] For example, the H_2O vapor response mechanism has been shown to involve dipole molecular effects with the polar PEDOT-PSS formulation.[173] Another "classic" polymer, polyaniline (PANI) was formulated with camphorsulfonic acid (CSA) and employed for sensing ammonia (NH_3) and H_2O vapors (see Figure 17c–d). The response mechanism of PANI-CSA to NH_3 involved polymer deprotonation, while the response mechanism to H_2O involved formation of hydrogen bonds and swelling.[165,174] The calculated detection limits for NH_3 using PANI-CSA were 20 – 80 ppb, which was 6 – 25 fold better than chemiresistor sensors with PANI nanowires.[175] Results of multivariate vapor-selectivity analysis using PEDOT- and PANI-based sensors showed excellent discrimination between different vapors (see Figure 17b, d).[75]

The detection limit of PANI-based RFID sensors has been further improved down to 500 part-per-trillion (ppt) followed by the demonstrations of these sensors for the monitoring of fish freshness. Five RFID sensors were arranged in separate plastic containers with ~ 200-mL headspace and were monitored at once using a multiplexed sensor reader. The headspace for three sensors contained ~ 20 g (each) of salmon filet on a water-soaked liner. Two other sensors served as negative controls with their headspace that was either dry or contained only a water-soaked liner. Figure 18 illustrates results of these experiments at room temperature. Control sensors exposed to low humidity and 100 %RH conditions demonstrated no increase in sensor impedance. Amines that were generated during salmon storage produced a significant increase in sensor impedance due to the deprotonation of PANI as detected in ~ 2 h with these un-optimized sensors.

New conjugated polymers have been synthesized and implemented for VOC detection with detection limits down to the low part-per-million – high part-per-billion range with reduced humidity effects.[71] Poly(fluorene)-diphenylpropane polymer (Figure 19a) was applied onto a multivariable RFID sensor and exposed to different concentrations of trichloroethylene (TCE), water, and toluene vapors (Figure 19b). This response demonstrated that the effect of RH was not only negligible but also was opposite in its response direction. The response magnitude and stability of the sensor were further tested at variable humidity levels as

shown in Figure 19c. This sensing material responded to TCE with a < 1 ppm detection limit.

Several routes to improve the selectivity and stability of conjugated polymers have been identified, including chemical modifications (e.g. side-group substitution of heterocycles, copolymerization, introduction of end-groups), doping, charge compensation for oxidized polymers by incorporation of functionalized counterions, formation of organic-inorganic hybrids, and surface functionalization.[158,176–178] Rational manipulation of polymerization conditions can also be used to control sensor-related properties of conjugated polymers (e.g. molecular weight, monomer connectivity, conductivity, band gap, morphology).[136].

Controlling chain orientation in conjugated polymers can be an important parameter in optimizing vapor-response performance. For example, ultra-high density arrays of polypyrrole nanorods have been fabricated by electropolymerization within a porous diblock copolymer template, demonstrating that nanorod conductivity is much higher than that of thin polypyrrole films, due to the high degree of chain orientation.[169] Controlling surface morphology on the nanoscale level can also be used to affect the performance of conjugated polymer-based vapor sensors.[162,179] It has been found that under certain conditions, regioregular poly(3-hexylthiophenes) self-assemble into highly ordered and partially crystalline structures with improved charge carrier mobility. A field-effect transistor readout was well suited to benefit from the improved field effect mobility in these conjugated polymers. Good contacts between the polythiophene polymer and the metal electrodes of a chemiresistor sensor were provided by combining nanotransfer printing and solventless polymerization.[160] Vapor-based polymerization of thiophene resulted in a highly oriented polythiophene film.

Deposition methods for conjugated polymers can facilitate the formation of different morphologies. For example, ink-jetted films can exhibit significantly different structures compared to films drop-cast from low vapor pressure solvents. The increased drying time of regioregular poly(3-hexylthiophene) polymer solution allowed polymer molecules to self assemble into dense 10 – 30 nm wide nanofibril structures when drop-cast.[179] Morphology of these regioregular poly(3-hexylthiophene) thin film is illustrated in Figure 20a. It was found that the response of these sensing films was strongly dependent on the applied gate voltage so that the source-drain current response was different in sign and magnitude for the same analyte (see Figure 20b). This sensor performance was explained by competing sensing mechanisms, specifically intra-grain effects causing the positive response and grain boundary effects causing the negative response. Thus, the overall response was dependent on the combined effects of both mechanisms originating from the nature of the particular vapor and applied gate voltage of the transducer.[162]

4.1.3. Micro- and Nanopatterning and Thin Films of Dielectric and Conjugated Polymers—Micro- and nanopatterning of polymeric sensing materials and the formation of thin polymeric films have been extensively demonstrated to facilitate enhanced vapor diffusion and response speed when compared to conventional polymeric films.[177,180–182] A variety of techniques have been demonstrated to fabricate features in polymeric materials ranging from 500 nm down to 2 nm feature sizes. Several examples of these techniques are presented in Table 4.[167,180,183–190] Representative examples of nanostructured polymeric materials employed for vapor sensing applications are illustrated in Figure 21.[180,184,191] Several recent reviews provide critical analysis of modern techniques for microand nanopatterning of polymeric materials[192] and electrospinning of polymers.[193]

It is important to note that in addition to the outstanding features of micro- and nano-patterned sensing films, these films can suffer from several practical challenges. In

particular, these structured films may be more prone to surface delamination, dewetting, and other surface effects particularly after exposure to relatively high analyte concentrations and/ or interference vapors. Although film conditioning may reduce these effects, care should be taken to understand the origin of these effects and to have practical technical solutions for these problems. An example of such effects is shown in Figure 22 where a microstructured polydiacetylene-based polymeric film was exposed to ~ 5000 ppm of dimethylformamide (DMF) vapor for 10 min. Upon such relatively short exposure, the original homogeneous, defect-free 24-μm wide patterned lines demonstrated a noticeable dilation and defect formation.[194] Unfortunately, effects from long term deployments in humid or harsh environments are even more pronounced in nano-structured materials. However some of these effects can be reduced by covalent linkage of the polymers to the sensor substrate.[195]

Thin polymeric films formed on a transducer surface can experience dewetting effects leading to modifications of the film morphology and causing sensor drift.[196] An efficient inhibition of dewetting effects of polymer films was demonstrated by changing the surface energy of the substrate, achieved by a careful cleaning of transducer surface, adding nanosize filler particles into film formulations, and inducing surface roughness.[196,197] Dewetting effects can also be utilized to produce useful chemical dosimeters when the morphology of a thin sensing film is altered upon vapor exposure. Figure 23 illustrates effects of methanol exposure on the morphology of an ink-jet printed PEDOT-PSS film.[198] This morphology change has been achieved by exposing the chemiresistor sensor to methanol concentration of 5000 ppm for 30 min.[198] In addition to dosimeters based on chemiresistors with conjugated polymer films[198] other examples include SAW resonators with dielectric polymer films.[196]

4.2. Carbon Allotrope-Based Sensing Materials

From the wide variety of carbon allotropes, amorphous carbon, fullerenes, carbon nanotubes, and graphene have been the most explored as gas-sensing materials. These carbon allotropes serve two main functions in sensing films, acting either as an additive in the sensing film matrix to provide signal transduction or as a main component in the sensing film to facilitate analyte-recognition and provide signal transduction. Amorphous carbon nanoparticles ("carbon black") have been extensively employed for sensing. These carbon nanoparticles serve as the additive in the sensing film matrix which provides electrical signal transduction in many chemiresistor sensors.[21,199–201] Fullerenes and carbon nanotubes are structurally formed from graphene, which is a planar monolayer of sp^2-bonded carbon atoms arranged in a honeycomb crystal lattice. Graphene can be wrapped up into zero-dimensional fullerene structures, or one-dimensional hollow single-wall carbon nanotube (SWNT) and multi-wall carbon nanotube (MWNT) structures, or can be free-standing planar two-dimensional sheets.[202,203] Unlike other semiconducting sensing materials such as nanobelts, nanowires, and nanoparticles, all atoms in fullerenes, SWNTs, or graphene are surface atoms, thus, electron transport through these materials can be efficiently modulated by the environment around these atoms, including adsorbed gas molecules. However, this also means that these materials suffer from non-selective gas responses unless properly functionalized. These 0-D, 1-D, and 2-D structures have been extensively explored for gas sensing as the main component in the sensing film to facilitate analyte-recognition and to provide signal transduction.

4.2.1. Amorphous Carbon Nanoparticles—In the mid 1980s, to combine the diversity of insulating polymeric sensing materials with the simplicity and low power consumption of chemiresistors, insulating polymers were formulated with conductive particle fillers near their percolation threshold.[204,205] The mechanism of response for these sensors involves the swelling of the polymer matrix in the presence of analyte molecules leading to an increase in

film resistance due to the disruption of conductive pathways. Initial reports by Lundberg and Sundqvist[204] and Ruschau et al.[205], in combination with work by Lewis and co-workers on arrays of these conducting polymer composites[206] initiated a new direction in gas sensing.

Significant achievements with conducting polymer composites were demonstrated including ppm detection limits for VOCs,[199,207], ppb detection limits of nerve agent simulants[21] and VOCs,[208] selective recognition of individual vapors in their mixtures,[84,209] discrimination between enantiomeric vapors,[200] and evaluation of effects of interfering vapors.[21] Chemiresistor arrays with conducting polymer composites were commercialized by Cyrano Sciences.[201] Wireless vapor sensors based on conducting polymer composites have been demonstrated based on both passive and battery-operated designs.[210–212] Several reviews provide details of developments in conducting polymer composites.[100,213]

4.2.2. Fullerenes—Fullerenes contain 20 or more carbon atoms bonded in pentagonal, hexagonal and sometimes heptagonal rings, forming roughly spherical molecules. Since the discovery of C_{60} molecules in 1985[214] and their synthesis in 1990[215], fullerenes were extensively explored from fundamental and applied perspectives as summarized in several reviews.[216,217] The high surface area, reactivity, and semiconducting properties of fullerenes led to their investigation as gas sensing and sorbing materials.[218]

Initial studies of fullerenes as sensor materials explored the semiconducting properties of C_{60} films deposited on interdigitated electrodes, where the C_{60} functioned as both sorbent and transducer.[219] Because of their semiconducting properties, fullerenes were studied for detection of reducing gases[219] with experiments at different temperatures (50 – 300°C) that revealed the need for 250°C or higher operating temperatures. Unfortunately, fullerenes also demonstrated significant humidity effects.[219] These humidity effects are well known for other semiconducting sensing materials such as metal oxides.[220–222] Operation at room temperature (adaptable for low-power and wireless sensing) was performed for the detection of polar organic vapors using TSM transducers.[223] Physisorption was the dominant mechanism for the majority of tested vapors while chemisorption of amine and thiol-containing vapors was also observed. The physisorption capabilities of pure fullerenes were thoroughly studied and further modeled using LSER relationships revealing the importance of dispersion, dipolarity/polarizability, and hydrogen-bond acidity interactions of fullerenes with vapor analytes.[224] In evaluating fullerene responses to non-polar vapors, it was found that the strongest responses were for vapors that were good solvents for fullerenes.[225] SAW transducers and LSER relationships were employed for the comparison of sorption of diverse vapors by fullerenes, graphite, and polymers.[226] It was found that fullerenes covalently attached to the SAW sensor surface had selectivity similar to graphite and low-polarity polymers but had lower sensitivities than linear polymers.

To improve selectivity and sensitivity of fullerenes, additional work focused on the functionalization of fullerenes. Sensitivity of fullerene sensors towards polar vapors (e.g. ethanol and water) was enhanced by > 50-fold through the deposition of a metal-fullerene hybrid film containing both C_{60} and aluminum due to higher surface areas and possibly metal-fullerene bonding.[227] UV exposure further enhanced the sensitivity of both pristine and C_{60}–Al hybrid films through the introduction of reactive sites on the C_{60} surface.[227] Sensitivity of C_{60}-based QCM and SAW sensors towards polar and non-polar vapors such as volatile organic alcohols, aldehydes and acids was enhanced by derivatizing the C_{60} with supramolecular host compounds such as crown ethers and cryptands.[228,229] The proposed mechanism of this sensitivity enhancement involved a combination of enhanced chelation by the cryptand/crown ether as well as enhanced reactivity of the C_{60} at the cryptand/crown ether binding site.[228,229] Another approach to generating supramolecular host compounds for vapor sensing with fullerenes involved liquid crystals[230] where rigid linear (thermotropic

liquid crystals) and globular (fullerenes) compounds formed a 1:1 stoichiometry sensing film, disturbing the close packing of both species and thus, forming cavities and diffusion channels.

4.2.3. Carbon Nanotubes—Multi-walled carbon nanotubes and single-walled carbon nanotubes were discovered in 1991 and 1993, respectively.[231,232] Several recent reviews cover the fundamentals of CNTs.[233,234] An example of CNTs is shown in Figure 24. Initial groundbreaking results of using carbon nanotubes for gas sensing demonstrated their extraordinary gas sensitivity,[235,236] and fast[237] and reversible[88] responses. These results inspired further comprehensive investigations of these sensing materials using conductometric detection of electron donating and withdrawing molecules undergoing charge transfer upon adsorption and using capacitive detection of molecules undergoing polarization upon adsorption. Applications of CNTs for sensing have been recently reviewed.[238–240]

CNTs have been extensively studied for sensing of reducing and oxidizing gases, VOCs, CWAs, TICs, and many other gases. The mechanisms of CNT gas response can involve charge transfer between analytes and p-type semiconducting CNTs,[235,237,241,242] gas-induced Schottky barrier modulation at CNT/metal contacts,[243] and/or polarization of molecular adsorbates on CNTs.[88] It was also reported that the dominant mode of resistive detection in nanotube networks changes according to the conductance level (defect level) in the nanotubes.[244]

Carbon nanotubes are also extensively used as conductive additives in vapor-responsive sensing film matrices.[245–247] Low-power transducers with SWNTs and MWNT-based films that are relevant to wireless sensing include chemiresistors,[103,235,245,248–250] capacitors,[88,251,252] FETs,[22,236,237,243] impedance sensors,[241,253,254] and SAW,[255,256] TSM,[257] and radio-frequency and microwave resonators.[242,258–262] With carefully designed wireless transducers, their performance was shown to exceed conventional wired sensors. For example, phase monitoring of reflected waves from a resistive load in a wireless radio-frequency resonator exhibited higher sensitivity than direct resistance measurements.[263] Resistance changes of SWNT films were also employed to modulate backscattered power in chipless RFID sensors.[264]

To measure changes in permittivity and conductivity of MWNTs upon exposure to vapors, highly conductive MWNTs were incorporated into a dielectric (SiO_2) matrix and deposited onto a wireless inductor-capacitor resonator.[258] The interaction of different gases with the MWNT-SiO_2 layer was monitored as changes in the resonant frequency of the sensor. This sensing approach was demonstrated for detection of CO_2, O_2, NH_3, and H_2O vapors. An example response of this sensor to CO_2 is illustrated in Figure 25. Sorption of CO_2 into the MWNTs decreased the effective permittivity of the sensing MWNT-SiO_2 layer since the permittivity of CO_2 ($\varepsilon'_r \sim 1$) was less than the permittivity of MWNTs ($\varepsilon_r \sim 15$). In addition, CO_2 acted as a reducing gas for the p-type semiconductor MWNTs, and injected electrons into the MWNTs, thus decreasing film conductivity. A three sensor array, comprised of the MWNT-SiO_2 sensing film and two reference sensors (a bare sensor and an SiO_2-coated sensor) were used to measure CO_2 in the presence of uncontrolled changes in humidity and temperature.[265]

Simultaneous measurements of capacitance and conductance of a SWNT network (related to permittivity and conductivity, respectively) were performed on SWNTs exposed to dilute individual vapors in dry air.[119] It was found that adsorbed vapors produced rapid responses in the capacitance and the conductance of SWNTs which originated from a combination of two distinct physiochemical properties of the adsorbed vapors, charge transfer and

polarizability. The ratio of the conductance response to the capacitance response ΔG/ΔC was found to be a concentration-independent intrinsic property of a chemical vapor that varied from analyte to analyte (Table 5), useful in assisting in the identification of unknown analytes.

Synthetic methods for CNTs include chemical vapor deposition (CVD),[266,267] laser ablation,[268] arc discharge,[269] and catalytic pyrolysis,[270] and govern the approaches that are used to apply these materials to transducers. In addition, carbon nanotubes can be surface modified, dissolved (dispersed) in different solvents, and solvent-cast onto transducers at ambient temperature. Depending on diameter and chirality, SWNTs can be either metallic or p-type semiconductors, while MWNTs generally demonstrate metallic behavior with electrons as the majority carriers due to the overlap of conduction and valence bands. However, p-type semiconducting MWNTs can also be present among the metallic MWNTs with Schottky barriers between the metallic and semiconducting nanotubes.[241]

Unfortunately, pristine CNTs non-selectively interact with numerous gases, typically with large binding energies, resulting in long gas-desorption time constants. Therefore, sensitivity, selectivity, and reversibility improvements for CNTs can be achieved through modification of gas-nanotube binding energies by introducing defect sites[271] and by doping.[272–274]

Defects along the sidewalls of CNTs can be introduced by various chemical and physical treatments. For example, acid oxidation increases the surface area of CNTs, creates sidewall defects, and simultaneously introduces functional groups at the defects on the nanotube surface.[271,275] Acid treatment can be also combined with plasma treatment for a two-step functionalization[276] or plasma treatment can be implemented as a stand-alone process to create oxygenated groups.[277] Besides enhancing organic and inorganic gas responses, CNT oxidation also promotes its response to polar vapors including water vapor,[257,278] bringing a significant problem of water interference. The mechanism of adsorption of polar molecules onto the oxidized surface of CNTs by dipole-dipole interactions is illustrated in Figure 26.[248]

Functionalization reactions of SWNTs and MWNTs can be broadly categorized as covalent and non-covalent. Covalent functionalization reactions include (1) direct attachment of functional groups to the graphene surface and (2) attachment of functional groups via amidation or esterification of the nanotube-bound carboxylic acid groups at the defect sites.[279–284] Non-covalent functionalization approaches are more diverse and include functionalization with organic molecules of different chain lengths, chain branchings, aromatic configurations, and functional groups;[103,274,285] biomolecules;[286,287] synthetic dielectric polymers;[88,236,245,248] conducting polymers;[277,288] metal nanoparticles;[257,267,289] metal oxide nanoparticles;[275,290] and infiltrated metals.[120,254]

An excellent example of response diversity for SWNTs functionalized with nonpolymeric organic materials has been recently demonstrated.[103] Ten chemiresistors were coated with a random network of SWNTs, functionalized with nonpolymeric organic materials (such as propyl gallate, authracene, tetracosanoic acid, tricosane, 3-methyl-2-phenyl valeric acid, tris(hydroxymethyl)nitro-methane, tetracosane + dioctyl phthalate, tetracosanoic acid + dioctyl phthalate, 1,2,5,6,9,10-hexabrormo-cyclododecane + dioctyl phthalate, and pentadecane + dioctyl phthalate), and were tested as a sensor array for detection of individual, diverse VOCs and water vapor. These VOCs were selected as representative biomarkers for lung cancer, while water vapor was an expected interferent in exhaled breath. The diversity and density of the non-polymeric functional groups were credited for the increase in interactions between the vapor molecules and the sorbent material, as compared

to polymer-based sorbents. These nonpolymeric functional materials were also shown to provide enhanced discrimination between closely related alkanes. The responses of these chemiresistors were attributed to several mechanisms including charge transfer from adsorbed species to the SWNTs, modification of contact work functions, and carrier scattering by adsorbed species. Figure 27 illustrates the scores plot of the PCA model of the sensor array response. Each tested VOC biomarker produced a unique response pattern with the pattern direction in principle component space diagnostic of the biomarker and the pattern height proportional to the biomarker concentration in the vapor phase.[103]

Water significantly affected the response of this sensor array, leading to the need for water vapor removal with a scrubber or preconcentration of analyte vapors. Similar humidity interference effects in bare and functionalized CNTs were also reported[265,291–294] with several proposed mechanisms that include electronic donation to the CNT, hydrogen bonding with oxygen defect sites on the CNT, and the introduction of charge-trapping sites on the CNT through direct water adsorption and/or interaction with the SiO_2 substrate.[239] Several methods for reducing the effects of water vapor were proposed, including the use of air filters coated with chemoselective polymer films[22] and functionalizing CNTs with additives that cancel humidity effect with an opposite resistance response.[295]

While most of the reported CNT-based sensors were tested at room temperature, recent studies of temperature-dependent responses revealed a general trend toward improved sensitivity and response kinetics at elevated temperatures[267,271,296] similar to other sensors based on semiconducting sensing materials such as metal oxide semiconductors.[297]

4.2.4. Graphene—Free-standing graphene was unexpectedly found in 2004[298], starting a graphene `gold rush'.[203] Recent results of using graphene for gas sensing have demonstrated its extreme gas sensitivity[299] and at present attract the attention of a growing number of research groups. Several prominent features of graphene-based materials include the 2-D geometry that enhances the effect of adsorbed species, its impermeability to gases, its metallic conductivity leading to low levels of Johnson noise, and the low levels of crystal defects minimizing 1/f noise.[298–300] Several recent reviews critically analyze the fundamental aspects of graphene[203,300,301] and its applications for sensing.[302,303] Low-power transducers with graphene-based films relevant to wireless sensing include chemiresistors,[304] FETs,[299,305] and SAW resonators[306] and have been employed for different types of gases.

Graphene isolation has been demonstrated using both mechanical[203] and chemical methods.[307] An example of a graphene material is illustrated in Figure 28. Because pristine graphene and bilayer graphene are zero-gap semiconductors, or zero-overlap semimetals,[203], adsorption of any gas with even a minor mismatch in chemical potential results in an easily detectable charge transfer, generating gas response sensitivities higher than in semiconducting materials with larger bandgaps.[302] An example of this high sensitivity to different gases is presented in Figure 29 where graphene monocrystals, obtained by mechanical cleavage of graphite, were exposed to 1 ppm concentrations of NO_2, NH_3, H_2O, and CO.[299] Similar to carbon nanotubes, pristine graphene interacts with numerous gases with large binding energies, causing long gas-desorption time constants. Thus, reversibility of this sensor was achieved by removal of the gas by vacuum, and heating the film to 150°C to desorb the gases. A short UV exposure provided an alternative way to recover sensor response.

Similar to carbon nanotubes, improvements in sensitivity and selectivity for graphene have been theoretically and experimentally studied by modifying the analyte binding energy using several approaches including reducing graphene oxide using chemical and thermal

methods,[304,306,308] inducing defect sites,[309,310] atomic-doping (Al, B, N, S),[310,311] functionalization with organic molecules,[312] coupling with nanoparticles,[313] and surface-contamination control.[305]

Graphene in its reduced graphene oxide form has also been tested as a sensing material.[308,314] It was found that the level of reduction affected both the sensitivity and the level of 1/f noise that originates from fluctuations in carrier mobility or carrier density in solid-state devices. The sensors were able to rapidly detect simulants of the three main classes of CWAs and an explosive at ppb concentrations.[308] In its oxidized state, oxygen functional groups of graphene oxide render it too electrically insulating for use as a conductance-based sensor. While chemical reduction restores the conductivity by removal of oxygen and recovery of aromatic double-bonded carbons, this process does not remove all oxygen groups. Thus, reduced graphene oxide is conductive and has chemically active defect sites available for efficient gas adsorption or surface functionalization. The largest portion of these unreduced groups are carboxyl groups, followed by epoxides and alcohols that can be utilized for covalent chemical functionalization for increased chemical or biological selectivity.

The 1/f noise originates from fluctuations in carrier mobility or carrier density in solid-state devices. In SWNT films, such fluctuations originate from trapped charges in the oxide or from the presence of defects within individual CNTs. The 1/f noise in a graphene bilayer is strongly suppressed compared to CNTs due to the effective screening of charge fluctuations from external impurity charges. Such screening was the origin of the 10–100 fold reduction in 1/f noise in graphene sensors over SWNT-based sensors. The noise level in graphene devices is inversely proportional to graphene film thickness. Figure 30 compares the amount of noise in SWNT responses and graphene devices to 0.5 ppb of DNT.[308] Detection limits obtained using graphene and SWNT sensors were measured in dry nitrogen and compared for several CWA simulants and explosive vapors. Because the 1/f noise levels in capacitance-based SWNT sensors were less than in conductance-based SWNT sensors,[238] capacitance-based SWNT sensors were used for comparison. It was found that graphene and SWNT sensors had the same detection limits for chloroethylethyl sulfide (CEES) and DNT, 0.5 ppb and 0.1 ppb, respectively. The graphene sensor demonstrated a 70 ppb detection limit for hydrogen cyanide (HCN), while the SWNT sensor did not respond even to the highest tested concentration of 4000 ppb. However, detection of DMMP was more attractive with the SWNT sensor because its 0.1 ppb detection limit was 50-fold better than 5-ppb obtained with the graphene sensor.[308] These initial comparitive results stimulated the need for more detailed further studies of relative performance of graphene and CNT sensors.

Similar to the performance of carbon nanotubes and other solid-state sensors, it was shown that operation at elevated temperatures improved the dynamic performance of graphene sensors[304] (see Figure 31). The temporal response was relatively slow at room temperature but was accelerated at elevated temperatures. The sensor response was consistent with a charge transfer mechanism between the analyte and graphene with a limited role for the electrical contacts. Similar to CNT sensors, graphene sensors also suffer from water interference effects.[315]

4.3. Monolayer-Protected Metal Nanoparticles

In the late 1990s, a revolutionary improvement in chemiresistor design was pioneered by Wohltjen and Snow.[316] They employed 2-nm diameter Au nanoparticles functionalized with octanethiol monolayers, forming a 3-D network, and achieved sub-ppm detection limits for non-polar VOCs. Figure 32 illustrates a schematic of such a sensing film with Au nanoparticles and alkanethiol ligand shells and a typical example of sensing Au nanoparticles. These new materials were initially termed colloidal metal-insulator metal-

ensemble (MIME) nanocluster structures,[316] followed by other names including monolayer-protected metal nanocluster interfaces[317] or monolayer-protected nanoparticle sensor films.[318]

This approach replaced not only relatively large (10 – 40 nm) carbon black particles in conducting polymer composites but also provided a well-controlled dielectric ligand shell around each metal nanoparticle. Changing the material and reducing the conductive particle size coupled with the reduction in spacing between the particles resulted in a different operational principle for these new chemiresistors as compared to conducting polymer composites. The mechanism for these new chemiresistors involves *electron tunneling* between metal cores through the dielectric ligand shell and *charge hopping* along the atoms of the dielectric ligand shell. The conductivity is very sensitive to the separation of the metal cores, giving nearly an order of magnitude decrease per angstrom increase in interparticle surface-to-surface separation.[319] Importantly, any process that affects either the interparticle surface-to-surface separation or the dielectric constant of the medium separating the metal cores can be detected by conductivity measurements. However, variations in the interparticle surface-to-surface separation or the dielectric constant of the medium separating the metal cores upon exposure of sensing films to different analytes or concentrations thereof may have the opposite effect on sensor conductivity. Thus, the conductivity response of chemiresistors can be either positive or negative depending on the rigidity of the linker, analyte concentration, and analyte dielectric constant.

A tremendous amount of work has been done in the area of these sensing materials with several recent reviews that detail conductivity measurements.[221,320,321] Although conductivity measurements are very attractive for low-power wireless sensors, other detection modalities have also been implemented with these materials.

The desired sensor response diversity is generally achieved by designing different ligands surrounding the metallic cores. Organic ligands that have been applied to metal (Au, Ag, Au/Ag alloys, Pt, Pd) nanoparticles include organothiol derivatives, dendrimers, organoamines, mercaptocarboxylic acids, and others.[319,322–327] These ligands can be broadly divided into two classes. One class constitutes soft linkers that change their length as a function of the amount of sorbed vapor. With these linkers, film swelling upon analyte exposure causes an increase in the film resistance with increased interparticle surface-to-surface separation. However, the dielectric constant of these films can also either increase or decrease depending on the dielectric constant of the analyte vapor causing resistance changes. The other class of ligands constitutes more rigid linkers that restrain swelling of sensing films and boost the effects of analyte-dependent changes of the dielectric constant of the film. Examples of soft and rigid linkers utilized with metal nanoparticles are presented in Figure 33.[328–330]

While general knowledge about the functional groups of organic linkers to create networks of metal nanoparticles is available,[331] the quantitative effects of different gases on the sensitivity and selectivity of organic linkers in metal nanoparticle networks are difficult to rationally predict based on existing knowledge. Thus, significant work has been done to explore the gas responses of metal nanoparticles networked with different types of linkers. Introduction of different chemical groups in aromatic organothiol linkers on 3 – 6-nm Au nanoparticles has been explored as illustrated in Figure 34.[319] The observed diversity of vapor responses for these chemiresistors demonstrates the importance of the nature of the functional group for controlling the relative strength of particle-particle and particle-solvent interactions.

To assess the performance of monolayer-protected metal nanoparticles in sensing films, it is important to compare the responses of these films when measured using different transducers. Such a comparison should not only provide insight into the relative contributions of variations of the interparticle surface-to-surface separation and the dielectric constant of the sensing film on sensor response but also should provide a critical comparison with already developed materials, and should provide guidance for the design of improved films. TSM transducers are commonly employed for reference measurements of vapor uptake by metal nanoparticle networked films.[332–334] In one evaluation, different types of interactions were explored between vapors and networked metal nanoparticles with four ligands chosen to provide different degrees of van der Waals force (*n*-octanethiol, C_8SH ligand), polarizibility (2-naphthalenethiol, NAP ligand), polarity (4-methoxythiolphenol, MOP ligand) and hydrogen bond acceptance (2-benzothiazolethiol, MBT ligand).[325] The responses of these ligands coupled to nanoparticles were investigated using ten diverse organic vapors and measured by both chemiresistors and TSM sensors with the goal of establishing a correlation between the chemical structure of a ligand shell of the networked metal nanoparticles and vapor response. Comparison of responses of sensing materials obtained with chemiresistors and TSMs revealed that chemiresistors had much higher sensitivity (Table 6) but with a less varied response pattern between different vapors.[325] Another study also indicated that the chemical diversity of monolayer-protected metal nanoclusters was more limited as compared to sorptive polymers.[335]

In a detailed study of the responses of C_8SH-capped metal nanoparticles to 25 vapors, a strong correlation between the responses of TSM and chemiresistor sensors was observed and explained by the predominant dependence on the partition coefficient of C_8SH ligand to these vapors. The fractional resistance changes of the chemiresistors were much larger than the fractional mass changes of the TSM sensors. Furthermore, detection limits obtained with chemiresistors were significantly lower than those for TSM sensors, (Table 7) explained by the more efficient signal transduction.[318] Significantly lower detection limits for chemiresistors as compared to SAW sensors were also reported.[317]

The effects of diverse vapors such as dimethyl methylphosphonate (DMMP) and toluene have been explored with a number of Au clusters (see Figure 35[336]) with the goal of further understanding the response mechanisms and exploring the potential to enhance sensor selectivity. The response of nonpolar toluene vapor showed only an increase in resistance (see Figure 35) for different films as a result of film swelling with the magnitudes of response determined by the toluene partition coefficient between the gas and sorbent phases. The DMMP vapor has strong hydrogen bond basic property[337] and showed more diverse interactions with studied nanocluster films. DMMP reaction with a Au:C_5COOH nanocluster film produced a large decrease in resistance due to the increase in the intercluster medium dielectric constant by to the formation of hydrogen bonds between the P=O moiety of DMMP and the protons of the COOH acid dimers in the film (see Figure 36a). The interaction of DMMP with a Au:HFIP film (HFIP = hexafluoroisopropanol) produced the inverse effect (Figure 36b) because two bulky –CF_3 groups sterically hindered the formation of any significant amount of intracluster dimer-like hydrogen bonding. The DMMP adsorption resulted in the formation of hydrogen bonds between P=O and the hydroxyls of HFIP with decreased intercluster hydrogen bonding which results in a decrease in the dielectric constant of the intercluster medium. This was reflected in a significant increase in the film resistance as shown in Figure 35.

Another class of organic ligands explored for use with metal nanoparticles are organic dendrimers[338] which are of interest because of their high solubilities, host–guest interactions with vapors, and their generation-controlled size that is favorable for metal networks. The combination of Au nanoparticles with polyfunctionalized dendrimers enables fabrication of

sensing films with controlled thickness and inter-particle separation using layer-by-layer self-assembly. Au nanoparticle/poly(propylene imine) (PPI) composite films comprising dendrimers of several generations (G1 – G5) were prepared via layer by layer self-assembly resulting in 19 – 32 nm thick films.[328]. An example of a PPI G3 dendrimer is illustrated in Figure 33a. The effects of the dendrimer size on selectivity and sensitivity to different vapors were studied using three vapors from different classes including hydrophobic hydrocarbons (toluene), amphiphilic H-bonding organic compounds (1-propanol), and polar H-bonding inorganic compounds (water). The resistivity of G1 – G5 films increased exponentially with increasing dendrimer generation because the size of the dendrimers controlled the separation between neighboring nanoparticles and, thus, the tunneling distances for charge transport. All films showed an increase in resistance upon vapor exposure (see Figure 37 for 5000 ppm exposures for each vapor) demonstrating that the dominant component of the sensing mechanism was swelling of sensing films. While the sensitivity to toluene and 1-propanol increased with dendrimer generation, the sensitivity to water vapor was almost independent of the dendrimer size, possibly because the molecular structure of the dendrimers provided different sites for interactions with different solvent molecules. Toluene and 1-propanol molecules were preferably "solvated" within the interior structure of the dendrimers and, therefore, the sensitivity for these solvents increased with the size of the dendrimers. The interaction sites for water sorption were the primary amino groups at the surface of the dendrimers. Concentration of these amino groups in the film was independent of the size of the dendrimers, leading to the similar sensitivity to water in G1 – G5 dendrimers.

Chemiresistors with diverse types of monolayer-protected metal nanoparticles were recently assembled into a nine-sensor array and tested for their response to simulated and real breath samples of lung cancer patients and healthy volunteers.[339] Monolayer capped 5-nm gold nanoparticles were fabricated with nine types of capping layers including dodecanethiol, decanethiol, 1-butanethiol, 2-ethylhexanethiol, hexanethiol, tert-dodecanethiol, 4-methoxy-toluenethiol, 2-mercaptobenzoxazole, and 11-mercapto-1-undecanol. This sensor array was able to discriminate between healthy and cancer breath samples as shown in Figure 38.[339] Most recently, a more advanced sensor array was developed for detection of lung, breast, colorectal, and prostate cancers from exhaled breath with 14 types of capping layers.[340]

At present, humidity effects on Au films have been investigated only in a limited number of reports,[324,341–343] although for practical applications of Au films chemiresistors, water vapor is one of the most significant interferents because of its abundance. In their pioneering work, Wohltjen and Snow showed that their Au:C_8SH sensor film did not respond to humidity as tested up to $P/P_0 = 0.6$ (~ 60% RH).[316] Since then, this octanethiol film and some other films have been tested for water response by several groups, most often as one of the analytes and less often as a potential interferent. For example, it was shown[342,343] that at humidities above 30 – 40 %RH, conductivity and capacitance of the sensors varies exponentially with humidity. Figure 39a illustrates the humidity-dependent response of a Au:C_8SH coated resistance – capacitance sensor. The humidity not only affected the baseline of the sensor response, but, unfortunately, reduced the sensitivity of the sensor to other vapors as tested with Au:C_8SH, Au:2-phenylethanethiol, and Au:1,6-hexanedithiol films.[342,343] Figure 39b illustrates humidity effects on the decrease in sensor sensitivity to diverse vapors. The largest effect of humidity was observed in acetone sensing (~40% signal loss at 60%RH) and the smallest effect was seen for toluene and ethyl acetate sensing (~12% signal loss at 60%RH). It was suggested[342] that such humidity dependence could be in part, due to residual tetraoctylammonium bromide (TOABr) present in films preparared by the Brust method[344] and due to aging of films over several months of storage under ambient conditions.

The ability of passive multivariable RFID sensors to operate with mixtures of water vapor and VOCs and to detect trace concentrations of VOCs has been evaluated with Au:C$_8$SH nanoparticle-based films.[71] An experimental design of a test cycle (see Figure 40a) included evaluation of sensor response to different concentrations of individual vapors (water and toluene), followed by exposure of the sensor to toluene at a single concentration with increasing concentrations of water vapor, and followed by re-testing of sensor response to different concentrations of individual water and toluene vapors. This experimental design provided the ability to assess sensor stability at variable RH levels and the magnitude of possible signal loss after humidity exposure. Results of these experiments are presented in Figures 40b–c demonstrating the ability to separate effects of water and toluene vapors based on the individual Fp and Zp responses of the sensor, respectively. This sensing material responded with the same magnitude to toluene at variable humidity levels with the detection limit of ~ 850 ppb.

Such passive multivariable response RFID sensor with the Au:C$_8$SH nanoparticle-based film was further tested for their selective quantitation of analyte vapors in the presence of multiple interferences. Similar to studies with PEUT sensing films (see Figure 14), acetone was selected as a model analyte vapor to be quantitated in mixtures with water and ethanol vapors. Figure 41a illustrates the PCA scores plot of sensor response to variable concentrations of acetone vapor in the presence of changing concentrations of water and ethanol vapors. A developed PCA model provided a full correction of acetone response at different levels of water and ethanol vapors removing the effects of water and ethanol vapors (Figure 41b). The sensor with Au:C$_8$SH sensing film provided ~ three-fold improvement in the standard error for the prediction of acetone as compared to the sensor with a PEUT sensing film.

The fundamentals of long-term stability in Au nanoparticle networks are becoming better understood. In one study, the long-term stability (12–16 months) of Au nanoparticles capped with C$_6$SH and TOABr ligands was explored by measurements of I–V curves and vapor responses.[326] Upon storage, C$_6$SH Au films showed a 2-fold decrease in baseline resistance while Au films with TOABr ligands demonstrated almost no changes in baseline resistance. Response magnitude to toluene vapor was decreased by 60% and 20% for Au:C$_6$SH and Au:TOABr films, respectively. The loss of performance of Au:C$_6$SH films was possibly due to sulfur oxidation, that occurs over time in air for thiols on Au.[326] Possible mechanisms for the loss of sensor performance include reactions of thiols with atmospheric ozone or with shorter-chain compounds leading to greater instability.[317]

The broad knowledge of susceptibility of thiolate SAM systems toward decomposition[331] is relevant to studies of nanoparticles with thiol shells. To identify aging processes under different storage conditions, films comprising 1,ω-alkyldithiol-interlinked (1,9-nonanedithiol and 1,16-hexadecanedithiol) nanoparticle networks were studied using elemental (XPS), morphological (SEM), and vapor-response analyses.[327] Under storage in air, oxidation of thiols dominated the degradation mechanisms including alkylsulfonate desorption and particle coalescence. However, under inert storage conditions in argon, the film morphology changed without detected oxidation. For nanoparticles interlinked with 1,ω-alkyldithiols, three possible sorption sites within the film can include hydrophobic and hydrophilic parts of the organic matrix for respective sorption of hydrophobic and hydrophilic vapors and the particle surface for sorption of gases. Responses of the AuC$_{16}$ networks to 5000 ppm toluene, 1-propanol, water, and 50 ppb hydrogen sulfide, before and after storage demonstrated changes in sensitivity and selectivity for the tested vapors. However, as expected, storage in argon resulted in smaller changes compared to storage in air. In studies aimed to reduce degradation of thiolate SAMs in ambient conditions, it was shown that nanostructured gold had higher resistance to SAM degradation and increased

electrochemical stability against thiolate desorption in relation to polycrystalline preferred orientation Au(111). The increased stability was related to the presence of a large number of defects, such as adatoms, vacancies, and steps where the thiolate binding energy is stronger than on terraces.[345]

The effects of reducing the size of the interdigitated electrode have been demonstrated for applications with monolayer-protected clusters of metal nanoparticles.[346–348] Under constant operating voltage, the absolute sensitivity of the chemiresistor is independent of geometric scaling, however, the effects of contact resistance tend to increase in the smallest devices.[346] While reductions in sensor size may increase the noise floor when performing measurements in the DC regime, operation of the sensors under AC conditions with filtering reduced the noise. Microdispensing thick sensing films onto interdigitated electrodes, rather than monolayer films, decreased the noise by five orders of magnitude.[347]. Although these films were non-uniform, their low noise performance made them preferable over the uniform monolayer films. It was also shown that 3-D layers of such nanoparticles significantly enhanced the amount of sorptive material on the surface as compared to 2-D monolayers, thus further enhancing the sensor sensitivity.[335]

4.4. Other Sensing Materials

In addition to the sensing materials detailed above, there are numerous other types of materials that are also applicable to wireless sensing. These materials include semiconducting metal oxides,[221,349–355] zeolites,[91,92] porphyrins,[93,94] cavitands,[96,356] ionic liquids,[357,358] liquid crystals,[359–361] crown ethers,[362–364], enzymes,[365,366] polysilsesquioxanes,[367,368] MOFs,[97,98] and others that can operate at room temperature. Several types of these materials are assessed below.

4.4.1. Semiconducting Metal Oxides—Semiconducting metal oxide gas sensors are one of the most advanced sensor types with pioneering reports on their gas sensitivity at elevated temperatures going back to the 1950s.[369,370] With more than 50 years of research, numerous metal oxides have been studied ranging from single-metal oxides (e.g. ZnO, CuO, CoO, SnO_2, TiO_2, ZrO_2, CeO_2, WO_3, MoO_3, In_2O_3) to perovskite oxides structures with two differently sized cations (e.g. $SrTiO_3$, $CaTiO_3$, $BaTiO_3$, $LaFeO_3$, $LaCoO_3$, $SmFeO_3$) that respond to reducing or oxidizing gases by their resistance change.[297,350] Depending on the type of metal oxide and employed dopants, operating temperatures for these sensors typically range from 200 to 1100°C leading to different gas-response mechanisms including adsorption/desorption, reduction/reoxidation, and bulk effects.[371]

The majority of semiconducting metal oxide sensors operate by the measurement of resistance changes.[297,350] However, there are several examples of mixed metal oxide compositions (e.g. CuO-$BaTiO_3$, ZnO-WO_3) that exhibit changes in permittivity, providing the ability to perform capacitance measurements using semiconducting metal oxides.[66,372–374] A careful selection of of mixed metal oxide SnO_2–TiO_2 compositions was recently demonstrated to significantly reduce (but not eliminate) humidity effects.[375]

Gas sensitivity in semiconducting metal oxide sensors is enhanced by forming 0-D, 1-D, 2-D, and 3-D nanostructures with high surface areas including nanoparticles, nanowires, nanotubes, nanobelts, nanosheets, and nanocubes.[353] Micro- and nano-structured sensing films have been fabricated using numerous methods including self-assembly, templating, and others.[353,376–379] Several excellent reviews summarize developments in semiconducting metal oxide gas sensors.[352–355]

Typical semiconducting metal oxide sensors do require a considerable amount power for the operation of their micromachined heaters (e.g., 5 – 170 mW for operation at 450°C[40] and

0.3 – 15 mW for operation at 300 °C[39]) making wireless sensing using these transducers difficult even with an on-board power supply. However, recently, the Joule self-heating effect for semiconducting metal oxide nanowire gas sensors has been demonstrated[380] enabling remotely powered wireless semiconducting metal oxide sensors. The small thermal mass and small thermal losses from the nanowire to its surroundings allow the sensor to operate without a dedicated heater. One such sensor based on the Joule self-heating effect employed SnO_2 nanowires (70 – 90 nm diameter, 5 – 15 μm length) and consumed only 20 μW to operate at 300 °C.[41]

For operation in high temperature environments with semiconducting metal oxide sensors, instead of having a dedicated heater, it is possible to utilize the high temperature of the measured environment itself. This approach further permits the design of passive wireless sensors based on semiconducting metal oxides. Realization of this concept has been demonstrated with two passive wireless chemical sensors where resistivity changes in $BaTiO_3$-La_2O_3 at 675°C were correlated with CO_2 concentrations and permittivity changes in ZnO-WO_3 at 600°C were correlated with NO concentrations.[66]

A limited number of semiconducting metal oxide sensors have also been reported operating at room temperature.[101,381,382] It was recently shown that the room temperature response mechanism in semiconducting metal oxide gas sensors is mediated by a thin layer of adsorbed water where the semiconductor materials act as pH sensors.[383] It was suggested that in this adsorbate-limited state, the gas sensitivity should be limited to molecular species that can easily dissolve in this thin layer of adsorbed water and subsequently undergo electrolytic dissociation.

4.4.2. Zeolites—Zeolites are crystalline nano- and mesoporous materials formed by the 3-D combination of tetrahedra TO_4 (T = Si, Al, B, Ga, Ge, Fe, P and Co) bonded by oxygen atoms.[91] The diversity of zeolites (more than 40 natural and 200 known synthetic zeolites) is provided by the T–O–Si links that form the framework of cages and channels of distinct constant sizes unaffected by vapor interactions. These T–O–Si links are also responsible for zeolites' molecular discrimination by size and shape and utility for molecular sieving.[91] In sensing applications, zeolites are employed either as sensing materials with capacitance, mass, calorimetric, resistive, or impedance readouts[384–390] or as membrane filters for selectivity improvement.[391–393] Recent reviews detail modern synthetic approaches,[394,395] molecular simulations of shape selectivity,[396] and sensing abilities of zeolites.[91,92]

The initial structure of zeolites can be controlled by tuning the tetrahedral building units (TO_4) and by the use of structure-directing agents.[397] Sensing properties can be further modified in post-synthesis steps by cation exchange and by incorporating catalytically active metal clusters, organic molecules, and polymers.[92,389] Partition coefficients of zeolites to VOCs were demonstrated to significantly exceed those of amorphous polymers.[398]

Depending on the type of detected gases and the types of surface modifications, zeolite-based sensors operate either at elevated (300 – 600 °C)[399,400] or at room temperature.[384,385,389] Operation of zeolites with a temperature programmed desorption[390] and with a high temperature activation and room temperature detection[401] provides additional sensing selectivity.

4.4.3. Supramolecular Materials—The development of new sensing materials with molecular recognition abilities that exceed the selectivity available by sorption into amorphous phases has been under pursuit for several decades.[96,402] Sensing films based on cavitands (e.g. cyclodextrins, calixarenes, resorcinarenes, cucurbiturils, chorands, etc.) promise responses with improved selectivity due to the presence of organic hosts with

enforced cavities whose rigid organization vastly enhances their ability to selectively bind guests.[356,403] However, selectivity response patterns of cavitands to small molecules can be similar to common amorphous polymers[404] indicating that cavitand sensors can respond not solely only to molecules with an ideal fit in the cavity but also to sorbed molecules occupying both intracavity and intercavity sites.[96,405–407] Nevertheless, the presence of a preorganized cavity in cavitands does promise an advantage in sensitivity compared to amorphous polymers, especially if applied to the sensor in multilayers.[406]

In applications of molecular receptors for gas sensing, there are well known competing phenomena including specific (complexation) interactions and nonspecific (dispersion) interactions in the sensing layer.[96] Phosphonate cavitands represent one class of molecular receptors that have been studied in detail to understand the factors that lead to selective binding using alcohols as model analyte vapors. These factors include: (1) simultaneous hydrogen bonding with a P=O group and CH–π interactions with the π-basic cavity, (2) a rigid cavity that provides a permanent free volume for the analyte around the inward facing P=O groups, essential for effective hydrogen bonding, and (3) a network of energetically equivalent hydrogen bonding sites available to the analyte.[95] The nonspecific dispersion interactions can be much stronger than the specific interactions and can depend on the chain length of sensed alcohols and their concentration.[408] Recently, it was shown that vacuum-evaporated phosphonate cavitands had a dominating intracavity complexation at low concentrations of ethanol vapor.[409] Quinoxaline cavitands solution-deposited onto a Si surface as a monolayer demonstrated a totally suppressed non specific extracavity adsorption of VOCs as compared to thicker sensing films.[410]

Clathrate materials that crystallize in phases with channels or cavities containing solvent molecules can also be used as sensing materials.[411–414] It was shown that these materials were ~100 times more sensitive to VOCs than polymer-coated TSM devices at low concentrations.[412]

In metalloporphyrins, metallophthalocyanines, and related macrocycles, gas sensing is accomplished either by π-stacking of the gas into organized layers of the flat macrocycles or by gas coordination to the metal center without the cavity inclusion.[96] Metalloporphyrins provide several mechanisms of gas response including hydrogen bonding, polarization, polarity interactions, metal center coordination interactions and molecular arrangements.[93] Porphyrins molecules can be also assembled into nanostructures using several methods.[415–417] Several reviews are available analyzing the performance of porphyrins and cyanines in gas sensing.[93,94,417,418]

MOFs, also referred to as porous coordination polymers (PCPs),[419,420] are relatively new highly porous hybrid organic-inorganic supramolecular materials comprised of ordered networks formed from organic electron donor linkers and metal cations.[97,420,421] In these materials, the specific recognition of gases is accomplished through several types of interactions that include van der Waals interactions of the framework surface with gases, coordination of the gas molecules to the central metal ion, and hydrogen bonding of the framework surface with gases.[421–423] The unusually high surface area (more than 3000 – 6000 m^2/g)[424,425] and the ability for tuning pore size, chemical functionality, and post-synthetic modifications make these materials attractive for gas sensing using different transduction principles. Transducers explored with MOF sensing materials range from impedometric[426] to gravimetric,[427,428] optical,[429,430] and mechanical.[431] Compared to crystalline and microporous fully inorganic zeolites, MOFs have much broader synthetic flexibility facilitated by the coordination environment provided by the metal ion and the geometry of the organic "linker" groups.[97] Several recent reviews summarize the gas adsorption isotherms and gas sensing applications of MOFs.[97,98,420,423]

5. Wireless Sensor Networks

Wireless sensor networks could be considered as a next step of the implementation of individual wireless sensors.[432] In a WSN, individual sensors are typically arranged into wireless sensing nodes, also known as motes, (see Figure 3) with the key hardware (long-lifetime battery or energy harvesting source, simple signal conditioning components, low-power processor) and software (small needed memory, computational capacity, high modularity) requirements for individual nodes.[25,433] Sometimes but not always, application-specific requirements for individual gas sensors in a WSN may include high analyte selectivity and high sensitivity.

The arrangement of individual wireless sensors into a distributed network brings new opportunities as described in section 5.2, but not without significant challenges to be solved first. The general challenges of WSNs for gas and physical sensing include power consumption of individual sensors and handling of massive heterogeneous data from the WSN. The inadequate long term stability of many research prototypes of gas sensors further prevents their reliable applications in WSNs. Thus, examples of gas sensor applications in WSNs include commercially available CO_2, CO, NO_2, SO_2, and VOC sensors[434–437] that often consume significant amounts of power (30 – 50 mW and up to 400 mW per sensor)[436,438] and simple humidity sensors with low power consumption.[434,435]

5.1. Stability Issues of Individual Sensors

Understandably, numerous published results do not report details on the long term stability or instability of sensing materials. This situation arises from the nature of projects that may focus only on the initial discoveries of sensing materials such as sensitivity,[235,299] response/recovery times,[88] or new transduction principles for gas sensors.[113,439] Nevertheless, it is critical to bring attention early to the possible challenges in materials stability. Some researchers provide information about materials instabilities,[317,326,327,412,440,441] serving the sensing community with important data and knowledge that truly facilitate decision-making in the broad area of sensor research.

A summary of representative reported results on the long term stability of diverse sensing materials is provided in Table 8.[83,176,317,326,442–445] As shown in this table, often, materials stability is evaluated either as the change in the baseline material property or the change in vapor sensitivity over time. Unfortunately, analysis of the stability of the sensor response pattern to several expected analyte and interference vapors is reported only rarely[83,317,441,446] because of the time and resource requirements to generate such data and the needed detailed knowledge about gas composition in an intended end-user application. However, this information presents the most value for the assessment of practical sensor implementations[441,446] and for appropriate multivariate data analysis algorithms that are most immune to long-term drift effects.[83]

5.2. Opportunities for Wireless Sensor Networks

The opportunities for WSNs with gas sensing nodes originate from the synergistic combination of new data-generation and processing concepts with new sensor-integration concepts. Representative examples of recent developments in these areas are illustrated in Table 9.[432–435,437,447–451]

Sensors arranged as networks can significantly benefit from novel data-generation and processing concepts currently unavailable for individual sensors. Three main aspects of these advantages can be summarized as (1) the ability for efficient sensors communications, (2) improvement of detection accuracy through data fusion, and (3) opportunities for automatic re-calibration of individual sensors on the network.

The broad opportunities for WSNs originate not only from the diverse applications as previously summarized[25,432] but also from the capabilities based on concepts of integration of individual sensors to form sensing nodes in a WSN. Indeed, a stationary or mobile origin of sensing nodes would dictate the diversity of application scenarios for a WSN.[448,450,451] Significant advantages in the reliability and accuracy of a WSN performance could be achieved upon an integration of sensing nodes into a component or a system that already has a maintenance schedule that could be matched to a maintenance schedule for sensing nodes.[435,448]

As a result of developments in the data-generation/processing and sensing node-integration concepts, the application concepts for WSNs can be broadly described as those that rely on stationary sensing nodes for mapping of chemical sources,[452,453] mobile sensing nodes for dynamic localization of chemical sources,[435,437] real-time chemical condition monitoring of high-value goods and their associated storage conditions,[454,455] and combination of sensing nodes with an intelligent inventory management.[456]

6. Summary and Perspective

Wireless and other gas sensors do not compete for resolution and selectivity with sophisticated high-end laboratory instrumentation that is designed to identify and quantify unknowns down to ppb-ppt levels in complex mixtures containing hundreds or thousands of volatiles. For example, detection of hundreds of individual unknowns in their mixtures at trace concentrations is the goal of the Panoptic Analysis of Chemical Traces program that is based on the orthogonal high-resolution analytical systems.[457] For comparison, a high-end laboratory instrument based on two-dimensional gas chromatography (GC × GC) followed by high-speed time-of-flight mass spectrometry (ToF-MS) detects ~ 1300 discrete volatiles in breath at a signal-to-noise of at least 100; a conventional GC system can detect ~ 200 peaks of compounds or their unresolved mixtures; and a sensor array can detect low resolution signatures of biomarkers if water vapor is partially removed.[15,103]

6.1. Competing With Other Fieldable Microanalytical Instruments

Gas sensors compete with other fieldable microanalytical instruments. Over the recent years, these instruments have become more portable, more energy-efficient, and less expensive.[458] For example, advances in miniaturization and ionization sources in mass spectrometry are bringing micromachined mass-spectrometry (MS) devices to the point of operating at ambient atmospheric pressure without vacuum pumps.[459] Advances in miniaturization in ion mobility spectrometry (IMS) are bringing these devices to form factors and power requirements similar to conventional packaged sensor systems.[460,461] Advances in miniaturization in gas chromatography are establishing the ability to detect and quantify 10 or more volatiles in less than 1 min with ppb detection limits in cell-phone-sized micro-gas analyzers (MGAs).[462,463] Advances in direct spectroscopic sensing that do not require a sensing material to generate the signal, are utilizing new physical principles and engineering designs to dramatically reduce the volume of analytical gas cells, improve detection sensitivity, and reduce device size.[464,465]

While we and other proponents of gas sensor technologies continue to bring the old arguments of low sensor cost and small size, these arguments, eventually, become less valid when comparing sensors with state-of-the-art, fieldable microanalytical instruments based on competing detection concepts. However, newly developed sensors continue to successfully compete with other types of microanalytical instrumentation based on certain performance parameters. For example, a significant advantage of sensors over IMS devices is in sensors' abilities to make quantitative measurements vs. the qualitative measurements done by IMS devices. An advantage of sensors over MGA devices could be in the

continuous nature of measurements performed with a sensor vs. periodic measurements done with MGA devices. Yet another advantage of wireless sensors is in their ability to protect the main readout/display instrument from environmental exposures (e.g. gases, temperature fluctuations) by exposing only a wireless transducer portion of the system to potentially dangerous or caustic environments. Multivariable wireless sensors provide an opportunity for simultaneous measurements of chemical (e.g. gas concentrations) and physical (e.g. temperature) parameters.

6.2. Reaching Beyond The "Valley Of Death"

To better understand the steps that are needed to bring a new sensor idea from a laboratory to practical application where it must outperform existing sensors and microanalytical instruments, it is useful to describe the sensor development process using technology readiness levels (TRLs) as shown in Figure 42. The concept of TRLs is an accepted way to assess technology maturity.[466] These TRLs provide a scale from TRL 1 (least mature) to TRL 9 (most mature) that describes the maturity of a technology with respect to a particular use. Sensor development requires several phases including discovery with initial observations, feasibility experimentation, and laboratory scale detailed evaluation (TRLs 1 – 4), followed by validation of components and the whole system prototype in the field (TRLs 5 – 6), followed by testing of the system prototype in the operational environment (TRL 7) and tests and end-use operation of the actual system (TRLs 8 – 9).

Understandably, numerous publications from academic and other teams do not go beyond laboratory testing with individual gases diluted with a dry carrier gas and reporting short-term detection limits. These initial experiments are critical because they explore innovative ideas in sensing materials, transducer designs, data analysis, sample handling, and packaging of sensor systems, and bring new sensing concepts up to TRL 2 – 3. Although initially very progressive and important, without further laboratory testing, for at least selectivity towards individual vapors, vapor mixtures with interfering gases, temperature effects, long term stability, and some others, these numerous developments often rapidly pile up in the "valley of death"[467] where they lack an additional driving force to advance into higher TRL levels. The lack of follow-up with more detailed laboratory and field tests after initial breakthrough results, is clearly the basis of most of R&D shortcomings and explains why, in spite of so many excellent laboratory results, the choice of sensors for real applications is still rather limited.[351,468] Thus, putting the sensor design phases into the broad perspective of TRLs should provide important guidance for more efficient sensor development. Over the years, representative examples of sensors that have matured for practical applications include those based on metal-oxide semiconductors,[469] dielectric polymers,[470] colorimetric films,[471] chemiluminescent films,[472] and conducting polymer composites.[201]

6.3. System Approach For Development Of Wireless Gas Sensors

Using the system approach for wireless gas sensor development, it is critical to identify and analyze all risks that could lead to a failure in making a practical sensor. This analysis should be followed by focusing on the most significant risk, identifying the mitigation actions to reduce or eliminate this risk, and performing these actions. After this major risk has been reduced to an acceptable level, the next biggest remaining risk is to be addressed, and so on. If a wireless gas sensor is to be designed to operate in complex environments for a period of time without manual maintenance, an initial list of development risks could include: (1, 2) insufficient sensor sensitivity and selectivity, (3) lack of routes to correct for uncontrolled variation of ambient temperature, (4) lack of reliable power for operation, (5, 6) aging of sensing material and transducer, (7, 8) sensor contamination and poisoning, (9) poor dynamic range, (10, 11) slow response/recovery times, (12, 13) initial cost of sensor

and its installation, (14) compatibility with available wireless communication protocols, and (15) others.

As shown in this review, all sensing materials that are attractive for wireless sensing applications with limited available power suffer from different levels of humidity effects. While ambient humidity in urban, industrial, environmental, battlefield, and other settings can fluctuate over the 5 – 95% RH range, humidity in breath (tracheal, expired, and alveolar air) reaches 100% RH.[473,474] In materials that rely on interactions between analyte molecules and sensing surfaces (e.g. carbon nanotubes, graphene, metal oxides, zeolites, and others), their response at room temperature is mediated by a thin hydration layer of adsorbed water.[291,383,475,476] While humidity effects may be less pronounced with catalytic materials and some doped and mixed semiconducting metal oxides at high operating temperatures,[375,477] operation of wireless sensors at high temperatures often requires significantly more power, which is typically unavailable. In materials that rely on partitioning of analytes into the sensing film, humidity effects are pronounced from the changes of the dielectric properties, mass, and dimensional properties of the film.

As conclusively demonstrated in this review, the major risk for such a sensor is its insufficient selectivity. Assuming that the sensor already can meet the goals of sensitivity and response/recovery times (e.g. using nanostructured sensing materials), the mitigation plan for the risk of insufficient selectivity could include: (1) to obtain quantitative details on the composition of gaseous samples to be analyzed with the sensor, number of analytes needed for quantitation, types and levels of expected interferences, chemical similarity of these interferences to analytes, temperature range of measurements and (2) to downselect the proper combination of sensing material with a proper transducer and proper signal generation and processing techniques.

6.4. Path Forward

Innovative approaches will continue to be developed to solve the remaining problems of sensor selectivity in realistic conditions. While significant problems of sensor response in the presence of uncontrolled humidity have been recently highlighted in several reviews,[19,79,100,239] the original literature remains too limited in describing innovative approaches to cope or eliminate humidity effects. To solve this fundamental selectivity problem, the system approach should involve the downselection of the proper combination of the three key sensor system components (1) sensing material, (2) proper transducer, and (3) proper signal generation and processing techniques.

First, the development of sensing materials based on new materials design concepts and new materials fabrication principles will produce a large impact for new sensor systems. *Synthetic dielectric and conducting polymers* will continue to impress with the development of polymers with ultra-high partition coefficients,[443] different response mechanisms to different gases,[165] different polymer side group functionalities, and different polymer formulations.[155] Significant work will continue with *carbon nanotubes and graphene* to meet the challenge of finding a functionalization approach that will suppress humidity effects. Computer simulations predicting binding affinities of different gases to bare and functionalized carbon nanotubes and graphene should be expanded to situations of non-zero ambient humidity and other gaseous interferences. *Networks of metal nanoparticles* with hydrophobic capping ligands have already been shown to be the sensing material with the smallest humidity effect. Research on these materials should expand into making these materials more stable under realistic conditions. Selectivity between different classes of gases has been demonstrated by using *cavitands* with carefully selected deposition methods that provided a dominating intracavity complexation[409] and even a totally suppressed non specific extracavity adsorption of VOCs.[410] The work on these materials should continue

with the emphasis of operating of these materials in the presence of interferences. Assembly of *porphyrins* and related molecules into polymers and nanostructures[415,416] could bring new sensing capabilities due to possible surpamolecular nature of these assemblies and charge distribution between individual molecules. *Metal-organic frameworks* (MOFs) promise to expand the applicability of mesoporous materials for sensing utilizing the tailored approach that can be adopted for their synthesis and post-synthesis modifications. In contrast to zeolites, where only cation exchange is feasible due to the anionic nature of zeolite frameworks, MOFs can undergo both anion and cation exchange depending on their framework charges.[478–480] To further improve selectivity of response, overcoating of sensing films with auxiliary membrane filter films will continue to be attractive. Among these, zeolite[391–393] and cavitand[481] filters have been demonstrated, with other materials to be further explored. The importance of studies on improvements of stability of sensing materials will increase because of the need for wireless sensing. Approaches for bio-inspired sensing materials[113,482–484] will attract more significant attention because of the opportunities for more sensitive, selective, and stable sensing. Nanomaterials are becoming the focus of increasingly important health-risk studies[485,486] and regulatory attention.[487] Thus, development of sensing nanomaterials should proceed with caution.

Second, a proper selection of a transduction principle is important for not only obtaining the best response of a sensing material, but also for the suppression[64] or elimination[488] of interference effects. Surface ionization gas detection was recently shown to have better detection selectivity vs conventional conductometric transducers.[489] Transducers based on self-heating of nanomaterials[380,490] could also improve response selectivity. Development of new transduction principles should also produce a significant impact for new sensor systems.

Third, new signal generation and processing techniques are needed to provide more selective responses in sensors. Unfortunately, it was shown that a simple addition of more sensors to correct for interference effects (humidity, etc.) generated new problems of cross-sensitivity to other interferences.[79] Thus, the enhanced selectivity can be achieved through the development of multitransducer arrays[87,150] or multi-variable response individual sensors.[33,73–75] Recently, to partially mimic biological olfaction, a chemical sensor system has been designed with up to 65,536 chemiresistors to be coated with organic conducting polymers.[491] Water removal before analyte measurement[145] and analyte gas preconcentration[103] may be useful for some applications, but for most wireless gas sensors new methods of interference rejection will be needed.

The development of new wireless gas sensors will continue to be a research area that benefits from contributions from numerous disciplines including analytical, polymer, and organic chemistry, materials science and nanotechnology, electrical, RF, and computer engineering, microfabrication and packaging, and many other disciplines. However, to successfully move the wireless sensor concepts from laboratory demonstrations to end-use applications, this research area should involve more system design and integration aspects and should engage more collaboration between diverse disciplines.

Acknowledgments

Biographies

Radislav A. Potyrailo is a Principal Scientist at General Electric Global Research Center in Niskayuna, New York and an Industrial Adjunct Professor of Chemistry at Indiana University. He holds an optoelectronics Degree from Kiev Polytechnic Institute, Ukraine and a PhD in Analytical Chemistry from Indiana University. His research is focused on new microanalytical instrumentation, sensing technologies, functional materials, and combinatorial materials science. He has coauthored/co-edited eight books, published 70+ peer-reviewed technical papers, holds 60+ US patents, and gave numerous invited lectures and four keynote lectures on national and international technical meetings. Dr. Potyrailo is Editor of the Springer book series Integrated Analytical Systems. Dr. Potyrailo serves as an editor of the Springer book series *Integrated Analytical Systems*, Consulting Editor of *ACS Combinatorial Science*, and Editorial Board Member of *Sensors*. Dr. Potyrailo received a GE 50 Patents Award in 2009 and a GE 125 Publications Award in 2010. He was a lead scientist for the development of an optical sensor array system for GE Water Technologies that has been awarded with the 2010 Prism Award for photonics innovation by SPIE and Photonics Media. He has been elected SPIE Fellow in 2011 for achievements in fundamental breakthroughs in optical sensing and innovative analytical systems.

Cheryl Surman (Bratu) is a Lead Scientist at General Electric Global Research Center in Niskayuna, New York. She received her BS in Chemistry and Biology from Valparaiso University in Valparaiso, Indiana in 1997 and her PhD in Bioanalytical Chemistry from Rensselaer Polytechnic Institute in 2006. She has 13 years of experience in the development of various analytical techniques including 5 years of experience in the online-process control. In addition, Surman has extensive background and practical experience in chemometric techniques and combinatorial methods. Prior joining GE, she worked at UOP, LLC developing data analysis techniques for process control and combinatorial screening of heterogeneous catalysts. At GE, Cheryl played the major role in the development of new sensing materials and an optical sensor array system for GE Water Technologies that has been awarded with the 2010 Prism Award for photonics innovation by SPIE and Photonics Media. Her current research is in the area of radio frequency identification (RFID) chemical, biological, and physical sensors. She has 14 technical publications and 14 filed patents.

Nandini Nagraj is a Lead Chemist at General Electric Global Research Center in Niskayuna, New York. She completed her Bachelor's degree in Chemistry at the University of Madras, India and her Master's degree at the University of Pune, India where she performed research on copper complexes targeting TB with Prof. Subhash Padhye. She completed her PhD in Chemistry from the University of Illinois at Urbana-Champaign in 2010 in the laboratory of Prof. Yi Lu where she worked on the isolation, mechanisms and sensing applications of functional DNA molecules including aptamers and DNAzymes. Her current research at GE is focused on the development of chemical and biological sensors, including new sensing materials and new transducers.

Andrew Burns is a Lead Materials Scientist at General Electric Global Research Center in Niskayuna, New York. He completed an undergraduate degree in Chemistry at the University of Delaware where he performed research on photocatalytic nanomaterials with Prof. S. Ismat Shah. He completed his PhD in Materials Science & Engineering at Cornell University in 2008 in the laboratory of Prof. Ulrich Wiesner where he developed fluorescent silica nanoparticles for in vitro and in vivo targeting, imaging and sensing. His research is focused on sensing materials, holographics, and micro-/nano-textured surfaces.

References

(1). Farrar JT, Zworykin VK, Baum J. Science. 1957; 126:975. [PubMed: 13486045]

(2). Mackay RS, Jaconson B. Nature. 1957; 179:1239. [PubMed: 13440945]

(3). Messer H, Zinevich A, Alpert P. Science. 2006; 312:713. [PubMed: 16675693]

(4). Receveur RAM, Lindemans FW, De Rooij NF. J. Micromech. Microeng. 2007; 17:R50.

(5). Fleming WJ. IEEE Sensors J. 2008; 8:1900.

(6). Kwong, KH.; Sasloglou, K.; Goh, HG.; Wu, TT.; Stephen, B.; Gilroy, M.; Tachtatzis, C.; Glover, IA.; Michie, C.; Andonovic, I. INSS2009 - 6th International Conference on Networked Sensing Systems; 2009. p. 66

(7). Sahandi R, Noroozi S, Roushan G, Heaslip V, Liu Y. J. Med. Eng. Technol. 2010; 34:51. [PubMed: 19929237]

(8). Daniel T, Gaura E, Brusey J. Lecture Notes in Computer Science. 2009; 5741:177. LNCS.

(9). Mitrokotsa, A.; Douligeris, C. Integrated RFID and Sensor Networks: Architectures and Applications. In: Zhang, Y.; Y. L. T.; C. J., editors. RFID and Sensor Networks: Architectures, Protocols, Security and Integrations. Auerbach Publications, CRC Press; 2009. p. 511

(10). Documentation for Immediately Dangerous to Life or Health Concentrations (IDLH): NIOSH Chemical Listing and Documentation of Revised IDLH Values. 1995. http://www.cdc.gov/niosh/idlh/intridl4.html

(11). USACHPPM Technical Guide 230: Chemical Exposure Guidelines for Deployed Military Personnel. 2006. http://chppm

(12). Annual Reports of the Committees on on TLVs and BEIs. 2008. https://www.acgih.org/Products/tlv_bei_intro.htm

(13). OSHA Regulations Standards 29CFR1910.1000 - Toxic and Hazardous Substances. 2006. http://www.osha.gov/pls/oshaweb/owadisp.show_document?p_table=STANDARDS&p_id=9991

(14). U.S. Environmental Protection Agency Acute Exposure Guideline Levels (AEGL). 2009. http://www.epa.gov/oppt/aegl/

(15). Pleil JD. J. Breath Res. 2010; 4:029001. [PubMed: 21383475]

(16). Lee WS, Alchanatis V, Yang C, Hirafuji M, Moshou D, Li C. Comput. Electron. Agr. 2010; 74:2.

(17). Casalinuovo IA, Di Pierro D, Coletta M, Di Francesco P. Sensors. 2006; 6:1428.

(18). Lide, DR., editor. CRC Handbook of Chemistry and Physics. 74 ed.. CRC Press: Boca Raton, FL; 1993.

(19). Röck F, Barsan N, Weimar U. Chem. Rev. 2008; 108:705. [PubMed: 18205411]

(20). Longworth, TL.; Ong, KY.; Baranoski, JM. Domestic Preparedness Program Testing of the VaporTracer Against Chemical Warfare Agents. U.S. Army Homeland Defense Publications; 2002. Summary Reporthttp://hld.sbccom.army.mil/

(21). Hopkins AR, Lewis NS. Anal. Chem. 2001; 73:884. [PubMed: 11289432]

(22). Novak JP, Snow ES, Houser EJ, Park D, Stepnowski JL, McGill RA. Appl. Phys. Lett. 2003; 83:4026.

(23). Meier DC, Evju JK, Boger Z, Raman B, Benkstein KD, Martinez CJ, Montgomery CB, Semancik S. Sens. Actuators B. 2007; 121:282.

(24). Byrne R, Diamond D. Nature Mater. 2006; 5:421. [PubMed: 16738672]

(25). Diamond D, Coyle S, Scarmagnani S, Hayes J. Chem. Rev. 2008; 108:652. [PubMed: 18215076]

(26). Zheng, J.; Jamalipour, A., editors. Wireless Sensor Networks: A Networking Perspective. Wiley-IEEE Press:; Hoboken NJ: 2009.

(27). Misra, S.; Woungang, I.; Misra, SC., editors. Guide to Wireless Sensor Networks. Springer; New York, NY: 2009.

(28). Tumanski S. Meas. Sci. Tech. 2007; 18:R31.

(29). Romero E, Warrington RO, Neuman MR. Physiological Measurement. 2009; 30:R35. [PubMed: 19687530]

(30). Federici JF, Schulkin B, Huang F, Gary D, Barat R, Oliveira F, Zimdars D. Semicond. Sci. Technol. 2005; 20:S266.

(31). Wolfbeis OS. Anal. Chem. 2008; 80:4269. [PubMed: 18462008]

(32). Wallin S, Pettersson A, Östmark H, Hobro A. Anal. Bioanal. Chem. 2009; 395:259. [PubMed: 19484226]

(33). Potyrailo RA, Morris WG. Anal. Chem. 2007; 79:45. [PubMed: 17194120]

(34). Lange U, Roznyatovskaya NV, Mirsky VM. Anal. Chim. Acta. 2008; 614:1. [PubMed: 18405677]

(35). Oprea A, Bârsan N, Weimar U, Bauersfeld M-L, Ebling D, Wöllenstein J. Sens. Actuators B. 2008; 132:404.

(36). Sin MLY, Chow GCT, Wong GMK, Li WJ, Leong PHW, Wong KW. IEEE Trans. Nanotechnol. 2007; 6:571.

(37). Thaker, DD.; Chen, A.; Amirtharajah, R.; Chong, FT. Proc. of IEEE International Workshop on Design and Test of Defect-Tolerant Nanoscale Architectures (NANOARCH'05); 2005. p. 4.9

(38). Löfgren, L.; Löfving, B.; Pettersson, T.; Ottosson, B.; Rusu, C.; Haasl, S.; Persson, K.; Vermesan, O.; Pesonen, N.; Enoksson, P. Low-power humidity sensor for RFID applications. In: Dimov, S.; Menz, W., editors. Multi-Material Micro Manufacture. Cardiff University; Cardiff, UK: 2008.

(39). Courbat J, Briand D, Yue L, Raible S, De Rooij NF. Transducers '09. 2009:584.

(40). Sayhan I, Helwig A, Becker T, Müller G, Elmi I, Zampolli S, Padilla M, Marco S. IEEE Sensors J. 2008; 8:176.

(41). Prades JD, Jimenez-Diaz R, Hernandez-Ramirez F, Barth S, Cirera A, Romano-Rodriguez A, Mathur S, Morante JR. Appl. Phys. Lett. 2008; 93 art. no. 123110.

(42). Cho TS, Lee K-J, Kong J, Chandrakasan AP. IEEE J. Solid-State Circuits. 2009; 44:659.

(43). Yokosawa K, Saitoh K, Nakano S, Goto Y, Tsukada K. Sens. Actuators B. 2008; 130:94.

(44). Adams JD, Parrott G, Bauer C, Sant T, Manning L, Jones M, Rogers B, McCorkle D, Ferrell TL. Appl. Phys. Lett. 2003; 83:3428.

(45). Cai QY, Cammers-Goodwin A, Grimes CA. J. Environ. Monit. 2000; 2:556. [PubMed: 11296740]

(46). Morris, WG.; Potyrailo, RA. Wireless Sensor Array System for Combinatorial Screening of Sensor Materials. In: Fasolka, M.; Wang, Q.; Potyrailo, RA.; Chikyow, T.; Schubert, US.; Korkin, A., editors. Combinatorial Methods and Informatics in Materials Science. MRS Symposium Proceedings; Warrendale, PA: Materials Research Society; 2006. p. 219

(47). Wagner J, Von Schickfus M. Sens. Actuators B. 2001; 76:58.

(48). Ong KG, Grimes CA. Smart Mater. Struct. 2000; 9:421.

(49). Ballantine, DS., Jr.; White, RM.; Martin, SJ.; Ricco, AJ.; Frye, GC.; Zellers, ET.; Wohltjen, H. Acoustic Wave Sensors: Theory, Design, and Physico-Chemical Applications. Academic Press; San Diego, CA: 1997. p. 436

(50). Baselt DR, Fruhberger B, Klaassen E, Cemalovic S, Britton CL Jr. Patel SV, Mlsna TE, McCorkle D, Warmack B. Sens. Actuators B. 2003; 88:120.

(51). DeHennis AD, Wise KD. J. Microelectromech. Syst. 2005; 14:12.

(52). Tsow F, Forzani E, Rai A, Wang R, Tsui R, Mastroianni S, Knobbe C, Gandolfi AJ, Tao NJ. IEEE Sensors J. 2009; 9:1734.

(53). Zeng K, Grimes CA. IEEE Trans. Magnetics. 2007; 43:2358.

(54). Reindl L, Scholl G, Ostertag T, Scherr H, Wolff U, Schmidt F. IEEE Trans. Ultrason. Ferroelectr. Freq. Control. 1998; 45:1281. [PubMed: 18244291]

(55). Dowling J, Tentzeris MM, Beckett N. Proc. IMWS. 2009 art. no. 5307884.

(56). Patil A, Patil V, Shin DW, Choi J-W, Paik D-S, Yoon S-J. Mater. Res. Bull. 2008; 43:1913.

(57). Simon P, Gogotsi Y. Nature Mater. 2008; 7:845. [PubMed: 18956000]

(58). Vullers RJM, van Schaijk R, Doms I, Van Hoof C, Mertens R. Solid-State Electronics. 2009; 53:684.

(59). Hayes J, Beirne S, Lau K-T, Diamond D. Proc. IEEE Sensors. 2008:530.

(60). Steinberg IM, Steinberg MD. Sens. Actuators B. 2009; 138:120.

(61). Finkenzeller, K. Fundamentals and applications in contactless smart cards and identification. 2 ed.. Wiley; Hoboken, NJ: 2003. RFID Handbook.

(62). Barandiaran JM, Gutierrez J, Gómez-Polo C. Sens. Actuators A. 2000; 81:154.

(63). Rabe J, Seidemann V, Buettgenbach S. Sens. Materials. 2003; 15:381.

(64). Wang W, Lee K, Kim T, Park I, Yang S. Smart Mater. Struct. 2007; 16:1382.

(65). Harpster TJ, Stark B, Najafi K. Sens. Actuators A. 2002; 95:100.

(66). Birdsell, E.; Allen, MG. Solid-State Sensors, Actuators, and Microsystems Workshop; Hilton Head Island, South Carolina. June 4–8; 2006. p. 212

(67). Tan EL, Ng WN, Shao R, Pereles BD, Ong KG. Sensors. 2007; 7:1747.

(68). Sridhar V, Takahata K. Sens. Actuators A. 2009; 155:58.

(69). Lei M, Baldi A, Nuxoll E, Siegel RA, Ziaie B. Biomedical Microdevices. 2009; 11:529. [PubMed: 18335316]

(70). Engheta N. Science. 2007; 317:1698. [PubMed: 17885123]

(71). Potyrailo RA, Surman C, Morris WG, Go S, Lee Y, Cella JA, Chichak KS. IEEE International Conference on RFID, IEEE RFID. 2010:22.

(72). Lehpamer, H. RFID Design Principles. Artech House; Norwood, MA: 2008.

(73). Potyrailo RA, Mouquin H, Morris WG. Talanta. 2008; 75:624. [PubMed: 18585123]

(74). Potyrailo RA, Morris WG, Sivavec T, Tomlinson HW, Klensmeden S, Lindh K. Wirel. Commun. Mob. Comput. 2009; 9:1318.

(75). Potyrailo RA, Surman C, Go S, Lee Y, Sivavec T, Morris WG. J. Appl. Phys. 2009; 106:124902.

(76). Fletcher, RR. Ph.D. thesis. Massachusetts Institute of Technology; Cambridge, MA: 2002. Low-Cost Electromagnetic Tagging: Design and Implementation.

(77). Shrestha S, Balachandran M, Agarwal M, Phoha VV, Varahramyan K. IEEE Trans. Microw. Theory. 2009; 57:1303.

(78). Sample AP, Yeager DJ, Powledge PS, Mamishev AV, Smith JR. IEEE Trans. Instrum. Meas. 2008; 57:2608.

(79). Hierlemann A, Gutierrez-Osuna R. Chem. Rev. 2008; 108:563. [PubMed: 18198903]

(80). Potyrailo RA, May RJ. Rev. Sci. Instrum. 2002; 73:1277.

(81). Potyrailo RA, Sivavec TM. Sens. Actuators B. 2005; 106:249.

(82). Peris M, Escuder-Gilabert L. Anal. Chim. Acta. 2009; 638:1. [PubMed: 19298873]

(83). Hierlemann A, Weimar U, Kraus G, Schweizer-Berberich M, Göpel W. Sens. Actuators B. 1995; 26:126.

(84). Severin EJ, Doleman BJ, Lewis NS. Anal. Chem. 2000; 72:658. [PubMed: 10701248]

(85). Hsieh M-D, Zellers ET. Anal. Chem. 2004; 76:1885. [PubMed: 15053648]

(86). Kummer AM, Hierlemann A. IEEE Sensors J. 2006; 6:3.

(87). Jin C, Zellers ET. Anal. Chem. 2008; 80:7283. [PubMed: 18771277]

(88). Snow ES, Perkins FK, Houser EJ, Badescu SC, Reinecke TL. Science. 2005; 307:1942. [PubMed: 15790850]

(89). Qi X, Osterloh FE. J. Am. Chem. Soc. 2005; 127:7666. [PubMed: 15913342]

(90). Haupt, K. Molecularly imprinted polymers as recognition elements in sensors. In: Mirsky, VM., editor. Ultrathin Electrochemical Chemo- and Biosensors. Springer; Berlin, Germany: 2004. p. 23

(91). Valdés MG, Pérez-Cordoves AI, Díaz-García ME. Trends Anal. Chem. 2006; 25:24.

(92). Sahner K, Hagen G, Schönauer D, Reiß S, Moos R. Solid State Ionics. 2008; 179:2416.

(93). Di Natale C, Paolesse R, D'Amico A. Sens. Actuators B. 2007; 121:238.

(94). Öztürk ZZ, Klnç N, Atilla D, Gürek AG, Ahsen V. J. Porphyrin. Phthalocyanin. 2009; 13:1179.

(95). Melegari M, Suman M, Pirondini L, Moiani D, Massera C, Ugozzoli F, Kalenius E, Vainiotalo P, Mulatier J-C, Dutasta J-P, Dalcanale E. Chem. Eur. J. 2008; 14:5772.

(96). Pirondini L, Dalcanale E. Chem. Soc. Rev. 2007; 36:695. [PubMed: 17471395]

(97). Meek ST, Greathouse JA, Allendorf MD. Adv. Mater. 2011; 23:249. [PubMed: 20972981]

(98). Shekhah O, Liu J, Fischer RA, Wöll C. Chem. Soc. Rev. 2011; 40:1081. [PubMed: 21225034]

(99). Potyrailo RA. Angew. Chem. Int. Ed. 2006; 45:702.

(100). Hatchett DW, Josowicz M. Chem. Rev. 2008; 108:746. [PubMed: 18171087]

(101). Potyrailo RA, Mirsky VM. Chem. Rev. 2008; 108:770. [PubMed: 18211102]

(102). Persaud K, Dodd G. Nature. 1982; 299:352. [PubMed: 7110356]

(103). Peng G, Trock E, Haick H. Nano Lett. 2008; 8:3631. [PubMed: 18839997]

(104). Hirschfeld T. Science. 1985; 230:286. [PubMed: 17782457]

(105). Joo S, Brown RB. Chem. Rev. 2008; 108:638. [PubMed: 18184017]

(106). Jurs PC, Bakken GA, McClelland HE. Chem. Rev. 2000; 100:2649. [PubMed: 11749299]

(107). Snopok BA, Kruglenko IV. Thin Solid Films. 2002; 418:21.

(108). Scott SM, James D, Ali Z. Microchim. Acta. 2007; 156:183.

(109). Potyrailo RA, May RJ, Sivavec TM. Sensor Lett. 2004; 2:31.

(110). Potyrailo RA, Wroczynski RJ, Lemmon JP, Flanagan WP, Siclovan OP. J. Comb. Chem. 2003; 5:8. [PubMed: 12523829]

(111). Potyrailo RA. Trends Anal. Chem. 2003; 22:374.

(112). Potyrailo RA. Appl. Phys. Lett. 2004; 84:5103.

(113). Potyrailo RA, Ghiradella H, Vertiatchikh A, Dovidenko K, Cournoyer JR, Olson E. Nature Photonics. 2007; 1:123.

(114). Zhong G, Bernhardt G, Lad R, Collins S, Smith R. Proc. IEEE Sensors. 2007:1225.

(115). Hagleitner C, Hierlemann A, Lange D, Kummer A, Kerness N, Brand O, Baltes H. Nature. 2001; 414:293. [PubMed: 11713525]

(116). Furuki M, Pu LS. Thin Solid Films. 1992; 210/211:471.

(117). Snow AW, Barger WR, Klusty M, Wohltjen H, Jarvis NL. Langmuir. 1986; 2:513.

(118). Di Natale C, Buchholt K, Martinelli E, Paolesse R, Pomarico G, D'Amico A, Lundstrom I, Lloyd Spetz A. Sens. Actuators B. 2009; 135:560.

(119). Snow ES, Perkins FK. Nano Lett. 2005; 5:2414. [PubMed: 16351188]

(120). Brahim S, Colbern S, Gump R, Grigorian L. J. Appl. Phys. 2008; 104 art. no. 024502.

(121). Hellmich W, Müller G, Braunmühl C. B.-v. Doll T, Eisele I. Sens. Actuators B. 1997; 43:132.

(122). Torsi L, Dodabalapur A, Sabbatini L, Zambonin PG. Sens. Actuators B. 2000; 67:312.

(123). Meier DC, Raman B, Semancik S. Annu. Rev. Anal. Chem. 2009; 2:463.

(124). Holloway AF, Nabok A, Thompson M, Ray AK, Wilkop T. Sens. Actuators B. 2004; 99:355.

(125). Josse F, Lukas R, Zhou R, Schneider S, Everhart D. Sens. Actuators B. 1996; 35–36:363.

(126). Martin SJ, Frye GC. Appl. Phys. Lett. 1990; 57:1867.

(127). Wessendorf, KO. The Lever Oscillator for Use in High Resistance Resonator Applications. Proc. 1993 Frequency Control Symp.; IEEE: New York, NY. 1993. p. 711

(128). Hwang BJ, Yang JY, Lin CW. Sens. Actuators B. 2001; 75:67.

(129). Fort A, Rocchi S, Serrano-Santos MB, Ulivieri N, Vignoli V, Pioggia G, Di Francesco F. Sens. Actuators B. 2005; 111–112:193.

(130). Tanaka H, Kanno Y. Jpn. J. Appl. Phys. Part 1. 2007; 46:7509.

(131). Woodard SE, Taylor BD. Meas. Sci. Tech. 2007; 18:1603.

(132). Amrani MEH, Persaud KC, Payne PA. Meas. Sci. Technol. 1995; 6:1500.

(133). Yang RD, Fruhberger B, Park J, Kummel AC. Appl. Phys. Lett. 2006; 88:074104.

(134). King WH Jr. Anal. Chem. 1964; 36:1735.

(135). Sugiyasu K, Swager TM. Bull. Chem. Soc. Jpn. 2007; 80:2074.

(136). McQuade DT, Pullen AE, Swager TM. Chem. Rev. 2000; 100:2537. [PubMed: 11749295]

(137). Grate JW. Chem. Rev. 2008; 108:726. [PubMed: 18220425]

(138). Grate JW, Abraham MH. Sens. Actuators B. 1991; 3:85.

(139). Patel SV, Mlsna TE, Fruhberger B, Klaassen E, Cemalovic S, Baselt DR. Sens. Actuators B. 2003; 96:541.

(140). Pinnaduwage LA, Thundat T, Hawk JE, Hedden DL, Britt PF, Houser EJ, Stepnowski S, McGill RA, Bubb D. Sens. Actuators B. 2004; 99:223.

(141). Stegmeier S, Fleischer M, Tawil A, Hauptmann P. Sens. Actuators B. 2010; 148:450.

(142). Grate, JW.; Abraham, H.; McGill, RA. Sorbent polymer materials for chemical sensors and arrays. In: Kress-Rogers, E., editor. Handbook of Biosensors and Electronic Noses. Medicine, Food, and the Environment. CRC Press; Boca Raton, FL: 1997. p. 593

(143). Harpster TJ, Hauvespre S, Dokmeci MR, Najafi K. J. Microelectromech. Syst. 2002; 11:61.

(144). Chang K, Kim YH, Kim YJ, Yoon YJ. Electron. Lett. 2007; 43:7.

(145). Kebabian PL, Freedman A. Meas. Sci. Technol. 2006; 17:703.

(146). Cai QY, Jain MK, Grimes CA. Sens. Actuators B. 2001; 77:614.

(147). Alentiev AY, Shantarovich VP, Merkel TC, Bondar VI, Freeman BD, Yampolskii YP. Macromolecules. 2002; 35:9513.

(148). Potyrailo RA, Leach AM, Morris WG, Gamage SK. Anal. Chem. 2006; 78:5633. [PubMed: 16906705]

(149). Bondar VI, Freeman BD, Yampolskii YP. Macromolecules. 1999; 32:6163.

(150). Kurzawski P, Hagleitner C, Hierlemann A. Anal. Chem. 2006; 78:6910. [PubMed: 17007514]

(151). Mlsna TE, Cemalovic S, Warburton M, Hobson ST, Mlsna D, Patel SV. Sens. Actuators B. 2006; 116:192.

(152). Collins GE, Buckley LJ. Synthetic Metals. 1996; 78:93.

(153). Grate JW, Patrash SJ, Kaganove SN, Wise BM. Anal. Chem. 1999; 71:1033. [PubMed: 21662772]

(154). Potyrailo RA, Morris WG. Rev. Sci. Instrum. 2007; 78:072214. [PubMed: 17672745]

(155). Potyrailo RA, Surman C, Morris WG. J. Comb. Chem. 2009; 11:598. [PubMed: 19413291]

(156). Travers JP, Nechtschein M. Synthetic Metals. 1986; 21:135.

(157). Chao S, Wrighton MS. J. Am. Chem. Soc. 1987; 109:6627.

(158). Li B, Santhanam S, Schultz L, Jeffries-EL M, Iovu MC, Sauvé G, Cooper J, Zhang R, Revelli JC, Kusne AG, Snyder JL, Kowalewski T, Weiss LE, McCullough RD, Fedder GK, Lambeth DN. Sens. Actuators B. 2007; 123:651.

(159). Jang J, Chang M, Yoon H. Adv. Mater. 2005; 17:1616.

(160). Xue M, Zhang Y, Yang Y, Cao T. Adv. Mater. 2008; 20:2145.

(161). Musio F, Ferrara MC. Sens. Actuators B. 1997; 41:97.

(162). Li B, Lambeth DN. Nano Lett. 2008; 11:3563. [PubMed: 18954129]

(163). Zeng X, Jin X, Huang Y, Mason A. Anal. Chem. 2009; 81:595. [PubMed: 19090744]

(164). Al-Mashat L, Tran HD, Wlodarski W, Kaner RB, Kalantar-zadeh K. Sens. Actuators B. 2008; 134:826.

(165). Virji S, Huang J, Kaner RB, Weiller BH. Nano Lett. 2004; 4:491.

(166). Hao Q, Wang X, Lu L, Yang X, Mirsky VM. Macromol. Rapid Comm. 2005; 26:1099.

(167). Arsat R, Yu XF, Li YX, Wlodarski W, Kalantar-zadeh K. Sens. Actuators B. 2009; 137:529.

(168). Gannot Y, Hertzog-Ronen C, Tessler N, Eichen Y. Adv. Funct. Mater. 2010; 20:105.

(169). Lee JI, Cho SH, Park S-M, Kim JK, Kim JK, Yu J-W, Kim YC, Russell TP. Nano Lett. 2008; 8:2315. [PubMed: 18642964]

(170). Krondak M, Broncova G, Anikin S, Merz A, Mirsky VM. J. Solid State Electrochem. 2006; 10:185.

(171). Ouyang J, Xu Q, Chu C-W, Yang Y, Li G, Shinar J. Polymer. 2004; 45:8443.

(172). Dan Y, Cao Y, Mallouk TE, Johnson AT, Evoy S. Sens. Actuators B. 2007; 125:55.

(173). Liu J, Agarwal M, Varahramyan K, Berney ES IV, Hodo WD. Sens. Actuators B. 2008; 129:599.

(174). Nicolas-Debarnot D, Poncin-Epaillard F. Anal. Chim. Acta. 2003; 475:1.

(175). Liu H, Kameoka J, Czaplewski DA, Craighead HG. Nano Lett. 2004; 4:671.

(176). Sasaki I, Janata J, Josowicz M. Polym. Degrad. Stab. 2007; 92:1408.

(177). Virji S, Fowler JD, Baker CO, Huang J, Kaner RB, Weiller BH. Small. 2005; 1:624. [PubMed: 17193496]

(178). Virji S, Kojima R, Fowler JD, Villanueva JG, Kaner RB, Weiller BH. Nano Research. 2009; 2:135.

(179). Zhang R, Li B, Iovu MC, Jeffries-El M, Sauvé G, Cooper J, Jia S, Tristram-Nagle S, Smilgies DM, Lambeth DN, McCullough RD, Kowalewski T. J. Am Chem. Soc. 2006; 128:3480. [PubMed: 16536496]

(180). Jung YS, Jung W, Tuller HL, Ross CA. Nano Lett. 2008; 8:3776. [PubMed: 18954147]

(181). Li Z-F, Blum FD, Bertino MF, Kim C-S, Pillalamarri SK. Sens. Actuators B. 2008; 134:31.

(182). Xie Z, Duan L, Jiang Y, Xue M, Zhang M, Cao T. Macromol. Rapid Comm. 2009; 30:1589.

(183). Hamedi M, Tvingstedt K, Karlsson RH, Åsberg P, Inganäs O. Nano Lett. 2009; 9:631. [PubMed: 19140695]

(184). Bearzotti A, MacAgnano A, Pantalei S, Zampetti E, Venditti I, Fratoddi I, Vittoria Russo M. J. Phys.: Condens. Matter. 2008; 20 art. no. 474207.

(185). Potyrailo RA, Ding Z, Butts MD, Genovese SE, Deng T. IEEE Sensors J. 2008; 8:815.

(186). Woodson M, Liu J. J. Am. Chem. Soc. 2006; 128:3760. [PubMed: 16536550]

(187). Schäffer E, Thurn-Albrecht T, Russell TP, Steiner U. Nature. 2000; 403:874. [PubMed: 10706280]

(188). Guan J, Yu B, Lee LJ. Adv. Mater. 2007; 19:1212.

(189). Zhou Y, Freitag M, Hone J, Staii C, Johnson AT, Pinto NJ, MacDiarmid AG. Appl. Phys. Lett. 2003; 83:3800.

(190). Hua F, Sun Y, Gaur A, Meitl MA, Bilhaut L, Rotkina L, Wang J, Geil P, Shim M, Rogers JA. Nano Lett. 2004; 4:2467.

(191). Lipomi DJ, Chiechi RC, Dickey MD, Whitesides GM. Nano Lett. 2008; 8:2100. [PubMed: 18517256]

(192). del Campo A, Arzt E. Chem. Rev. 2008; 108:911. [PubMed: 18298098]

(193). Ding B, Wang M, Yu J, Sun G. Sensors. 2009; 9:1609.

(194). Jiang H, Wang Y, Ye Q, Zou G, Su W, Zhang Q. Sens. Actuators B. 2010; 143:789.

(195). Loui A, Ratto TV, Wilson TS, McCall SK, Mukerjee EV, Love AH, Hart BR. Analyst. 2008; 133:608. [PubMed: 18427681]

(196). Grate JW, McGill RA. Anal. Chem. 1995; 67:4015.

(197). Barnes KA, Karim A, Douglas JF, Nakatani AI, Gruell H, Amis EJ. Macromolecules. 2000; 33:4177.

(198). Mabrook MF, Pearson C, Petty MC. Appl. Phys. Lett. 2005; 86:013507.

(199). Sisk BC, Lewis NS. Langmuir. 2006; 22:7928. [PubMed: 16922586]

(200). Severin EJ, Sanner RD, Doleman BJ, Lewis NS. Anal. Chem. 1998; 70:1440. [PubMed: 21644739]

(201). Li J. Sensors. 2000; 17:56.

(202). Dresselhaus, MS.; Dresselhaus, G.; Eklund, PC. Science of Fullerenes and Carbon Nanotubes. Academic Press; San Diego, CA: 1996.

(203). Geim AK, Novoselov KS. Nature Materials. 2007; 6:183.

(204). Lundberg B, Sundqvist B. J. Appl. Phys. 1986; 60:1074.

(205). Ruschau GR, Newnham RE, Runt J, Smith BE. Sens. Actuators. 1989; 20:269.

(206). Lonergan MC, Severin EJ, Doleman BJ, Beaber SA, Grubbs RH, Lewis NS. Chem. Mater. 1996; 8:2298.

(207). Matthews B, Li J, Sunshine S, Lerner L, Judy JW. IEEE Sensors J. 2002; 2:160.

(208). Kang NK, Jun TS, La D-D, Oh JH, Cho YW, Kim YS. Sens. Actuators B. 2010; 147:55.

(209). Patel SV, Jenkins MW, Hughes RC, Yelton WG, Ricco AJ. Anal. Chem. 2000; 72:1532. [PubMed: 10763250]

(210). Mascaro DJ, Baxter JC, Halvorsen A, White K, Scholz B, Schulz DL. Sens. Actuators B. 2007; 120:353.

(211). Marinov VR, Atanasov YA, Khan A, Vaselaar D, Halvorsen A, Schulz DL, Chrisey DB. IEEE Sensors J. 2007; 7:937.

(212). De Girolamo Del Mauro A, Burrasca G, De Vito S, Massera E, Loffredo F, Quercia L, Di Francia G, Della Sala D. Transducers '07. 2007:1011.

(213). Lewis NS. Acc. Chem. Res. 2004; 37:663. [PubMed: 15379582]

(214). Kroto HW, Heath JR, O'Brien SC, Curl RF, Smalley RE. Nature. 1985; 318:162.

(215). Kratschmer W, Lamb L, Fostiropoulos K, Huffman DR. Nature. 1990; 347:354.

(216). Martin N. Chem. Commun. 2006:2093.

(217). Darwish AD. Annu. Reports Progr. Chem. A. 2009; 105:363.

(218). Serrano A, Gallego M. J. Sep. Sci. 2006; 29:33. [PubMed: 16485707]

(219). Sberveglieri G, Faglia G, Perego C, Nelli P, Marks RN, Virgili T, Taliani C, Zamboni R. Synthetic Metals. 1996; 77:273.

(220). Barsan N, Weimar U. J. Phys.: Condens. Matter. 2003; 15:R813.

(221). Franke ME, Koplin TJ, Simon U. Small. 2006; 2:36. [PubMed: 17193551]

(222). Korotcenkov G. Sens. Actuators B. 2005; 107:209.

(223). Chao Y-C, Shih J-S. Anal. Chim. Acta. 1998; 374:39.

(224). Abraham MH, Du CM, Grate JW, McGill RA, Shuely WJ. J. Chem. Soc., Chem. Comm. 1993:1863.

(225). Li D, Swanson BI. Langmuir. 1993; 9:3341.

(226). Grate JW, Abraham MH, Du CM, McGill RA, Shuely WJ. Langmuir. 1995; 11:2125.

(227). Grynko D, Burlachenko J, Kukla O, Kruglenko I, Belyaev O. Semiconductor Physics, Quantum Electronics & Optoelectronics. 2009; 12:287.

(228). Shih J-S, Mao Y-C, Sung M-F, Gau G-J, Chiou C-S. Sens. Actuators B. 2001; 76:347.

(229). Lin H-B, Shih J-S. Sens. Actuators B. 2003; 92:243.

(230). Dickert FL, Zenkel ME, Bulst W-E, Fischerauer G, Knauer U. Fresenius J. Anal. Chem. 1997; 357:27.

(231). Iijima S. Nature. 1991; 354:56.

(232). Iijima S, Ichihashi T. Nature. 1993; 363:603.

(233). Dai H. Surf. Sci. 2002; 500:218.

(234). Zhao Y-L, Stoddart JF. Acc. Chem. Res. 2009; 42:1161. [PubMed: 19462997]

(235). Collins PG, Bradley K, Ishigami M, Zettl A. Science. 2000; 287:1801. [PubMed: 10710305]

(236). Qi P, Vermesh O, Grecu M, Javey A, Wang Q, Dai H, Peng S, Cho KJ. Nano Lett. 2003; 3:347.

(237). Kong J, Franklin NR, Zhou C, Chapline MG, Peng S, Cho K, Dai H. Science. 2000; 287:622. [PubMed: 10649989]

(238). Snow ES, Perkins FK, Robinson JA. Chem. Soc. Rev. 2006; 35:790. [PubMed: 16936927]

(239). Kauffman DR, Star A. Angew. Chem. Int. Ed. 2008; 47:6550.

(240). Cao Q, Rogers JA. Adv. Mater. 2009; 21:29.

(241). Varghese OK, Kichambre PD, Gong D, Ong KG, Dickey EC, Grimes CA. Sens. Actuators B. 2001; 81:32.

(242). McGrath M, Pham A. Int. J. High Speed Electron. Syst. 2006; 16:913.

(243). Peng N, Zhang Q, Chow CL, Tan OK, Marzari N. Nano Lett. 2009; 9:1626. [PubMed: 19281216]

(244). Salehi-Khojin A, Khalili-Araghi F, Kuroda MA, Lin KY, Leburton J-P, Masel RI. ACS Nano. 2011; 5:153. [PubMed: 21186822]

(245). Yoon H, Xie J, Abraham JK, Varadan VK, Ruffin PB. Smart Mater. Struct. 2006; 15:S14.

(246). Wang F, Gu H, Swager TM. J. Am. Chem. Soc. 2008; 130:5392. [PubMed: 18373343]

(247). Castro M, Lu J, Bruzaud S, Kumar B, Feller J-F. Carbon. 2009; 47:1930.

(248). Abraham JK, Philip B, Witchurch A, Varadan VK, Channa Reddy C. Smart Mater. Struct. 2004; 13:1045.

(249). Rajaputra S, Mangu R, Clore P, Qian D, Andrews R, Singh VP. Nanotechnology. 2008; 19 art. no. 345502.

(250). Faizah MY. Europ. J. Sci. Res. 2009; 35:142.

(251). Robinson JA, Snow ES, Perkins FK. Sens. Actuators A. 2007; 135:309.

(252). Chen Y, Meng F, Li M, Liu J. Sens. Actuators B. 2009; 140:396.

(253). Esen G, Fuhrer MS, Ishigami M, Williams ED. Appl. Phys. Lett. 2007; 90 art. no. 123510.

(254). Brahim S, Colbern S, Gump R, Moser A, Grigorian L. Nanotechnology. 2009; 20 art. no. 235502.

(255). Penza M, Rossi R, Alvisi M, Aversa P, Cassano G, Suriano D, Benetti M, Cannatà D, Di Pietrantonio F, Verona E. Proc. IEEE Ultrason. Symp. 2008:1850.

(256). Penza M, Antolini F, Vittori-Antisari M. Thin Solid Films. 2005; 472:246.

(257). Su P-G, Tsai J-F. Sens. Actuators B. 2009; 135:506.

(258). Ong KG, Zeng K, Grimes CA. IEEE Sensors J. 2002; 2:82.

(259). Chopra S, McGuire K, Gothard N, Rao AM, Pham A. Appl. Phys. Lett. 2003; 83:2280.

(260). Picaud F, Langlet R, Arab M, Devel M, Girardet C, Natarajan S, Chopra S, Rao AM. J. Appl. Phys. 2005; 97:1.

(261). McGrath M, Pham A-VH. Sensor Lett. 2008; 6:719.

(262). Tooski SB. J. Appl. Phys. 2010; 107 art. no. 014702.

(263). Yoon H, Philip B, Xie J, Ji T, Varadan VK. Proc. SPIE. 2004; 5389:101.

(264). Yang L, Staiculescu D, Zhang R, Wong CP, Tentzeris MM. IEEE Anten. Propag. Soc., AP-S Int. Symp. 2009 art. no. 5171787.

(265). Ong KG, Grimes CA. Sensors. 2001; 1:193.

(266). Nguyen LH, Phi TV, Phan PQ, Vu HN, Nguyen-Duc C, Fossard F. Physica E. 2007; 37:54.

(267). Penza M, Rossi R, Alvisi M, Cassano G, Signore MA, Serra E, Giorgi R. Sens. Actuators B. 2008; 135:289.

(268). Bhuiyan MMH, Mitsugi F, Ueda T, Ikegami T. Int. J. Nanomanufactur. 2009; 4:186.

(269). Ebbesen TW, Ajayan PM. Nature. 1992; 358:220.

(270). Zhu HW, Xu CL, Wu DH, Wei BQ, Vajtai R, Ajayan PM. Science. 2002; 296:884. [PubMed: 11988567]

(271). Xu M, Sun Z, Chen Q, Tay BK. Int. J. Nanotechn. 2009; 6:735.

(272). Peng S, Cho K. Nano Lett. 2003; 3:513.

(273). Star A, Han T-R, Joshi V, Gabriel J-CP, Grüner G. Adv. Mater. 2004; 16:2049.

(274). Lee CY, Strano MS. J. Am. Chem. Soc. 2008; 130:1766. [PubMed: 18189400]

(275). Hashishin T, Tamaki J. Sens. Materials. 2009; 21:265.

(276). Tseng W-S, Tseng C-Y, Kuo C-T. J. Nanosci. Nanotechnol. 2009; 9:6889. [PubMed: 19908694]

(277). Yoo K-P, Kwon K-H, Min N-K, Lee MJ, Lee CJ. Sens. Actuators B. 2009; 143:333.

(278). Watts PCP, Mureau N, Tang Z, Miyajima Y, David Carey J, Silva SRP. Nanotechnology. 2007; 18 art. no. 175701.

(279). Wong SS, Joselevich E, Woolley AT, Cheung CL, Lieber CM. Nature. 1998; 394:52. [PubMed: 9665127]

(280). Williams KA, Veenhuizen PTM, De la Torre BG, Eritja R, Dekker C. Nature. 2002; 420:761. [PubMed: 12490938]

(281). Asuri P, Bale SS, Pangule RC, Shah DA, Kane RS, Dordick JS. Langmuir. 2007; 23:12318. [PubMed: 17944500]

(282). Kong L, Wang J, Fu X, Zhong Y, Meng F, Luo T, Liu J. Carbon. 2010; 48:1262.

(283). Sun Y-P, Fu K, Lin Y, Huang W. Acc. Chem. Res. 2002; 35:1096. [PubMed: 12484798]

(284). Hussain CM, Saridara C, Mitra S. Analyst. 2009; 134:1928. [PubMed: 19684921]

(285). Kauffman DR, Shade CM, Uh H, Petoud S, Star A. Nature Chem. 2009; 1:500. [PubMed: 21378918]

(286). Staii C, Johnson AT Jr. Chen M, Gelperin A. Nano Lett. 2005; 5:1774. [PubMed: 16159222]

(287). Kuang Z, Kim SN, Crookes-Goodson WJ, Farmer BL, Naik RR. ACS Nano. 2010; 4:452. [PubMed: 20038158]

(288). Wu R-J, Huang Y-C, Yu M-R, Lin TH, Hung S-L. Sens. Actuators B. 2008; 134:213.

(289). Kauffman DR, Sorescu DC, Schofield DP, Allen BL, Jordan KD, Star A. Nano Lett. 2010 DOI: 10.1021/nl903888c.

(290). Leghrib R, Pavelko R, Felten A, Vasiliev A, Cané C, Gràcia I, Pireaux J-J, Llobet E. Sens. Actuators B. 2010; 145:411.

(291). Kim W, Javey A, Vermesh O, Wang Q, Li Y, Dai H. Nano Lett. 2003; 3:193.

(292). Kuzmych O, Allen BL, Star A. Nanotechnology. 2007; 18 art. no. 375502.

(293). Mendoza D, Santiago P. J. Nanosci. Nanotechnol. 2008; 8:6523. [PubMed: 19205234]

(294). Peng N, Zhang Q, Lee YC, Huang H, Tan OK, Tian J, Chan L. Sensor Lett. 2008; 6:796.

(295). Zhang T, Mubeen S, Yoo B, Myung NV, Deshusses MA. Nanotechnology. 2009; 20 art. no. 255501.

(296). Santucci S, Picozzi S, Di Gregorio F, Lozzi L, Cantalini C, Valentini L, Kenny JM, Delley B. J. Chem. Phys. 2003; 119:10904.

(297). Lampe, U.; Fleischer, M.; Reitmeier, N.; Meixner, H.; McMonagle, JB.; Marsh, A. New Materials for Metal Oxide Sensors. In: Baltes, H.; Göpel, W.; Hesse, J., editors. Sensors Update. Vol. Vol. 2. VCH; Weinheim: 1996. p. 1

(298). Novoselov KS, Geim AK, Morozov SV, Jiang D, Zhang Y, Dubonos SV, Grigorieva IV, Firsov AA. Science. 2004; 306:666. [PubMed: 15499015]

(299). Schedin F, Geim AK, Morozov SV, Hill EW, Blake P, Katsnelson MI, Novoselov KS. Nature Materials. 2007; 6:652.

(300). Geim AK. Science. 2009; 324:1530. [PubMed: 19541989]

(301). Rao CNR, Sood AK, Subrahmanyam KS, Govindaraj A. Angew. Chem. Int. Ed. 2009; 48:7752.

(302). Ratinac KR, Yang W, Ringer SP, Braet F. Environ. Sci. Technol. 2010; 44:1167. [PubMed: 20099803]

(303). Yang W, Ratinac KR, Ringer SP, Thordarson P, Gooding JJ, Braet F. Angew. Chem. Int. Ed. 2010; 49:2114.

(304). Fowler JD, Allen MJ, Tung VC, Yang Y, Kaner RB, Weiller BH. ACS Nano. 2009; 3:301. [PubMed: 19236064]

(305). Dan Y, Lu Y, Kybert NJ, Luo Z, Johnson ATC. Nano Lett. 2009; 9:1472. [PubMed: 19267449]

(306). Arsat R, Breedon M, Shafiei M, Spizziri PG, Gilje S, Kaner RB, Kalantar-zadeh K, Wlodarski W. Chem. Phys. Lett. 2009; 467:344.

(307). Park S, Ruoff RS. Nature Nanotechn. 2009; 4:217.

(308). Robinson JT, Perkins FK, Snow ES, Wei Z, Sheehan PE. Nano Lett. 2008; 8:3137. [PubMed: 18763832]

(309). Huang B, Li Z, Liu Z, Zhou G, Hao S, Wu J, Gu B-L, Duan W. J. Phys. Chem. C. 2008; 112:13442.

(310). Zhang Y-H, Chen Y-B, Zhou K-G, Liu C-H, Zeng J, Zhang H-L, Peng Y. Nanotechnology. 2009; 20 art. no. 185504.

(311). Dai J, Yuan J, Giannozzi P. Appl. Phys. Lett. 2009; 95 art. no. 232105.

(312). Zhang Y-H, Zhou K-G, Xie K-F, Zeng J, Zhang H-L, Peng Y. Nanotechnology. 2010; 21 art. no. 065201.

(313). Mizuno M, Kim EH. Appl. Phys. Lett. 2009; 94 art. no. 082108.

(314). Dua V, Surwade SP, Ammu S, Agnihotra SR, Jain S, Roberts KE, Park S, Ruoff RS, Manohar SK. Angew. Chem. Int. Ed. 2010; 49:2154.

(315). Jung I, Dikin D, Park S, Cai W, Mielke SL, Ruoff RS. J. Phys. Chem. C. 2008; 112:20264.

(316). Wohltjen H, Snow AW. Anal. Chem. 1998; 70:2856.

(317). Cai Q-Y, Zellers ET. Anal. Chem. 2002; 74:3533. [PubMed: 12139065]

(318). Steinecker WH, Rowe MP, Zellers ET. Anal. Chem. 2007; 79:4977. [PubMed: 17523593]

(319). Evans SD, Johnson SR, Cheng YL, Shen T. J. Mater. Chem. 2000; 10:183.

(320). Drake C, Deshpande S, Bera D, Seal S. Intern. Mat. Rev. 2007; 52:289.

(321). Zabet-Khosousi A, Dhirani A-A. Chem. Rev. 2008; 108:4072. [PubMed: 18811216]

(322). Wang L, Shi X, Kariuki NN, Schadt M, Wang GR, Rendeng Q, Choi J, Luo J, Susan Lu S, Zhong C-J. J. Am Chem. Soc. 2007; 129:2161. [PubMed: 17253690]

(323). Joseph Y, Guse B, Yasuda A, Vossmeyer T. Sens. Actuators B. 2004; 98:188.

(324). Wang L, Luo J, Yin J, Zhang H, Wu J, Shi X, Crew E, Xu Z, Rendeng Q, Lu S, Poliks M, Sammakia B, Zhong C-J. J. Mater. Chem. 2010; 20:907.

(325). Yang C-Y, Li C-L, Lu C-J. Anal. Chim. Acta. 2006; 565:17. [PubMed: 17723413]

(326). Ibañez FJ, Zamborini FP. ACS Nano. 2008; 2:1543. [PubMed: 19206357]

(327). Joseph Y, Guse B, Nelles G. Chem. Mater. 2009; 21:1670.

(328). Krasteva N, Guse B, Besnard I, Yasuda A, Vossmeyer T. Sens. Actuators B. 2003; 92:137.

(329). Krasteva N, Fogel Y, Bauer RE, Müllen K, Joseph Y, Matsuzawa N, Yasuda A, Vossmeyer T. Adv. Funct. Mater. 2007; 17:881.

(330). Joseph Y, Peie A, Chen X, Michl J, Vossmeyer T, Yasuda A. J. Phys. Chem. C. 2007; 111:12855.

(331). Love JC, Estroff LA, Kriebel JK, Nuzzo RG, Whitesides GM. Chem. Rev. 2005; 105:1103. [PubMed: 15826011]

(332). Zotti G, Vercelli B, Berlin A. Chem. Mater. 2008; 20:397.

(333). Vörös NM, Patakfalvi R, Dékány I. Coll. Surfaces A. 2008; 329:205.

(334). Im J, Chandekar A, Whitten JE. Langmuir. 2009; 25:4288. [PubMed: 19366214]

(335). Grate JW, Nelson DA, Skaggs R. Anal. Chem. 2003; 75:1868. [PubMed: 12713045]

(336). Smardzewski RR, Jarvis NL, Snow AW, Wohltjen H. Proc. Sci. Conf. Chem. Bio. Defense Res. 2004 ADM001849.

(337). McGill RA, Abraham MH, Grate JW. ChemTech. 1994; 9:27.

(338). Crooks RM, Ricco AJ. Acc. Chem. Res. 1998; 31:219.

(339). Peng G, Tisch U, Adams O, Hakim M, Shehada N, Broza YY, Billan S, Abdah-Bortnyak R, Kuten A, Haick H. Nature Nanotechn. 2009; 4:669.

(340). Peng G, Hakim M, Broza YY, Billan S, Abdah-Bortnyak R, Kuten A, Tisch U, Haick H. British Journal of Cancer. 2010; 103:542. [PubMed: 20648015]

(341). Krasteva N, Möhwald H, Krastev R. C. R. Chimie. 2009; 12:129.

(342). Pang P, Guo Z, Cai Q. Talanta. 2005; 65:1343. [PubMed: 18969951]

(343). Pang P, Guo J, Wu S, Cai Q. Sens. Actuators B. 2006; 114:799.

(344). Brust M, Walker M, Bethell D, Schiffrin DJ, Whyman RJ. J. Chem. Soc., Chem. Commun. 1994:801.

(345). Cortés E, Rubert AA, Benitez G, Carro P, Vela ME, Salvarezza RC. Langmuir. 2009; 25:5661. [PubMed: 19348488]

(346). Ancona MG, Snow AW, Foos EE, Kruppa W, Bass R. IEEE Sensors J. 2006; 6:1403.

(347). Covington EL, Turner RW, Kurdak C, Rowe MP, Xu C, Zellers ET. Proc. IEEE Sensors. 2008

(348). Bohrer FI, Covington E, Kurdak Ç, Zellers ET. Proc. Transducers '09. 2009:148.

(349). Kolmakov A, Moskovits M. Annu. Rev. Mater. Res. 2004:151.

(350). Fergus JW. Sens. Actuators B. 2007; 123:1169.

(351). Barsan N, Koziej D, Weimar U. Sens. Actuators B. 2007; 121:18.

(352). Comini E, Baratto C, Faglia G, Ferroni M, Vomiero A, Sberveglieri G. Prog. Mater. Sci. 2009; 54:1.

(353). Lee J-H. Sens. Actuators B. 2009; 140:319.

(354). Korotcenkov G, Cho BK. Crit. Rev. Solid State Mater. Sci. 2010; 35:1.

(355). Choi KJ, Jang HW. Sensors. 2010; 10:4083.

(356). Cram DJ. Science. 1983; 219:1177. [PubMed: 17771285]

(357). Xu X, Li C, Pei K, Zhao K, Zhao ZK, Li H. Sens. Actuators B. 2008; 134:258.

(358). Tseng M-C, Chu Y-H. Chem. Commun. 2010; 46:2983.

(359). Dickert FL, Zwissler GK, Obermeier E. Phys. Chem. Chem. Phys. 1993; 97:184.

(360). Patrash SJ, Zellers ET. Anal. Chim. Acta. 1994; 288:167.

(361). Feresenbet EB, Taylor F, Chinowsky TM, Yee SS, Shenoy DK. Sensor Lett. 2004; 2:145.

(362). Lu C-J, Shih J-S. Anal. Chim. Acta. 1995; 306:129.

(363). Xing W-L, He X-W. Analyst. 1997; 122:587.

(364). Kuchmenko TA, Lisitskaya RP, Bobrova OS. J. Anal. Chem. 2010; 65:195.

(365). Mitsubayashi K, Matsunaga H, Nishio G, Toda S, Nakanishi Y. Biosens. Bioelectron. 2005; 20:1573. [PubMed: 15626611]

(366). Perinotto AC, Caseli L, Hayasaka CO, Riul A Jr. Oliveira ON Jr. Zucolotto V. Thin Solid Films. 2008; 516:9002.

(367). Castaldo A, Massera E, Quercia L, Di Francia G. Macromol. Symp. 2007; 247:350.

(368). Patel SV, Hobson ST, Cemalovic S, Mlsna TE. J. Sol-Gel Sci. Technol. 2010; 53:673.

(369). Heiland G. Zeit. Phys. 1954; 138:459.

(370). Bielanski A, Deren J, Haber J. Nature. 1957; 179:668.

(371). Korotcenkov G. Mater. Sci. Eng. B. 2007; 139:1.

(372). Ishihara T, Kometani K, Mizuhara Y, Takita Y. Sens. Actuators B. 1991; 5:97.

(373). Ishihara T, Sato S, Takita Y. Sens. Actuators B. 1996; 30:43.

(374). Herran J, Mandayo GG, Castano E. Sens. Actuators B. 2008; 129:705.

(375). Tricoli A, Righettoni M, Pratsinis SE. Nanotechnology. 2009; 20 art. no. 315502.

(376). Scott RWJ, Yang SM, Coombs N, Ozin GA, Williams DE. Adv. Funct. Mater. 2003; 13:225.

(377). Kim I-D, Rothschild A, Hyodo T, Tuller HL. Nano Lett. 2006; 6:193. [PubMed: 16464033]

(378). Zuruzi AS, MacDonald NC, Moskovits M, Kolmakov A. Angew. Chem. Int. Ed. 2007; 46:4298.

(379). Jia L, Cai W, Wang H, Sun F, Li Y. ACS Nano. 2009; 3:2697. [PubMed: 19702282]

(380). Strelcov E, Dmitriev S, Button B, Cothren J, Sysoev V, Kolmakov A. Nanotechnology. 2008; 19 art. no. 355502.

(381). Zhao J, Wu S, Liu J, Liu H, Gong S, Zhou D. Sens. Actuators B. 2010; 145:788.

(382). Xu L, Dong B, Wang Y, Bai X, Chen J, Liu Q, Song H. J. Phys. Chem. C. 2010; 114:9089.

(383). Helwig A, Müller G, Sberveglieri G, Eickhoff M. J. Sensors. 2009 art. no. 620720.

(384). Bein T, Brown K, Frye GC, Brinker CJ. J. Am. Chem. Soc. 1989; 111:7640.

(385). Yan Y, Bein T. Chem. Mater. 1992; 4:975.

(386). Fischerauer A, Gollwitzer A, Thalmayr F, Hagen G, Moos R, Fischerauer G. Sensor Lett. 2008; 6:1019.

(387). Gora L, Kuhn J, Baimpos T, Nikolakis V, Kapteijn F, Serwicka EM. Analyst. 2009; 134:2118. [PubMed: 19768223]

(388). Yasuda KE, Visser JH, Bein T. Microporous Mesoporous Materials. 2009; 119:356.

(389). Urbiztondo MA, Pellejero I, Villarroya M, Sesé J, Pina MP, Dufour I, Santamaría J. Sens. Actuators B. 2009; 137:608.

(390). Rodríguez-Gonzlez L, Simon U. Meas. Sci. Tech. 2010; 21 art. no. 027003.

(391). Tavolaro A, Drioli E. Adv. Mater. 1999; 11:975.

(392). Vilaseca M, Coronas J, Cirera A, Cornet A, Morante JR, Santamaría J. Catalysis Today. 2003; 82:179.

(393). Fong YY, Abdullah AZ, Ahmad AL, Bhatia S. Sensor Lett. 2007; 5:485.

(394). Snyder MA, Tsapatsis M. Angew. Chem. Int. Ed. 2007; 46:7560.

(395). Coronas J. Chem. Eng. J. 2010; 156:236.

(396). Smit B. Chem. Rev. 2008; 108:4125. [PubMed: 18817356]

(397). Akporiaye DE. Angew. Chem. Int. Ed. 1998; 37:2456.

(398). Yan Y, Bein T. J. Phys. Chem. 1992; 96:9387.

(399). Li X, Dutta PK. J. Phys. Chem. C. 2010; 114:7986.

(400). Neumeier S, Echterhof T, Bölling R, Pfeifer H, Simon U. Sens. Actuators B. 2008; 134:171.

(401). Zhang J, Tang X, Dong J, Wei T, Xiao H. Sens. Actuators B. 2009; 135:420.

(402). Rebek J Jr. Science. 1987; 235:1478. [PubMed: 3823899]

(403). Schierbaum KD, Weiss T, Thoden Van Velzen EU, Engbersen JFJ, Reinhoudt DN, Göpel W. Science. 1994; 265:1413. [PubMed: 17833812]

(404). Grate JW, Patrash SJ, Abraham MH, Du CM. Anal. Chem. 1996; 68:913. [PubMed: 21619189]

(405). Dickert FL, Schuster O. Mikrochim. Acta. 1995; 119:55.

(406). Grate JW. Chem. Rev. 2000; 100:2627. [PubMed: 11749298]

(407). Schneider H-J. Angew. Chem. Int. Ed. 2009; 48:3924.

(408). Pinalli R, Suman M, Dalcanale E. Eur. J. Org. Chem. 2004:451.

(409). Tonezzer M, Melegari M, Maggioni G, Milan R, Della Mea G, Dalcanale E. Chem. Mater. 2008; 20:6535.

(410). Condorelli GG, Motta A, Favazza M, Gurrieri E, Betti P, Dalcanale E. Chem. Commun. 2010; 46:288.

(411). Ehlen A, Wimmer C, Weber E, Bargon J. Angew. Chem. Int. Ed. 1993; 32:110.

(412). Finklea HO, Phillippi MA, Lompert E, Grate JW. Anal. Chem. 1998; 70:1268. [PubMed: 21644723]

(413). Yakimova LS, Ziganshin MA, Sidorov VA, Kovalev VV, Shokova EA, Tafeenko VA, Gorbatchuk VV. J. Phys. Chem. B. 2008; 112:15569. [PubMed: 19368014]

(414). Cha J-H, Lee W, Lee H. Angew. Chem. Int. Ed. 2009; 48:8687.

(415). Kosal ME, Chou J-H, Wilson SR, Suslick KS. Nature Mater. 2002; 1:118. [PubMed: 12618827]

(416). Medforth CJ, Wang Z, Martin KE, Song Y, Jacobsen JL, Shelnutt JA. Chem. Commun. 2009:7261.

(417). Di Natale C, Monti D, Paolesse R. Materials Today. 2010; 13(7–8):46.

(418). Di Natale C, Macagnano A, Repole G, Saggio G, D'Amico A, Paolesse R, Boschi T. Matl. Sci. Eng. C. 1998; 5:209.

(419). Rowsell JLC, Yaghi OM. Microporous Mesoporous Materials. 2004; 73:3.

(420). Fang Q-R, Makal TA, Young MD, Zhou H-C. Comm. Inorg. Chem. 2010; 31:165.

(421). MacGillivray, LR., editor. Metal-Organic Frameworks: Design and Application. Wiley; Hoboken, NJ: 2010.

(422). Zacher D, Schmid R, Wöll C, Fischer RA. Angew. Chem. Int. Ed. 2011; 50:176.

(423). Chen B, Xiang S, Qian G. Acc. Chem. Res. 2010; 43:1115. [PubMed: 20450174]

(424). Ferey C, Mellot-Draznieks C, Serre C, Millange F, Dutour J, Surble S, Margiolaki I. Science. 2005; 309:2040. [PubMed: 16179475]

(425). Furukawa H, Ko N, Go YB, Aratani N, Choi SB, Choi E, Yazaydin AO, Snurr RQ, O'Keeffe M, Kim J, Yaghi OM. Science. 2010; 329:424. [PubMed: 20595583]

(426). Achmann S, Hagen G, Kita J, Malkowsky IM, Kiener C, Moos R. Sensors. 2009; 9:1574.

(427). Biemmi E, Darga A, Stock N, Bein T. Microporous and Mesoporous Materials. 2008; 114:380.

(428). Zybaylo O, Shekhah O, Wang H, Tafipolsky M, Schmid R, Johannsmann D, Wöll C. Phys. Chem. Chem. Phys. 2010; 12:8092. [PubMed: 20532258]

(429). Lu G, Hupp JT. J. Am Chem. Soc. 2010; 132:7832. [PubMed: 20486704]

(430). Kreno LE, Hupp JT, Van Duyne RP. Anal. Chem. 2010; 82:8042. [PubMed: 20839787]

(431). Allendorf MD, Houk RJT, Andruszkiewicz L, Talin AA, Pikarsky J, Choudhury A, Gall KA, Hesketh PJ. J. Am. Chem. Soc. 2008; 130:14404. [PubMed: 18841964]

(432). Akyildiz IF, Su W, Sankarasubramaniam Y, Cayirci E. Computer Networks. 2002; 38:393.

(433). De Vito S, Di Palma P, Ambrosino C, Massera E, Burrasca G, Miglietta ML, Di Francia G. IEEE Sensors J. 2011; 11:947.

(434). Tsujita W, Yoshino A, Ishida H, Moriizumi T. Sens. Actuators B. 2005; 110:304.

(435). Al-Ali AR, Zualkernan I, Aloul F. IEEE Sensors J. 2010; 10:1666.

(436). Becher C, Kaul P, Mitrovics J, Warmer J. Sens. Actuators B. 2010; 146:513.

(437). Lane G, Brueton C, Diall D, Airantzis D, Jeremijenko N, Papamarkos G, Roussos G, Martin K. IET Conf. Public. 2006; 518:23.

(438). Chen L, Yang S, Xi Y. International Conference on Computer, Mechatronics, Control and Electronic Engineering. 2010; 4:425.

(439). Salehi-Khojin A, Lin KY, Field CR, Masel RI. Science. 2010; 329:1327. [PubMed: 20829482]

(440). Potyrailo RA, Morris WG, Wroczynski RJ. Rev. Sci. Instrum. 2004; 75:2177.

(441). Steinecker WH, Kim SK, Bohrer FI, Farina L, Kurdak Ç, Zellers ET. IEEE Sensors J. 2011; 11:469.

(442). Hartmann-Thompson C, Hu J, Kaganove SN, Keinath SE, Keeley DL, Dvornic PR. Chem. Mater. 2004; 16:5357.

(443). Potyrailo RA, Sivavec TM. Anal. Chem. 2004; 76:7023. [PubMed: 15571355]

(444). Pestov D, Guney-Altay O, Levit N, Tepper G. Sens. Actuators B. 2007; 126:557.

(445). Garg N, Mohanty A, Lazarus N, Schultz L, Rozzi TR, Santhanam S, Weiss L, Snyder JL, Fedder GK, Jin R. Nanotechnology. 2010; 21 art. no. 40550.

(446). Martinelli E, Santonico M, Pennazza G, Paolesse R, D'Amico A, Di Natale C. Sens. Actuators B. 2011 ASAP paper.

(447). Liu S, Tu D, Zhang Y. Proc. IEEE Int Conf. Intelligent Comput. Intelligent Syst. 2009; 3 art. no. 5358197.

(448). Diamond D. Anal. Chem. 2004; 76:278A.

(449). Bicelli S, Depari A, Faglia G, Flammini A, Fort A, Mugnaini M, Ponzoni A, Vignoli V, Rocchi S. IEEE Trans. Instrum. Meas. 2009; 58:1324.

(450). The Times (London). March 28th. 2004

(451). Ramachandra Rao GV, Murali M, Satya Prasad K, Rama Rao CB. Pollution Res. 2009; 28:561.

(452). Grimes CA, Ong KG, Varghese OK, Yang X, Mor G, Paulose M, Dickey EC, Ruan C, Pishko MV, Kendig JW, Mason AJ. Sensors. 2003; 3:69.

(453). Shepherd R, Beirne S, Lau KT, Corcoran B, Diamond D. Sens. Actuators B. 2007; 121:142.

(454). Yingjun Z, Shengwei X, Peng X, Xinquan W. Proc. Intl Conf. Networked Comput. 2010 art. no. 5484814.

(455). Gutierrez A, González-Mas MC, Bernet GP, López S. Acta Horticulturae. 2010; 877:1357.

(456). Mason A, Al-Shamma'a AI, Shaw A. Proc. Intl Conf. Developm. eSyst. Eng. 2009 art. no. 5395161.

(457). Panoptic Analysis of Chemical Traces (PACT), DARPA-BAA-08-62. 2008.

(458). Janasek D, Franzke J, Manz A. Nature. 2006; 442:374. [PubMed: 16871204]

(459). Ramsey, JM.; Whitten, W.; Pau, S.; Denton, MB. Highly Miniaturized Mass Spectrometer. Pittsburgh Conference on Analytical Chemistry and Applied Spectroscopy; Orlando, FL USA. February 28 – March 4; 2010.

(460). Zimmermann S, Barth S, Baether WKM, Ringer J. Anal. Chem. 2008; 80:6671. [PubMed: 18665610]

(461). Babis JS, Sperline RP, Knight AK, Jones DA, Gresham CA, Denton MB. Anal. Bioanal. Chem. 2009; 395:411. [PubMed: 19424683]

(462). Zampolli S, Elmi I, Mancarella F, Betti P, Dalcanale E, Cardinali GC, Severi M. Sens. Actuators B. 2009; 141:322.

(463). Serrano G, Chang H, Zellers ET. Transducers '09. 2009:1654.

(464). Chen R, Codella PJ, Guida R, Zribi A, Vert A, Potyrailo R, Baller M. Photonic bandgap fiber enabled Raman detection of nitrogen gas, Proc. SPIE-Int. Soc. Opt. Eng. 2009; 7322 (Photonic Microdevices/Microstructures for Sensing) 73220N1.

(465). Modi A, Koratkar N, Lass E, Wei B, Ajayan PM. Nature. 2003; 424:171. [PubMed: 12853951]

(466). Department of Defence, Prepared by the Deputy Under Secretary of Defense for Science and Technology (DUSD(S&T)). 2005. https://acc.dau.mil/CommunityBrowser.aspx?id=18545

(467). Butler D. Nature. 2008; 453:840. [PubMed: 18548043]

(468). Korotcenkov G, Cho BK. Sens. Actuators B. 2011 In Press.

(469). Arnold C, Harms M, Goschnick J. IEEE Sensors J. 2002; 2:179.

(470). Wohltjen, H. A Journey: From Sensor Ideas to Sensor Products. Plenary talk at the 11th International Meeting on Chemical Sensors; July 16–19, 2006; Italy: University of Brescia; Elsevier Science; 2006.

(471). Lim SH, Feng L, Kemling JW, Musto CJ, Suslick KS. Nature Chemistry. 2009:562.

(472). Ohira SI, Dasgupta PK, Schug KA. Anal. Chem. 2009; 81:4183. [PubMed: 19402646]

(473). Lambertsen, CJ. The atmosphere and gas exchanges with the lungs and blood. In: Mountcastle, VB., editor. Medical Physiology. The C. V. Mosby Company; Saint Louis, MO: 1968. p. 629

(474). Dubowski KM. Clin. Chem. 1974; 20:966. [PubMed: 4850825]

(475). Bradley K, Cumings J, Star A, Gabriel J-CP, Gruner G. Nano Lett. 2003; 3:639.

(476). Kleine-Ostmann T, Jördens C, Baaske K, Weimann T, De Angelis MH, Koch M. Appl. Phys. Lett. 2006; 88 art. no. 102102.

(477). Righettoni M, Tricoli A, Pratsinis SE. Anal. Chem. 2010; 82:3581. [PubMed: 20380475]

(478). Janiak C. Angew. Chem. Int. Ed. 1997; 36:1431.

(479). Wang Z, Cohen SM. Chem. Soc. Rev. 2009; 38:1315. [PubMed: 19384440]

(480). Tanaka D, Henke A, Albrecht K, Moeller M, Nakagawa K, Kitagawa S, Groll J. Nature Chem. 2010; 2:410. [PubMed: 20414244]

(481). Zampolli S, Betti P, Elmi I, Dalcanale E. Chem. Commun. 2007:2790.

(482). McConney ME, Anderson KD, Brott LL, Naik RR, Tsukruk VV. Adv. Funct. Mater. 2009; 19:2527.

(483). Song F, Su H, Han J, Zhang D, Chen Z. Nanotechnology. 2009; 20 art. no. 495502.

(484). Biró LP, Vigneron JP. Laser & Photon. Rev. 2010; 1–26

(485). Kumar, CSSR., editor. Nanomaterials: toxicity, health and environmental issues. Wiley-VCH; Weinheim, Germany: 2006.

(486). Donaldson K, Murphy FA, Duffin R, Poland CA. Particle and Fibre Toxicology. 2010; 7:5. [PubMed: 20307263]

(487). Houlton, S. 2010. http://www.rsc.org/chemistryworld/News/2010/June/14061001.asp

(488). Surman, C.; Morris, WG.; Potyrailo, RA. Quantitation of toxic vapors in variable humidity atmosphere using individual passive radio frequency identification (RFID) sensors. 12th International Meeting on Chemical Sensors; Columbus, OH: Elsevier Science; 2008. Talk SADA 12

(489). Hackner A, Habauzit A, Müller G, Comini E, Faglia G, Sberveglieri G. IEEE Sensors J. 2009; 9:1727.

(490). Kawano T, Chiamori HC, Suter M, Zhou Q, Sosnowchik BD, Lin L. Nano Lett. 2007; 7:3686. [PubMed: 18001108]

(491). Beccherelli R, Zampetti E, Pantalei S, Bernabei M, Persaud KC. Sens. Actuators B. 2010; 146:446.
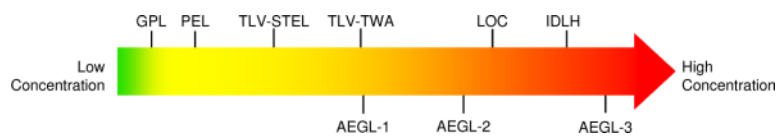
Figure 1.
Examples of regulated vapor-exposure limits established by different organizations:

GPL: General Population Limit, established by USACHPPM – U.S. Army Center for Health Promotion and Preventative Medicine;

PEL: Permissible Exposure Limit, established by OSHA, Occupational Safety and Health Administration;

TLV-STEL: Threshold Limit Value (Short Term Exposure Limit) and TLV-TWA: Threshold Limit Value (Time Weighted Average), established by ACGIH, American Conference of Governmental Industrial Hygenists;

IDLH: Immediately Dangerous to Life or Health and *LOC: Level of Concern*, 0.1×IDLH, established by NIOSH, U.S. National Institute for Occupational Safety and Health;

AEGL-1,2,3: Acute Exposure Guideline Levels, established by EPA – U.S. Environmental Protection Agency.

Figure 2.
Number of publications on wireless sensors (as searched in Inspec and Scopus databases).
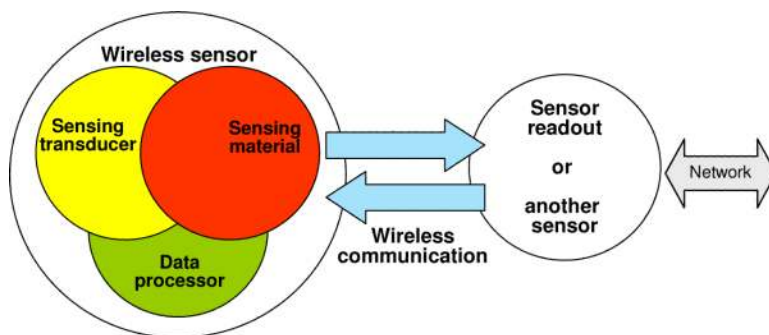
Figure 3.
Subsystem schematic of a typical wireless sensor and its wireless communication with a sensor reader/display.
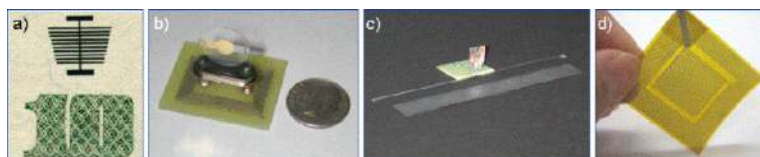
Figure 4.
Examples of battery-free (passive) wireless sensors based on (a) magnetoelastic, (b) thickness shear mode, (c) surface acoustic wave, and (d) resonant inductor–capacitor-resistor transducers. Figure 5d is photo courtesy of K. G. Ong (Michigan Technological University), used by permission. (a) Reprinted with permission from reference[53]. Copyright 2007 IEEE.
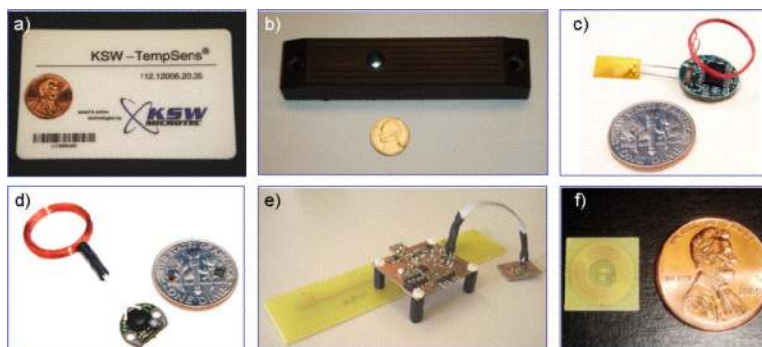
Figure 5.
Examples of active and passive RFID sensors. Active sensors with (a) thin-film and (b) AAA-type batteries. Passive sensors with an analog input into an IC memory chip for operation at (c), LF (d), HF and (e) UHF frequency ranges; (f) passive sensor based on a common HF RFID tag with a sensing material applied directly to the resonant antenna of the sensor. Figures 5c–d are courtesy of Phase IV Engineering, Inc., used by permission. Figure 5e is courtesy of Schneider Electric, used by permission.
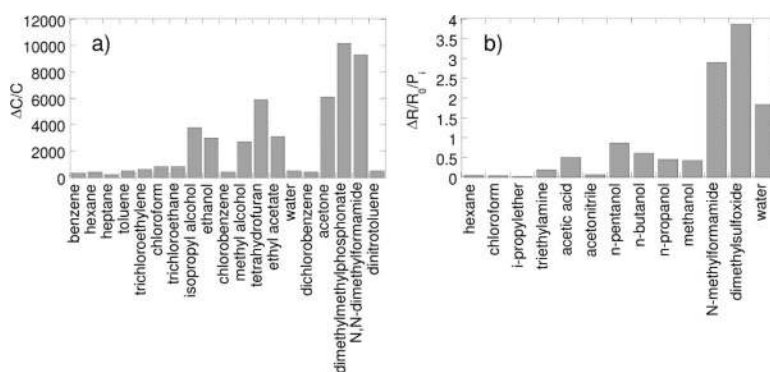
Figure 6.
Typical response cross-sensitivity of different types of sensing materials to a variety of vapors: (a) capacitance response pattern of single-wall carbon nanotubes and (b) resistance response pattern of $LiMo_3Se_3$ nanowires. (a) Reprinted with permission from reference[88]. Copyright 2005 AAAS. (b) Reprinted with permission from reference[89]. Copyright 2005 American Chemical Society.
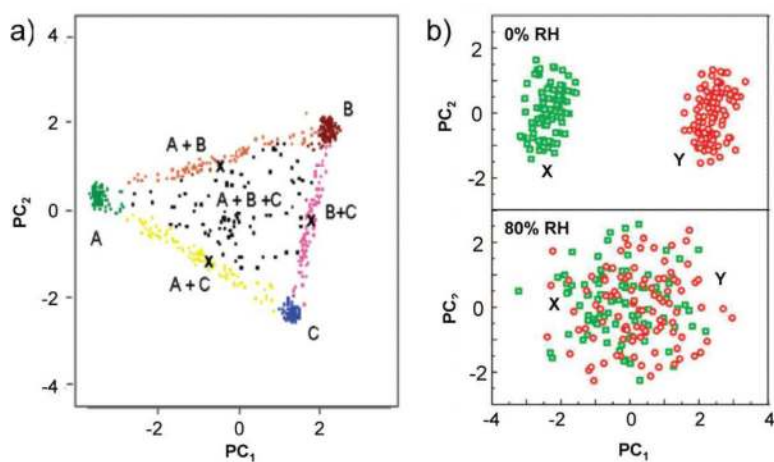
Figure 7.
Operation of sensor arrays for detection of several components in gas mixtures depicted as scores plots from principal components analysis. (a) Monte Carlo simulated response of a sensor array to three individual vapors A, B, and C and their binary and ternary mixtures. Sensor array responses were normalized by dividing each response by the sum of the responses from all sensors for a given vapor or vapor mixture. (b) Response of an array of 10 chemiresistors coated with diverse surface-functionalized single wall carbon nanotubes sensing films upon exposure to two types of vapor mixtures (X, green squares and Y, red circles) at 0 and 80 % RH. (a) Reprinted with permission from reference[85]. Copyright 2004 American Chemical Society. (b) Reprinted with permission from reference[103]. Copyright 2008 American Chemical Society.
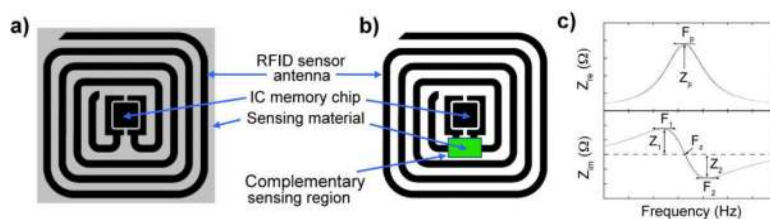
Figure 8.
The operating principle of passive battery-free RFID sensors with multivariable response:
(a) Sensing material is applied onto the resonant antenna of the RFID tag. (b)
Complementary sensor is attached across an antenna and memory chip. In both cases (a, b)
the electrical response of the sensing material is translated into changes in the impedance
response of the sensor. (c) Measured impedance spectrum (real part $Z_{re}(f)$ and imaginary
part $Z_{im}(f)$ of impedance) and examples of parameters for multivariate analysis: frequency
position F_p and magnitude Z_p of $Z_{re}(f)$ and resonant F_1 and antiresonant F_2 frequencies of
$Z_{im}(f)$.
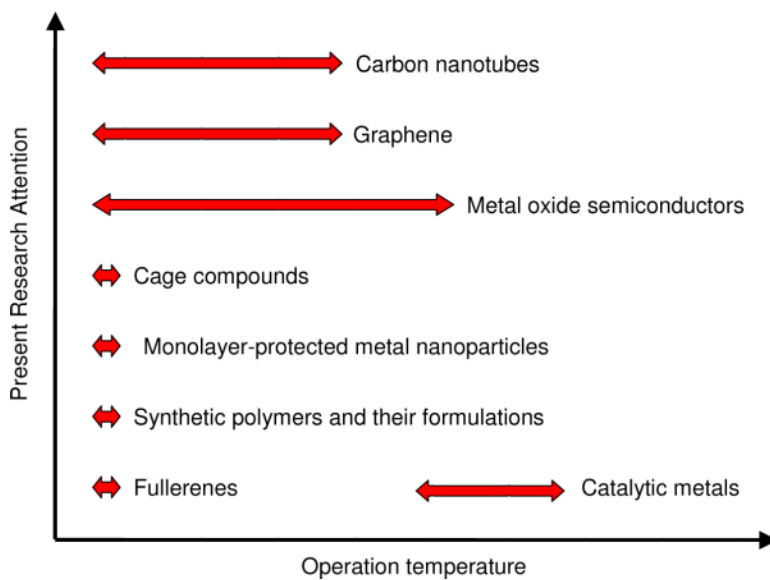
Figure 9.
General summary of research activities in development of sensing materials for transducers
with different power requirements applicable for wireless sensing.
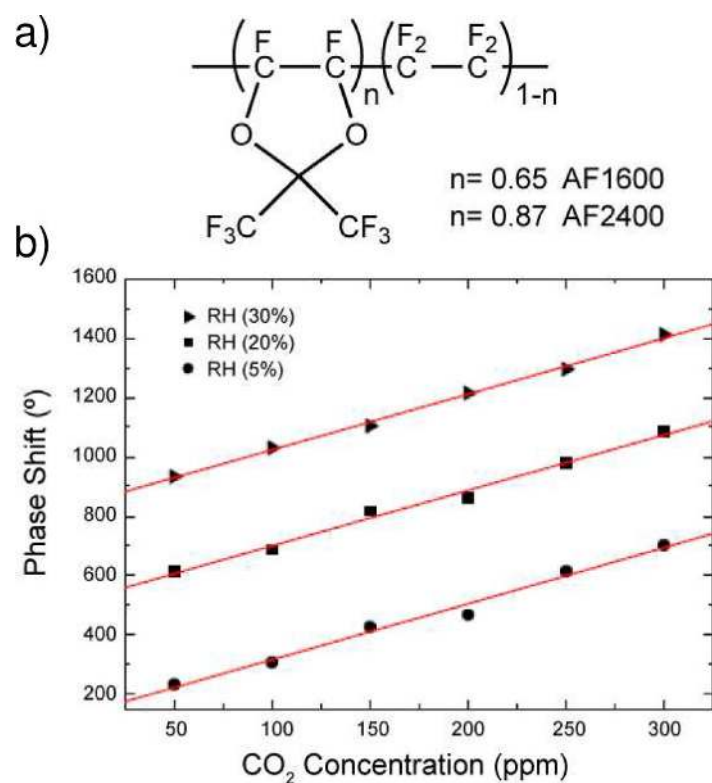
Figure 10.
Application of a random copolymer Teflon AF2400 prepared from tetrafluoroethylene and 2,2-bis(trifluoromethyl)-4,5-difluoro-1,3-dioxole for CO_2 sensing using a wireless SAW sensor. (a) Chemical structures of Teflon AF2400 and AF1600. (b) Sensor response to CO_2 at different humidity levels. Reprinted with permission from reference[64]. Copyright 2007 IOP Publishing.
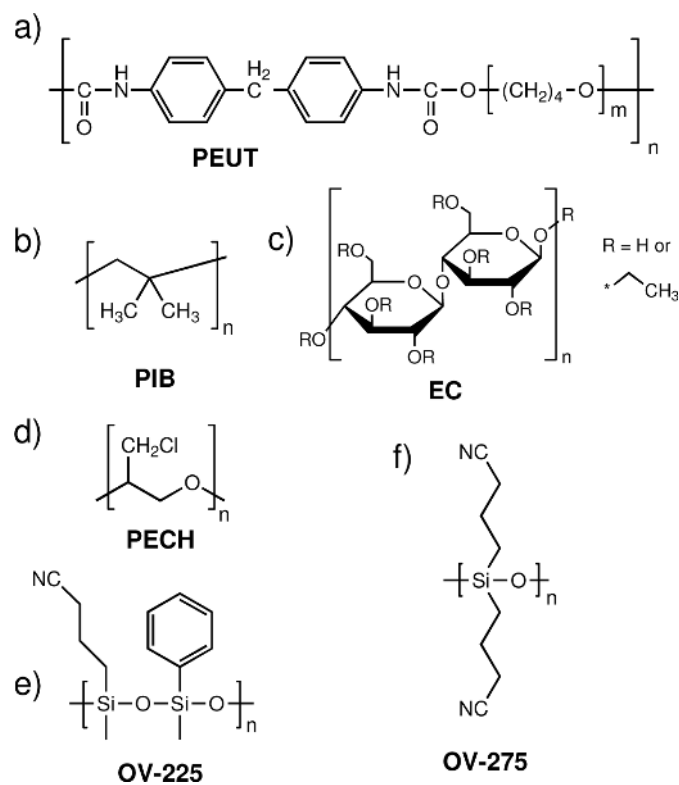
Figure 11.
Representative examples of low-T_g polymers that became "classic" benchmark sensing materials. (a) polyetherurethane (PEUT), (b) polyisobutylene (PIB), (c) ethyl cellulose (EC), (d) polyepichlorihydrin (PECH), (e) cyanopropyl methyl phenylmethyl silicone (OV-225), and (f) dicyanoallyl silicone (OV-275).
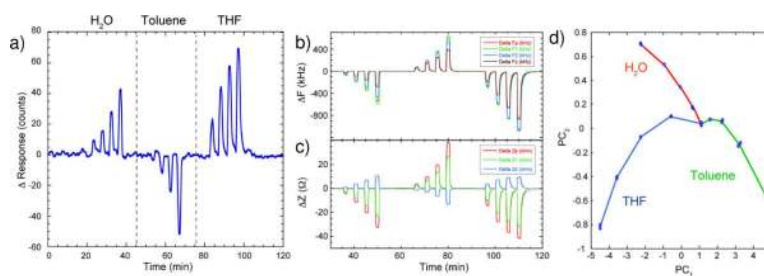
Figure 12.
Comparison of the ability to discriminate between three individual vapors (water, toluene, and THF) using different transducers coated with the same PEUT films: (a) Performance of a passive RFID sensor with a capacitance transducer. (b–d) Performance of an RFID sensor with multi-variable signal transduction; individual sensor responses (b) Fp, F1, F2, Fz, and (c) Zp, Z1, Z2; and (d) Scores plot of a PCA model of an individual RFID sensor response.
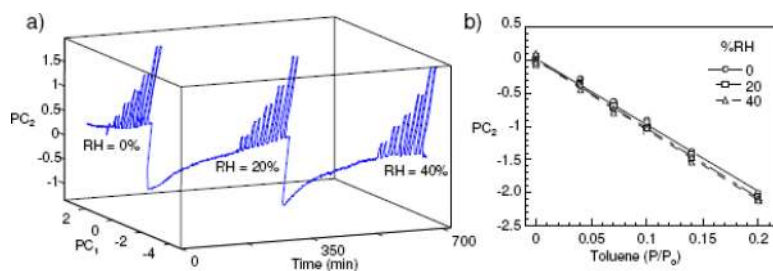
Figure 13.
Demonstration of humidity-independent operation using a single RFID sensor with multivariable signal transduction and PEUT sensing polymer. (a) Plot of PC_1 vs. PC_2 vs. time illustrates sensor response to five concentrations of toluene vapor (0.04, 0.07, 0.10, 0.14, and 0.20 P/P_o, two replicates each) at three humidity levels. (b) Multivariate calibration curves for toluene detection at 0, 20, and 40 %RH.
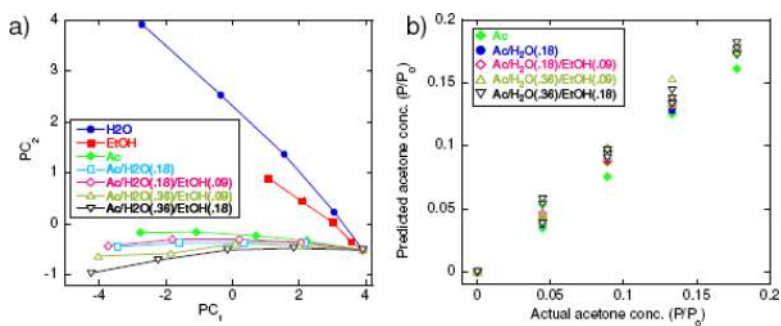
Figure 14.
Quantitation of an analyte vapor (acetone) in the presence of multiple interferences (water and ethanol vapors) using a single RFID sensor with multi-variable signal transduction and PEUT sensing polymer. (a) Plot of PC_1 vs. PC_2 illustrates sensor response to four concentrations of acetone vapor (0.044, 0.089, 0.133, and 0.178 P/P_o) at two concentrations of water vapor (0.18 and 0.36 P/P_o) and two concentrations of ethanol vapor (0.09 and 0.18 P/P_o). (b) Multivariate calibration curves for acetone detection in the presence of two interferences (water and ethanol vapors).
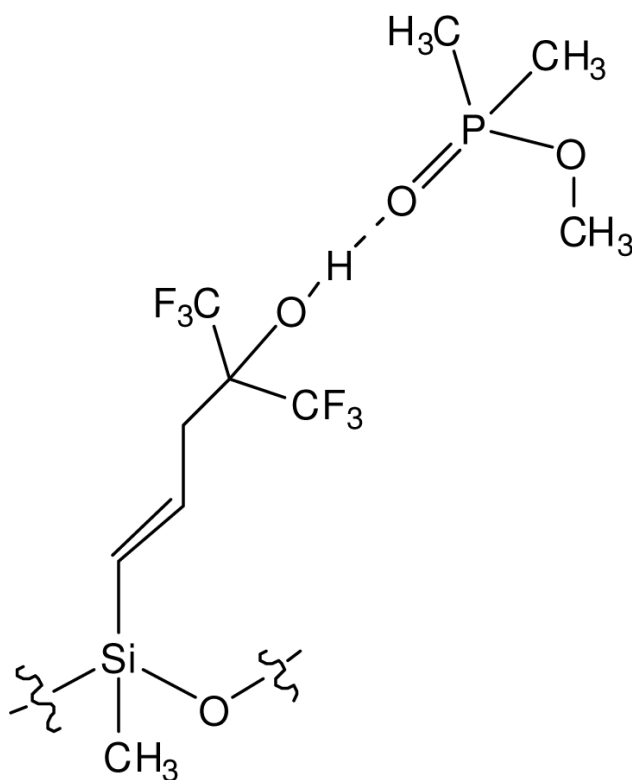
Figure 15.
Example of selective molecular association between DMMP and the hexafluoroisopropanol group in SXFA polymer.
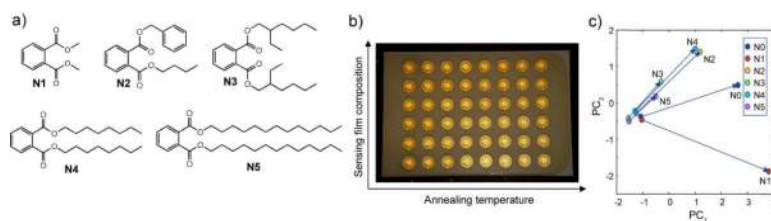
Figure 16.
Combinatorial screening of sensing film compositions using passive RFID sensors. (a) Phthalate plasticizers dimethyl phthalate **N1**, butyl benzyl phthalate **N2**, di-(2-ethylhexyl) phthalate **N3**, dicapryl phthalate **N4**, and diisotridecyl phthalate **N5**. (b) Photo of an array of 48 RFID sensors prepared for temperature-gradient evaluations of response of Nafion/phthalate compositions. (c) Results of principal components analysis of F_1, F_2, F_p, and Z_p responses of RFID sensors with six types of sensing films to H_2O and ACN vapors upon annealing at 110 °C. Arrows illustrate the H_2O – ACN Euclidean distances and the response direction of sensing films **N0** – **N5** starting with ACN and ending with H_2O response. Reprinted with permission from reference[155]. Copyright 2009 American Chemical Society.
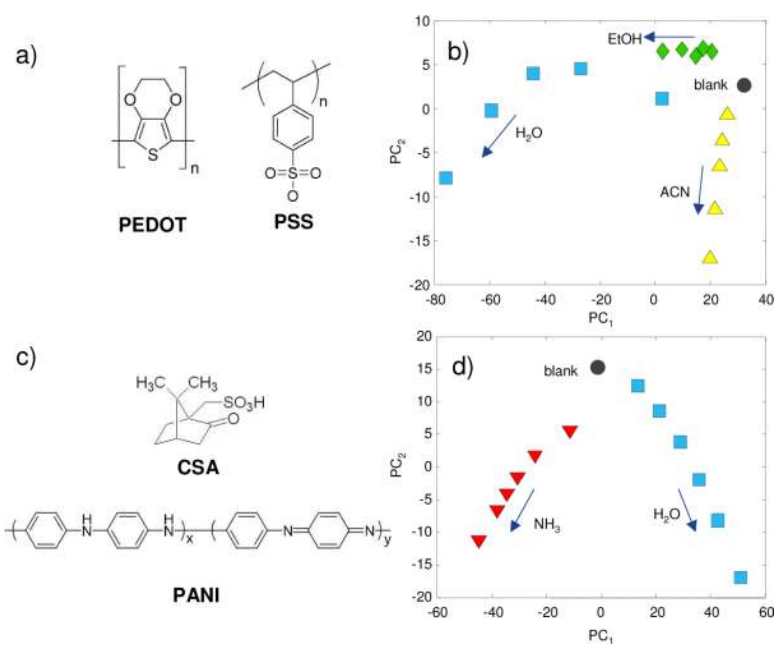
Figure 17.
Application of conjugated polymer compositions with diverse vapor-response mechanisms on multi-variable RFID transducers. Conjugated polymer compositions: (a) PEDOT/PSS. (c) PANI/CSA. PCA scores plots demonstrating selective analysis of vapors using individual RFID sensors with the multi-variable signal transduction. (b) Discrimination between EtOH, ACN, and H_2O vapors using PEDOT-PSS film, concentrations of all vapors were 0.04, 0.07, 0.1, 0.14, and 0.2 P/P_o. (d) Discrimination between NH_3 and H2O vapors using PANI-CSA film, concentrations of H_2O vapor were 0.02, 0.04, 0.07, 0.1, 0.14, and 0.2 P/P_o and concentrations of NH_3 vapor were 1×10^{-5}, 2×10^{-5}, 3.5×10^{-5}, 5×10^{-5}, 7×10^{-5}, and 1×10^{-4} P/P_o. Reprinted with permission from reference[74] Copyright 2009 Wiley.
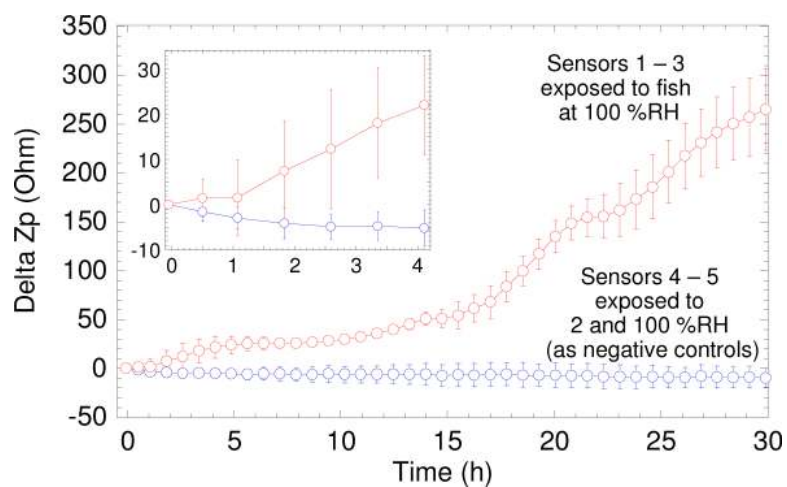
Figure 18.
Monitoring of fish freshness using PANI-based RFID sensors. Sensors 1 – 3 were positioned in a headspace with ~ 20 g (each) of salmon filet on a water-soaked liner. Sensor 4 served as the first negative control positioned in a low humidity headspace. Sensor 5 served as the second negative control positioned in a headspace only with a water-soaked liner. Sensors 1 − 5 were monitored at once at room temperature using a multiplexed sensor reader after 1 h of equilibration time to reach the state-state condition in all four sensors. Results are plotted as means and SD for sensors 1 – 3 (red trace) and 4 – 5 (blue trace). Inset, initial response of sensors 1 – 5.
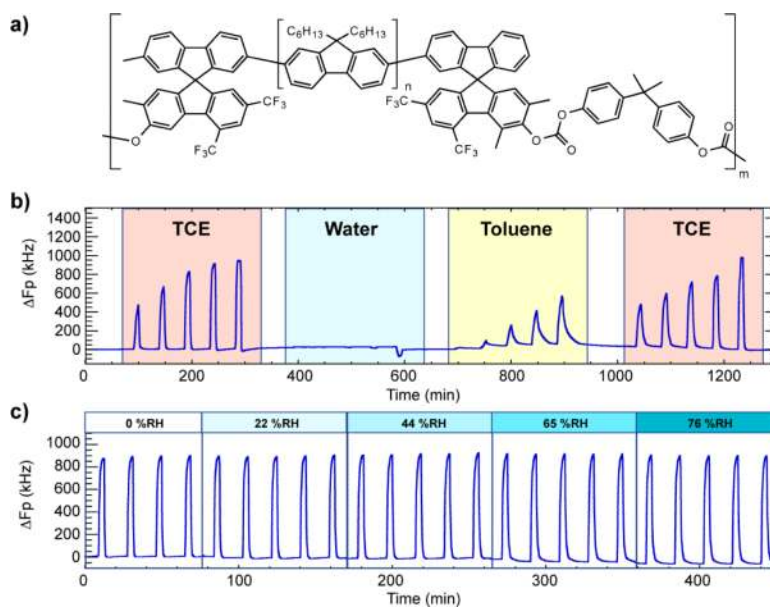
Figure 19.
Humidity-independent operation using a conjugated polymer sensing film on a multivariable RFID transducer. (a) Structure of poly(fluorene)-diphenylpropane polymer. (b) Response to different concentrations of TCE, water, and toluene vapors. TCE and toluene vapor concentrations are 0.02, 0.03, 0.5, 0.7, and 0.1 P/P_o; water concentration corresponds to relative humidity of 4, 10, 20, 48, and 76 %RH. (c) Sensor response stability to TCE vapor ($P/P_o = 0.1$) at different RH of carrier gas.
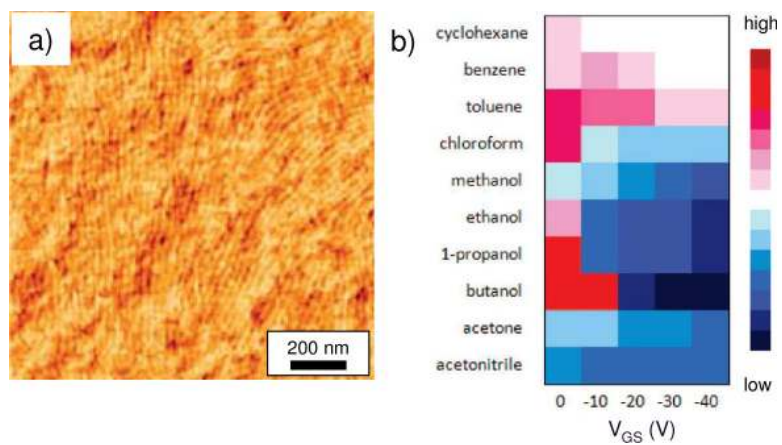
Figure 20.
Demonstration of morphology effects of a drop-cast regioregular poly(3-hexylthiophene) thin film on vapor-response selectivity. (a) AFM image of sensing film inside the transistor channel; (b) Contour map illustrating the effect of applied gate voltage on transistor drain-source current response to ten vapors normalized to 1 ppm of each vapor. Reprinted with permission from reference[162]. Copyright 2008 American Chemical Society.
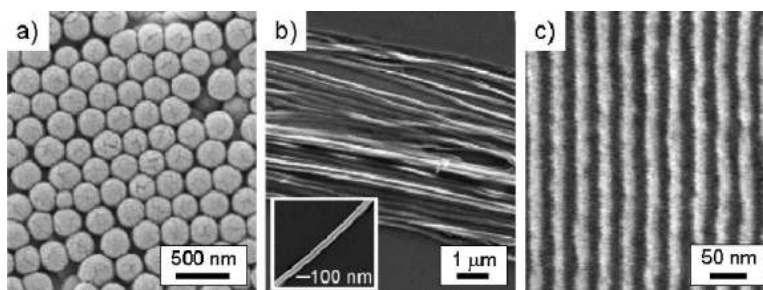
Figure 21.
Representative examples of nanostructured polymeric materials employed for vapor sensing with progressively decreasing feature size. SEM images of (a) self assembled film from phenylacetylene nanospheres; reprinted with permission from reference[184] (b) poly(2-methoxy-5-(2′-ethylhexyloxy)-1,4-phenylenevinylene nanowires fabricated by edge lithography; reprinted with permission from reference[191] and (c) PEDOT/PSS nanowires fabricated by self-assembled block copolymer lithography., Reprinted with permission from[180]. (a) Copyright 2008 IOP Publishing.(b) Copyright 2008 American Chemical Society (c) Copyright 2008 American Chemical Society.
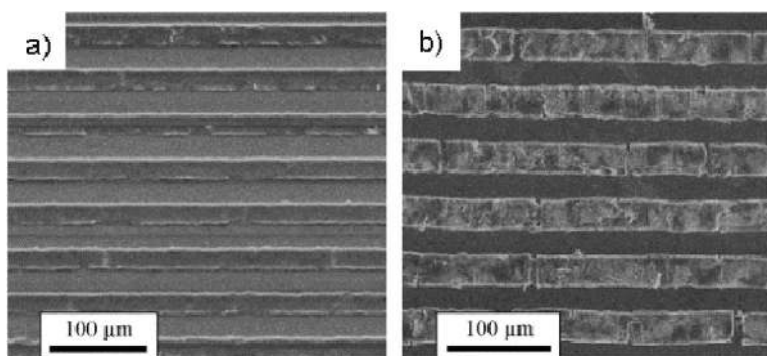
Figure 22.
SEM images of a microstructured polydiacetylene-based polymeric film (a) before and (b) after exposure to ~ 5000 ppm of dimethylformamide vapor for 10 min. Reprinted with permission from[194] Copyright 2010 Elsevier.
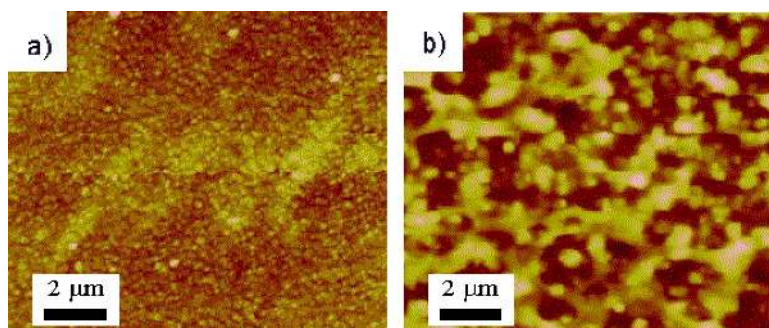
Figure 23.
Example of utilization of sensing film dewetting effects for chemical dosimetry. Atomic force micrographs of an ink-jet printed PEDOT-PSS film (a) before and (b) after exposure to ~ 5000 ppm of methanol vapor for 30 min Reprinted with permission from reference[198]. Copyright 2005 American Institute of Physics.
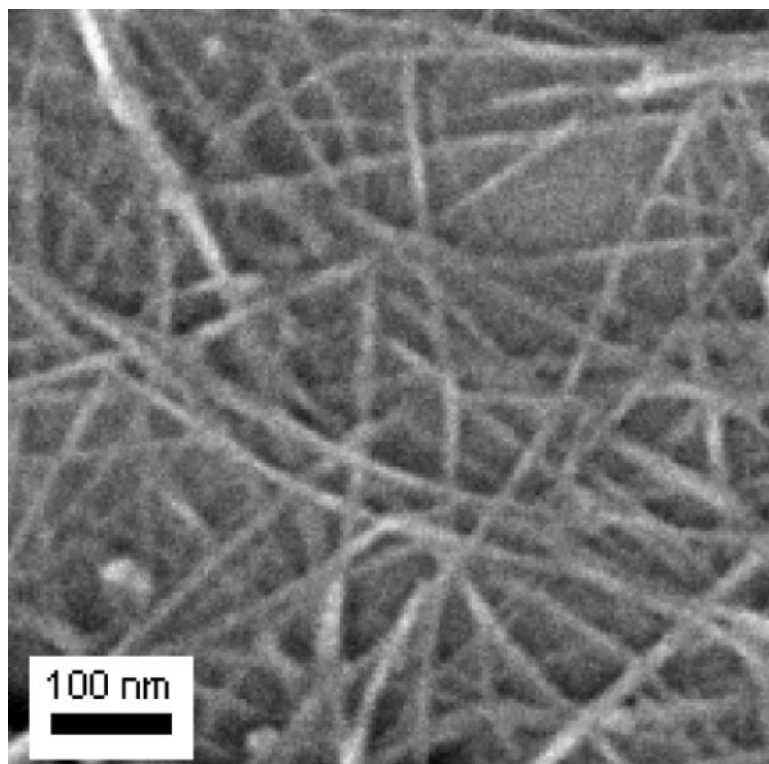
Figure 24.
SEM image of SWNTs.
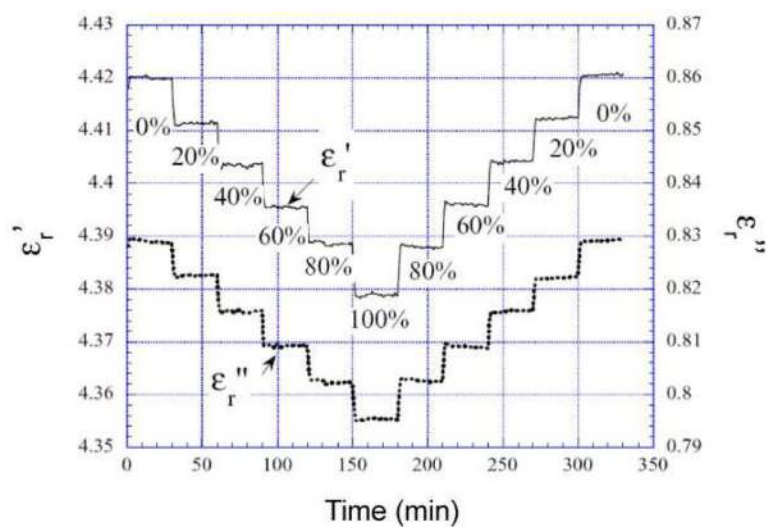
Figure 25.
Monitoring of CO_2 using wireless LCR transducer coated with a MWNT-SiO_2 composite film. Hysteresis-free sensor response as ε'_r and ε''_r upon sensor exposure to CO_2 concentrations varying from 0% to 100% vol. Reprinted with permission from reference[265]. Copyright 2001 MDPI.
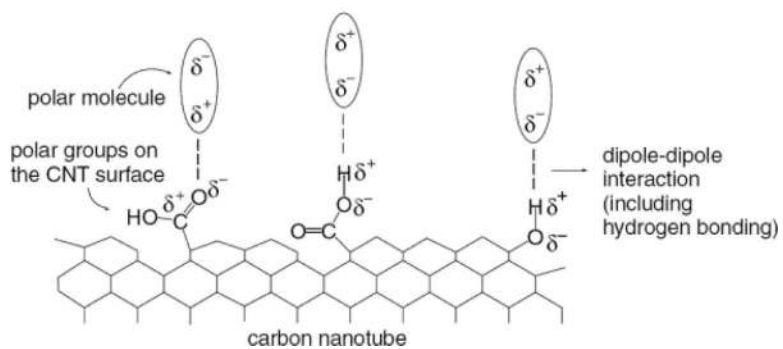
Figure 26.
Mechanism of interactions of polar gas molecules with surface-modified carbon nanotubes. Reprinted with permission from reference[248]. Copyright 2004 IOP Publishing.
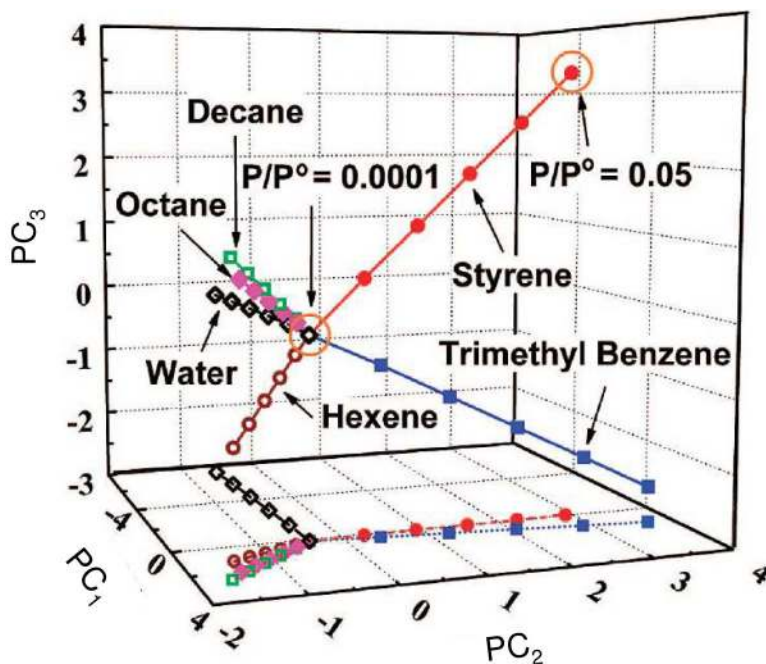
Figure 27.
Scores plot from a 10-detector array exposed to the representative VOC biomarkers of lung cancer as well as to water (to simulate the humidity effect in the exhaled breath) at P/P_o = 0.0001–0.05 in air. Reprinted with permission from reference[103]. Copyright 2008 American Chemical Society
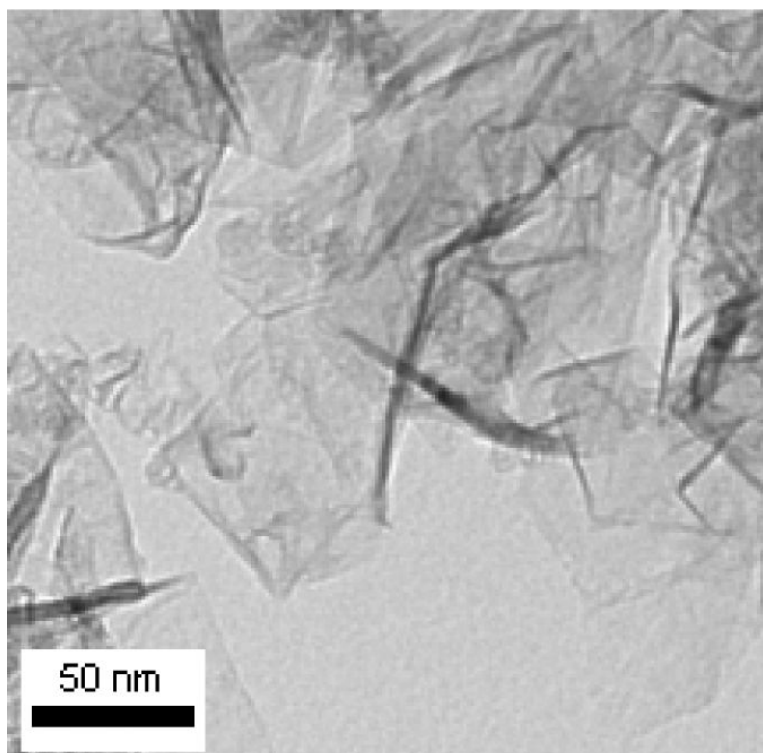
Figure 28.
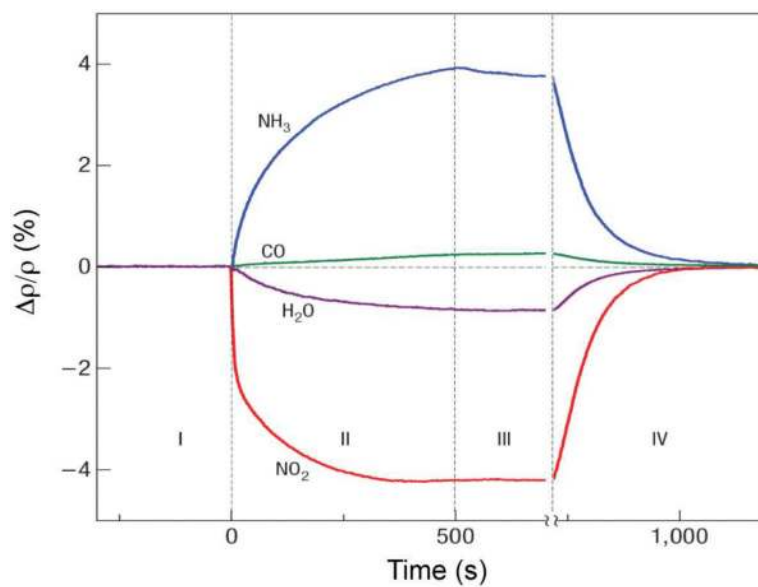SEM image of graphene.

Figure 29.
Resistivity response of pristine graphene monocrystals to 1 ppm concentrations of different reducing and oxidizing gases. Regions: (I) response in vacuum before gas exposure; (II) exposure to 1 ppm of gases; (III) gas removed by vacuum; (IV) gas desorption by annealing at 150°C. Reprinted with permission from reference[299]. Copyright 2007 Nature Publishing Group.
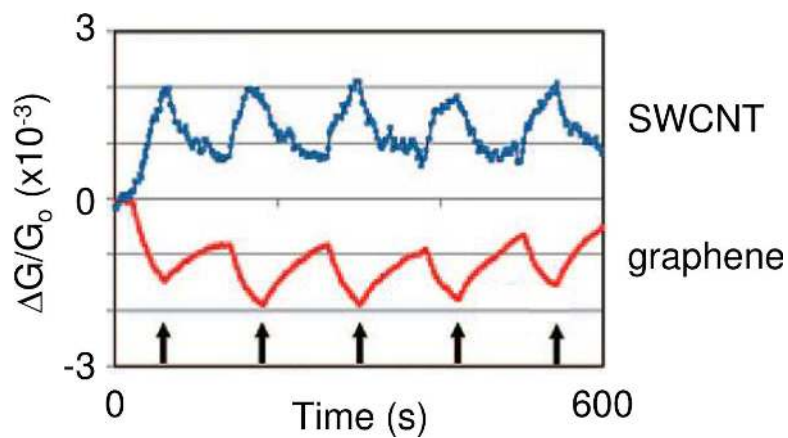
Figure 30.
Conductance response ($\Delta G/G_0$) of SWNT and graphene devices to periodic 30 s pulses of 0.5 ppb DNT. Vertical arrows in the plot mark the end of each 30 s pulse. Reprinted with permission from reference[308]. Copyright 2008 American Chemical Society.
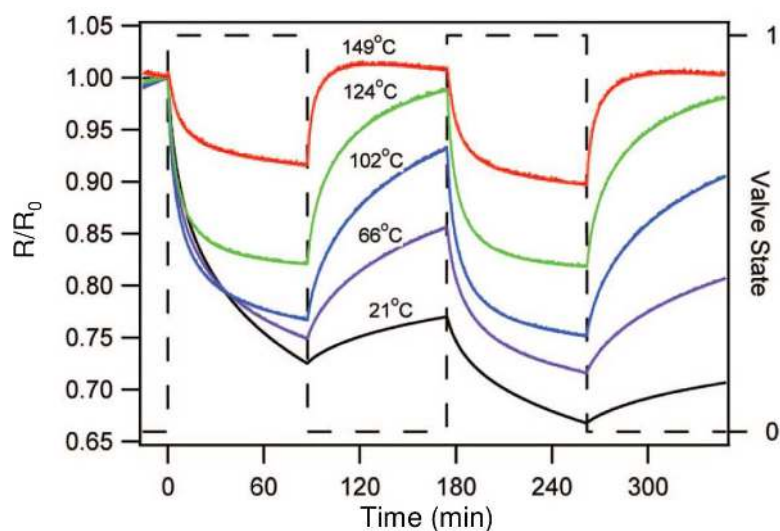
Figure 31.
Dynamics of operation for a graphene sensor at variable temperatures ranging from 21 to 149 °C for detection of 5 ppm of NO_2. Reprinted with permission from reference[304]. Copyright 2009 American Chemical Society.
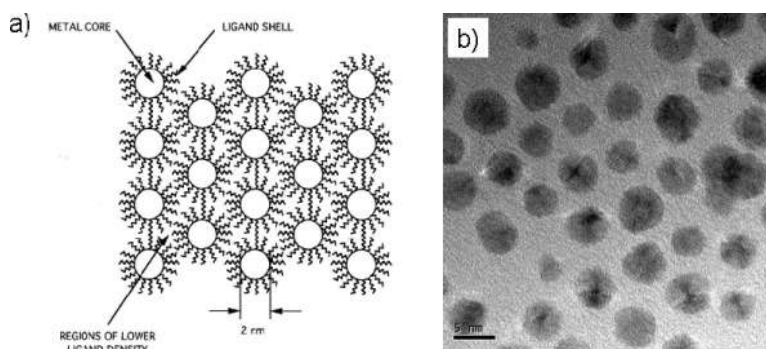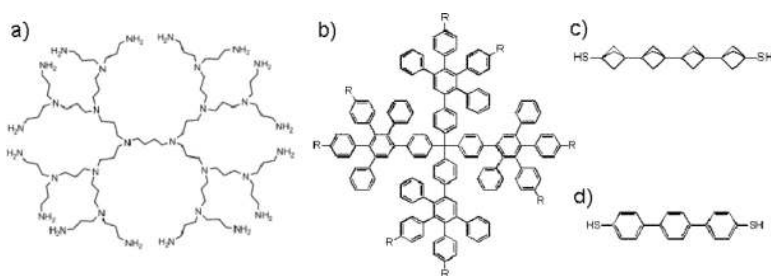
Figure 32.
Sensing films based on metal nanoparticles with dielectric ligand shells around each nanoparticle. (a) Schematic of a sensing film with Au nanoparticles and alkanethiol ligand shells. (b) Typical example of a fabricated film, TEM image of Au nanoparticles network.

Figure 33.
Examples of soft (a–b) and rigid (c–d) linkers utilized to form metal nanoparticle networks: (a) poly(propyleneimine) dendrimer of third generation; (b) polyphenylene dendrimer of first generation; (c) 4-staffane-3,3‴-dithiol; (d) 4,4′-terphenyldithiol. (a) Reprinted with permission from reference[328]. Copyright 2003 Elsevier; (b) Reprinted with permission from reference[329]. Copyright 2007 Wiley; (c–d) Reprinted with permission from reference[330]. Copyright 2007 American Chemical Society.
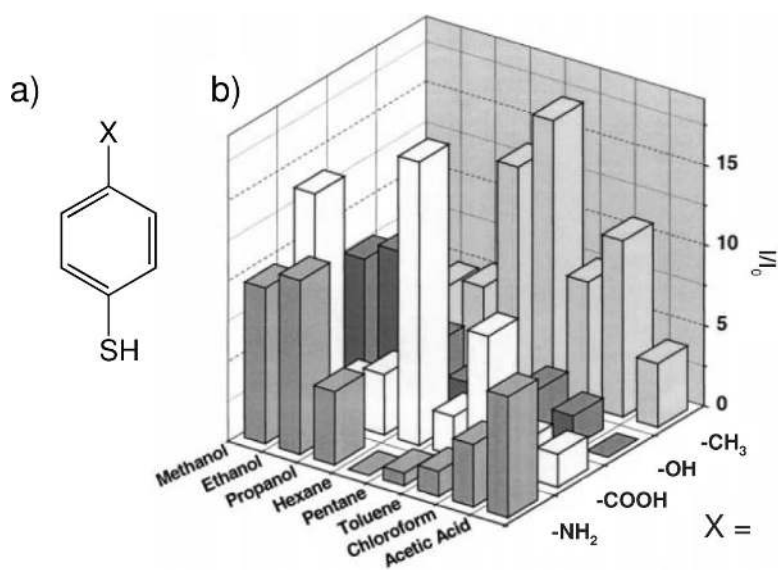
Figure 34.
Response of chemiresistors with short aromatic organothiol linkers of 3 – 6 nm Au
nanoparticles upon exposure to diverse vapors. (a) Chemical structures of linkers. (b)
Chemiresistor responses to diverse vapors. Reprinted with permission from reference[319].
Copyright 2000 Royal Society of Chemistry.
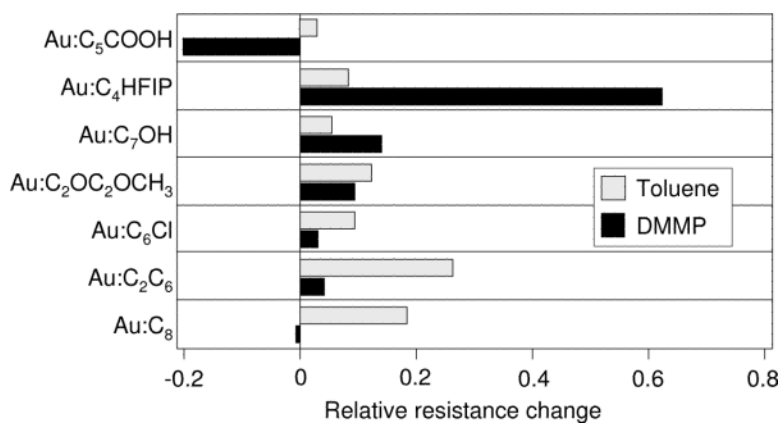
Figure 35.
Responses of several functionalized nanocluster films to toluene and DMMP vapors (both vapors were at $P/P_0 = 0.1$) Reprinted with permission from reference[336].
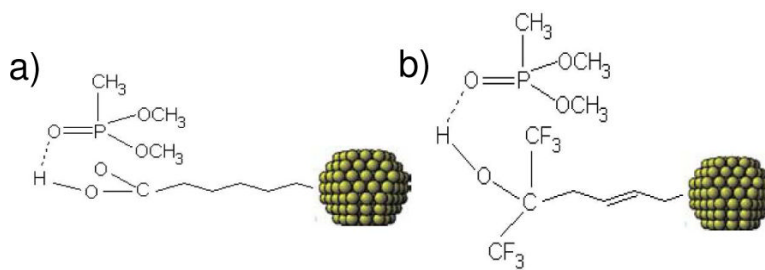
Figure 36.
Interaction mechanisms of DMMP vapor with different nanocluster films: (a) Au:C$_5$COOH and (b) Au:HFIP. Reprinted with permission from reference[336].
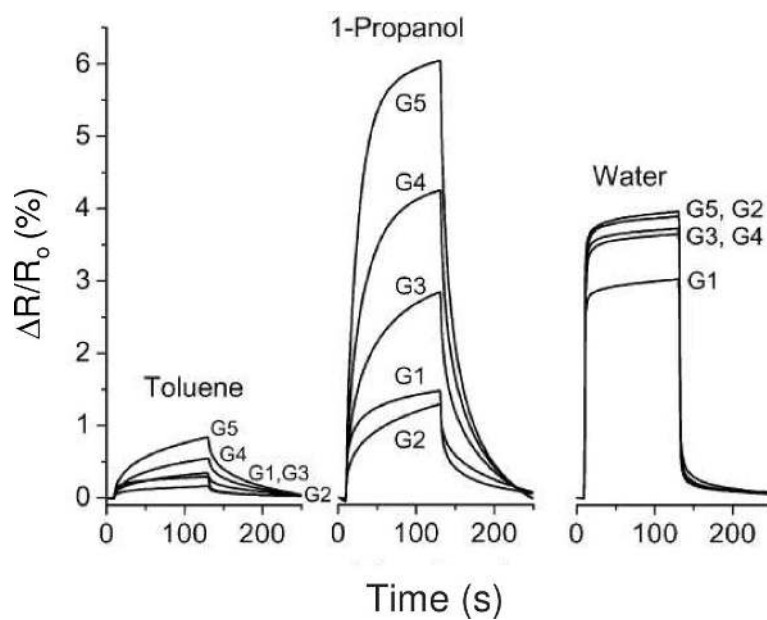
Figure 37.
Responses of chemiresistors based on Au nanoparticle films with PPI G1 – G5 dendrimers
to toluene, 1-propanol, and water vapors. Reprinted with permission from reference[328].
Copyright 2003 Elsevier.
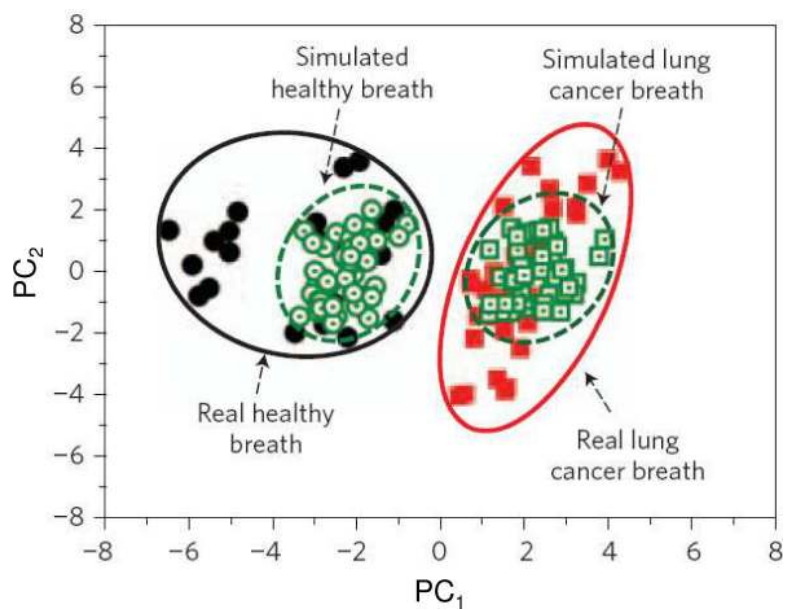
Figure 38.
Scores plot of a PCA model of response a nine-sensor array with diverse types of monolayer-protected metal nanoparticles to samples of real and simulated breath from lung cancer patients and healthy volunteers. Reprinted with permission from reference[339]. Copyright 2009 Nature Publishing Group.
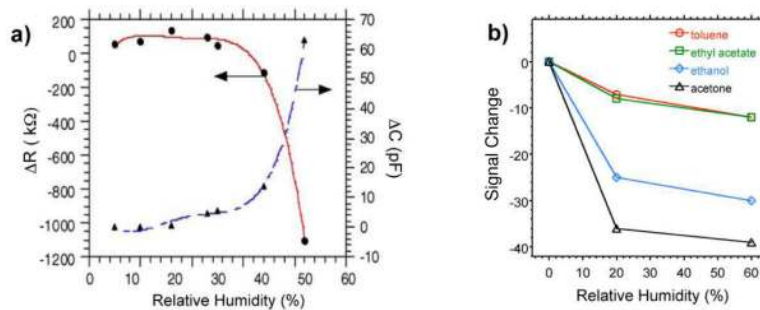
Figure 39.
Effects of humidity on sensor performance with C_8SH film. (a) Humidity-dependent resistance-capacitance response. (b) Decrease of sensitivity to analyte vapors in presence of humidity Reprinted with permission from reference[342]. Copyright 2005 Elsevier.
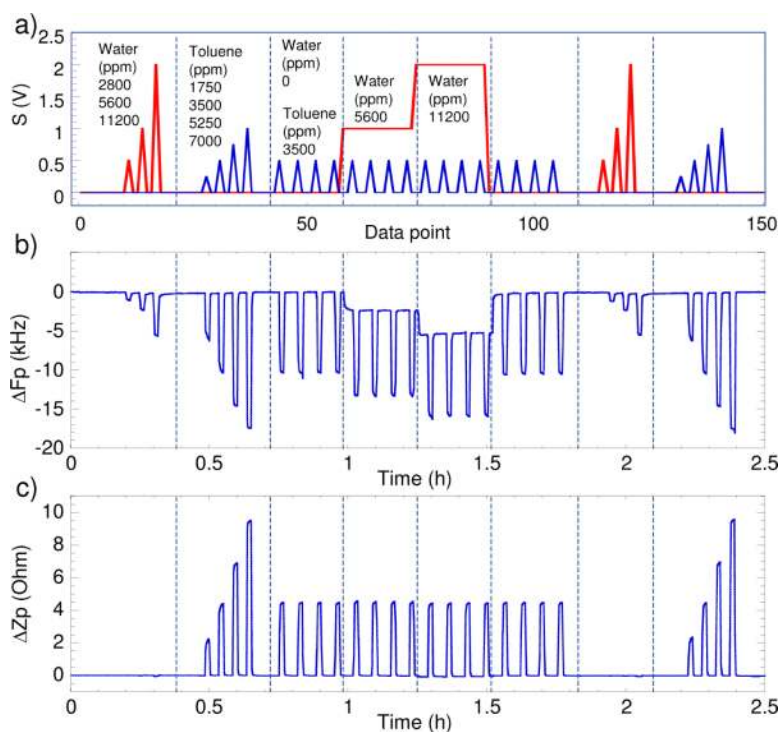
Figure 40.
Humidity-independent operation using a single RFID sensor with the multivariable signal transduction and a monolayer capped Au nanoparticles as a sensing film. (a) Experimental design of a test cycle for evaluation of sensor response to different concentrations of individual vapors (water and toluene) and their mixtures; (b) Sensor Fp response; and (c) Sensor Zp response.
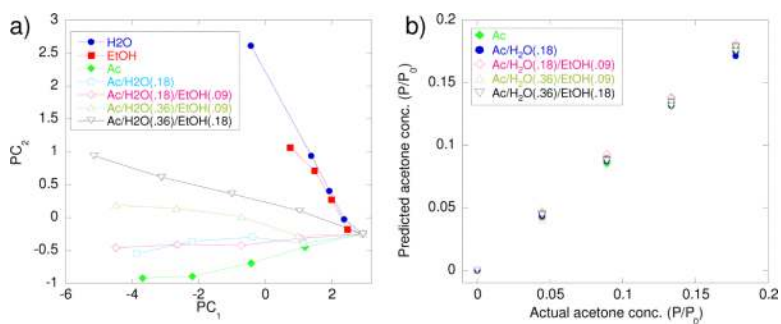
Figure 41.
Quantitation of an analyte vapor (acetone) in the presence of multiple interferences (water and ethanol vapors) using a single RFID sensor with multi-variable signal transduction and Au:C_8SH nanoparticle-based film. (a) Plot of PC_1 vs. PC_2 illustrates sensor response to four concentrations of acetone vapor (0.044, 0.089, 0.133, and 0.178 P/P_o) at two concentrations of water vapor (0.18 and 0.36 P/P_o) and two concentrations of ethanol vapor (0.09 and 0.18 P/P_o). (b) Multivariate calibration curves for acetone detection in the presence of two interferences (water and ethanol vapors).

Figure 42.
Technology readiness levels in development of new gas sensors.

Table 1

Examples of regulated concentration levels (in ppm by volume) from three representative classes of toxic gases: VOCs, TICs, and CWAs.[10–14]

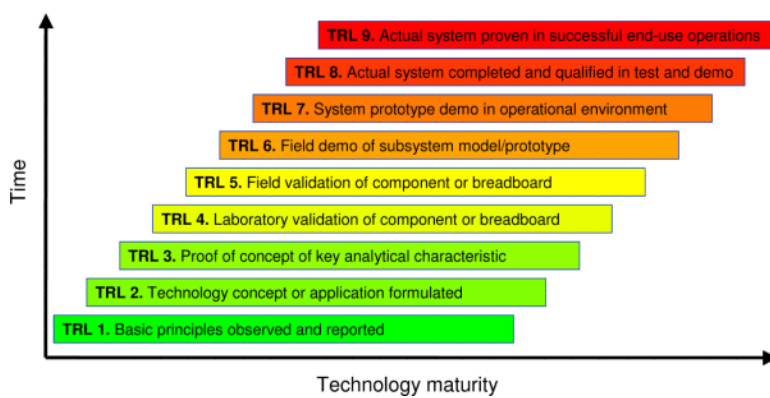| Class	Chemical or agent	IDLH (ppm)	LOC (ppm)	TLV-TWA (ppm)	TLV-STEL (ppm)	PEL (ppmv)	GPL (ppm)	AEGL-3 (ppm)	AEGL-2 (ppm)	AEGL-1 (ppm)
VOCs	Acetone	2500	250	750	1000	1000		1700	950	200
	Benzene	500	50	0.5	2.5	1		990	200	9
	Chloroform	500	50	10	2	50		1600	29	
	Methanol	6000	600	200	250	250		1600	520	270
	Methylene Chloride	2300	230	25	125			2100	60	
	Phenol	250	25	5	10	5		23	6.3	1.9
TICs	Ammonia	300	30	25	25	50		390	110	30
	Carbon monoxide	1200	120	25	400	50		130	27	
	Chlorine	10	1	0.5	1	1		7.1	0.71	0.5
	Formaldehyde	20	2	0.3	0.75	0.75		35	15	0.9
	Nitrogen dioxide	20	2	3	5	5		11	6.7	0.5
	Phosphine	50	5	0.3	0.3	0.3		0.45	0.25	
	Sulfur dioxide	100	10	2	5	5		9.6	0.75	0.2
CWAs	Chemical Mustard	0.0004	0.00004	0.00006	0.00046		3.1×10^{-6}	0.04154	0.002	0.0012
	Lewisite	0.0003	0.00003	0.00035			0.00035	0.013	0.0021	
	Sarin	0.03	0.003	9.0×10^{-6}	0.00003		3.0×10^{-7}	0.0087	0.0022	0.0002
	Soman	0.008	0.0008	4.03×10^{-6}	7.0×10^{-6}		1.3×10^{-7}	0.0066	0.0009	7.0×10^{-5}
	Tabun	0.03	0.003	9.0×10^{-6}	0.00003		3.0×10^{-7}	0.015	0.002	0.0002
	VX	0.002	0.0002	7.0×10^{-7}	7.0×10^{-6}		4×10^{-7}	0.00035	0.0001	7.0×10^{-7}

GPL: General Population Limit, established by USACHPPM – U.S. Army Center for Health Promotion and Preventative Medicine;

PEL: Permissible Exposure Limit, established by OSHA, Occupational Safety and Health Administration;

TLV-STEL: Threshold Limit Value (Short Term Exposure Limit) and *TLV-TWA: Threshold Limit Value (Time Weighted Average)*, established by ACGIH, American Conference of Governmental Industrial Hygienists;

IDLH: Immediately Dangerous to Life or Health and *LOC: Level of Concern*, 0.1×IDLH, established by NIOSH, U.S. National Institute for Occupational Safety and Health;

AEGL-1,2,3: Acute Exposure Guideline Levels, established by EPA – U.S. Environmental Protection Agency.

Table 2

Examples of power requirements for different gas sensing transducers and sensing systems.

Sensing scheme	Required power	Reference
Sensing transducers		
Capacitor[*]	30 pW – 30 μW	[35]
Resistor[*]	10 nW – 64μW	[36 – 38]
Microcantilever[*]	200 pW – 20 nW	[44]
Field-effect transistor[*]	32 μW	[42]
Resistor[**]	20 μW at 300°C 0.3 – 15 mW at 300°C 5 – 170 mW at 450°C	[41] [39] [40]
Field-effect transistor[**]	20 – 200 mW	[43]
Magnetoelastic wireless passive resonator[***]	0	[45]
TSM wireless passive resonator[***]	0	[46]
SAW wireless passive resonator[***]	0	[47]
LCR wireless passive resonator[***]	0	[48]
Sensing systems		
Surface-acoustic wave sensor array system	120 mW	[49]
Wireless sensor system with eight microcantilevers, humidity, and temperature sensors	84 mW	[50]
Capacitance three sensor array for humidity, temperature, and pressure	0.3 mW	[51]
Wireless sensor system with arrays of tuning fork sensors, collection/conditioning subsystem, Bluetooth communication	~ nW - tuning forks ~ 100 mW - communication ~ 800 mW pump/valve	[52]
Reader for magnetoelastic wireless passive resonator sensors	9 V battery for 10,000 measurements	[53]
Reader for TSM wireless passive resonator sensors	0.1 – 10 mW	[46]
Reader for SAW wireless passive resonator sensors	0.5 – 25 mW	[54,55]
Reader for LCR wireless passive resonator sensors	1 mW	[48]

[*] operation at ambient room temperature

[**] operation at elevated temperature

[***] passive sensor operation without a power source on board, required energy has been delivered wirelessly by a reader

Table 3

Typical characteristics of various energy sources available for the ambient and harvested power[58].

Source	Source power	Harvested Power
Ambient light- indoor	100 μW/cm^2	10 μW/cm^2
Ambient light – outdoor	100 mW/cm^2	10 mW/cm^2
Human motion	0.5 m @ 1 Hz 1 m/s^2 @ 50 Hz	4 μW/cm^2
Industrial vibration	1 m @ 5 Hz 10 m/s^2 @ 1 kHz	100 μW/cm^2
Thermal energy – human	20 mW/cm^2	30 μW/cm^2
Thermal energy – industrial	100 mW/cm^2	10 mW/cm^2
Radio frequency energy - cell phones	0.3 μW/cm^2	0.1 μW/cm^2

Table 4

Examples of techniques demonstrated for fabrication of nanoscale features in polymeric materials.

Demonstrated feature size	Technique	Reference
~500 nm linewidth	Nanoassembly from fluids	183
200 – 300-nm nanoparticle diameter	Fabrication and self-assembly of polymeric and composite nanobeads	184,185
~ 150 nm feature	guided growth of polymeric structures on surface-functionalized nanopatterns	186
~ 100 nm lateral dimension	Electrostatic lithography for polymeric patterns	187
40 – 50 nm nanofiber diameter	Electropolymerization techniques	167
15-nm width of nanowire	Self-assembled block copolymer lithography for large-scale fabrication of well-ordered nanowires	180
< 10 nm lateral size of nanowire	Dewetting technique for highly ordered arrays of nanowires	188
5 nm nanofibers diameter	Electrospinning techniques	189
~ 2nm feature	Polymer imprint lithography with single-walled carbon nanotubes as templates	190

Table 5

Values of ΔG/ΔC of SWNTs networks measured for various dilute individual chemical vapors in dry air[119].

chemical vapor	ΔG/ΔC
dinitrotoluene	0.20
dichloropentane	0.10
nitrobenzene	0.080
water	0.045
hexane	0.043
toluene	0.025
benzene	0.013
2-propanol	−0.027
acetone	−0.03
tetrahydrofuran	−0.10
DMMP	−0.12

Table 6

Ratios of response sensitivity of chemiresistors to TSM sensors for four metal cluster-capping ligands.[325]

	MOP	C8SH	MET	NAP
Toluene	1.5	8.9	4.3	1.3
2-Butanone	2.7	18.6	4.4	5.5
iso-Propanol	4.5	24.9	5.5	4.1
Octane	0.5	17.8	3.9	0.3
Butyl acetate	1.3	13.7	5.6	1.1
1,2-Dichloroethane	1.1	10.2	2.1	1.9
Perchloroethylene	1.0	5.4	3.3	1.1
n-Butanol	2.2	22.5	1.7	4.0
1,4-Dioxane	3.6	22.3	12.9	2.7
m-Xylene	0.4	24.6	3.5	0.7
Average	1.9	16.9	4.7	2.3

Table 7

Vapor properties, calculated partition coefficients, and calculated detection limits for chemiresistors and TSM sensors coated with C_8SH ligand.[318]

vapor (abbreviation)	ε_v	Kb	CR, DL (ppm)	TSM, DL (ppm)
n-butane (C_4)				
n-pentane (C_5)	1.84	51	2.0	4300
2-methylpentane (2MP)	1.89	100	0.81	1800
chloroform (CHL)	4.71			
n-hexane (C_6)	1.88	150	0.53	1200
methanol (MEOH)	32.6	97	150	5100
1,1,1-trichloroethane (TCA)	7.08			
benzene (BEN)	2.27	380	0.24	540
1,2-dichloroethane (DCE)	10.1	260	0.92	610
ethanol (ETOH)	24.9	180	4.9	1900
2,2,4-trimethylpentane (IC8)	1.94	340	0.20	410
n-heptane (C_7)	1.91	410	0.18	390
2-propanol (IPA)	19.3	210	2.2	1300
toluene (TOL)	2.37	1000	0.082	170
1-propanol (PROH)	20.5	480	1.1	540
perchloroethylene (PCE)	2.27	1600	0.065	59
2-butanol (2BOH)	15.9	460	0.64	460
n-octane (C_8)	1.94	1500	0.046	95
ethylbenzene (ETB)	2.43	2600	0.027	57
p-xylene (pXYL)	2.27	2500	0.029	60
m-xylene (mXYL)	2.35	2600	0.028	57
1-butanol (1BOH)	17.3	760	0.32	280
o-xylene (oXYL)	2.55	3300	0.023	45
isopropylbenzene (IPB)	2.37	3500	0.017	37
n-nonane (C_9)	1.96	3100	0.020	39
o-chlorotoluene (oCLT)	4.63	7900	0.011	16
1,3,5-trimethylbenzene (TMB)	2.27	6400	0.010	21
n-decane (C_{10})	1.98	7500	0.0079	15

Table 8

Representative results on the long term stability of diverse sensing materials.

Type of sensing material	Duration of testing (months)	Summary of results	Ref.
Dielectric Polymers	6.3	Comparison between SAW vapor responses of hyperbranched hydrogen-bond acidic polymers: phenolic hyperbranched polymers lost 70–80% of their response, while polymer with hexafluoro-2-propanol groups maintained a steady response	[442]
Dielectric Polymers	10	Evaluation of side-chain-modified polysiloxanes: the long term stability without the need for calibration demonstrated over 10 months with artificial neural networks and only over 6 months with partial least squares concentration prediction	[83]
Dielectric Polymers	36	Evaluation of silicone block polyimide polymer: X-ray photoelectron spectroscopy showed no detectable differences in the amount and type of oxygen on the surface of fresh and old films, QCM measurements showed negligible variation in film thickness.	[443]
Dielectric Polymers	46	Evaluation of submicron particles of diethyl ester of *p*-phenylenediacrylic acid that were polymerized directly onto SAW transducers: sensor vapor response decreased only 20 % over 46 months	[444]
Conjugated Polymers	4	Evaluation of UV-treated PANI-CSA films as changes in the bulk resistance and in the interface resistance between the film and sensor substrate and the interface resistance between sensing film and air: no detectable change in relative resistance	[176]
Monolayer-Protected Metal Nanoparticles	6	Comparison between Au:BC2 (17% reduction in vapor response, 15% decrease in baseline resistance) and more stable Au:C8 (1% reduction in vapor response, 5% decrease in baseline resistance) sensing films	[317]
Monolayer-Protected Metal Nanoparticles	6	Comparison between monothiol-Au (50% reduction in vapor response) and more stable trithiol-Au (10% reduction in vapor response) sensing films	[445]
Monolayer-Protected Metal Nanoparticles	12 – 16	Comparison between unstable Au:C6S (60% reduction in vapor response, decrease in baseline current from 4.5 to 2.0 nA) and more stable Au:TOABr (20% reduction in vapor response, insignificant descrease in baseline current) sensing films	[326]

Table 9

Attractive features of wireless gas sensing networks.

WSN features	Reference
Novel data-generation and processing concepts	
Implementation of available infrastructure for communications of sensors	432,433
Heterogeneous sensors coupled to multiparameter coincidence techniques to improve detection accuracy	447
Fusion and processing strategies for massive and dynamic data from WSNs for time-critical decision-making and for providing ability to identify spurious signals and malfunction of individual sensors on the network	448
Data acquisition algorithms for individual sensors to reduce power consumption and to extend operational lifetime before battery replacement	433,449
Auto-calibration methods for maintenance-free operation of individual gas sensors in WSN. Responses of sensors are calibrated against local reference monitoring stations	434
Internet-enabled pollution monitoring server interfaced to Google Maps to display real time pollutants levels and locations in large metropolitan areas	435
Novel sensor-integration concepts	
Integration of sensors into mobile phones	448,450,451
Autonomous sensor- and GPS-equipped mobile robotic devices for location and validation of pollution, homeland security threat, and other sources	437,448
Integration of sensors into public or personal transportation vehicles for pollution and homeland security threat monitoring with a significant benefit of matching vehicle/sensor maintenance schedules	435,448